"Dynamic Regulation of RUNX2 and AMPK in Metabolic Disorders and Stress"

Thesis submitted for the degree of

DOCTOR OF PHILOSOPHY

To

Department of Animal Biology

School of Life Sciences

University of Hyderabad

By

Chava Suresh

[Enrolment No: 12LAPH14]

Department of Animal Biology

School of Life Sciences

University of Hyderabad

Hyderabad - 500046

India

--June 2018--

University of Hyderabad
(A central university established in 1974 by an act of parliament)
Hyderabad-500046, INDIA

CERTIFICATE

This is to certify that the thesis entitled **"Dynamic Regulation of RUNX2 and AMPK in Metabolic Disorders and Stress"** submitted by **Mr. Chava Suresh** bearing registration number **12LAPH14** in partial fulfilment of the requirements for award of Doctor of philosophy in the Department of Animal Biology, School of Life Sciences is a bonafide work carried out by him under my supervision and guidance.

This thesis is free from plagiarism and has not been submitted previously in part or in full to this or any other University or Institution for award of any degree or diploma.

The results of this thesis have been:

A. Published in the following publications:

1. **Suresh C,** Chennakesavulu S, Gayatri MB, Reddy AB. A Novel Phosphorylation by AMP-activated Kinase regulates RUNX2 from Ubiquitination in Osteogenesis over Adipogenesis. (2018) *Cell death and disease* (ISSN: 2041-4889)

2. Devi A, Chennakesavulu S, **Suresh C**, Reddy AB. Chapter-17 "Nutraceuticals in Health and Disease". "Functional food and human health". (2018) *Springer-Nature Inc.* (Book chapter ISBN: 978-981-13-1122-2)

B. Presented in the following conferences:

1. Presented in "The international congress for cell biology (ICCB-2018) Conference on the dynamic cell: Molecules and Networks to form and function" at CCMB, Hyderabad, 2018 (International).

Further, the student has passed the following courses towards fulfillment of coursework requirement for Ph.D.

Course Code	Name	Credits	Pass/Fail
1. AS 801	Seminar 1	1	PASS
2. AS 802	Research Ethics & Management	2	PASS
3. AS 803	Biostatistics	2	PASS
4. AS 804	Analytical Techniques	3	PASS
5. AS 805	Lab Work	4	PASS

Supervisor **Head of Department** **Dean of School**

University of Hyderabad
(A central university established in 1974 by an act of parliament)
Hyderabad-500046, INDIA

DECLARATION

I hereby declare that the results of the study incorporated in the thesis entitled **"Dynamic Regulation of RUNX2 and AMPK in Metabolic Disorders and Stress"** has been carried out by me under the supervision of **Dr. A. Bindu Madhava Reddy** and this work has not been submitted for any degree or diploma of any other university earlier.

Dated:

Chava Suresh
(12LAPH14)
(Research Scholar)

Supervisor
Dr. A. Bindu Madhava Reddy

Acknowledgements

- I would like to express my deepest sense of gratitude to my supervisor ***Dr. A. Bindu Madhava Reddy***, for giving me an opportunity to work under his guidance, constant cooperation, and encouragement throughout my work. I have been inspired by his meticulousness, his attention to detail and his energetic application to any problem. I value his concern and support at all times, good and bad. The door to Dr. A. Bindu Madhava Reddy's office was always open whenever I ran into a trouble spot or had a question about my research or writing. I am highly grateful to him for all the efforts he has put in for the successful completion of this thesis.
- I thank Head, Dept. of Animal Biology, Prof. Anita Jagota, and previous HOD's Prof. Jagan Pongubala, Prof. Senthilkumaran, and Prof. Manjula Sritharan for allowing me to use the departmental facilities.
- I thank the Dean, School of Life Sciences, Prof. K.V.A. Ramaiah and former Dean Prof. M. N. V. Prasad, Prof. P. Reddanna, Prof. A.S. Raghavendra, Prof. Aparna Dutta Gupta, Prof. R.P. Sharma and Prof. M. Ramanadham for providing the central facilities at the School of Life Sciences.
- I thank the doctoral committee experts who were involved in the validation survey for this research work Prof. Naresh Babu V. Sepuri and Prof. Sreenivasulu kurukuti for constructive criticism and valuable guidance, without their passionate participation and inputs, the validation survey could not have been successfully conducted.
- I thank Dr. Kota Arun Kumar and Dr. Arunasree MK for allowing me to use their laboratory facilities as on when needed.
- I have been privileged to have worked with Dr. Navin Viswakarma, Dr. Kishore Parsa and Dr. Parimal Mishra, during my stay in DRILS. I have learnt several things from them and highly indebted to them. Their continuous support, encouragement and appreciation have been extremely valuable to me.
- I thank Dr. Aparna Rachamallu for her critical suggestions and constant encouragement throughout my study.

- I thank Dr. Prashanth Maitreya for his help and support in PSP imaging.
- I thank Dr. Uma Krishnan for her help and support in µCT studies.
- I thank all my present and past lab mates Chenna keshavulu, Preeti vyakaranam, Gaythri, Naga Chaitanya, Navya Naidu, Arpitha devi, Nikhitha, shruti, Priya Madhesia and Ram Gopal Reddy for their help and support during my stay in lab.
- I thank my best friends (Doctor Bava's) Dr. Ravi Boya, Dr. Prasad Tammineni, Dr. Sai Naresh Kona and Dr. Keshavardhana Sannula, for their care, Love and Support in even and odd times. I am always fortunate to have these people in my life.
- I thank all my friends Dr. Tapan, Dr. Soma Behera, Dr. Bandish, Dr. Malathi, Chandana, Dr. Neeraja, for their help as on when needed.
- I thank all my friends & Seniors Dr. Papa Rao, Dr. Maruthi Mulaka, Dr. Subramanyam, Dr. Suresh Kumar Kalangi, Dr. Suman, Dr. Rameswar Reddy, Dr. Ravi Jillapalli and Dr. Madhavi Reddy for their help as on when needed.
- I thank Bangaraiah, Kumar, Chandram and Prashanth Kumar Yadav for their assistance in the laboratory.
- I thank Mr. Ankineedu, Mrs. Jyothi, Mrs. Vijaya Lakshmi, Mr. Sreenu, Mr. Gopala Krishna, and Mr. Jagan for their help in office work during my course of study.
- The financial support from DBT-RGYI, DBT-RNAi, DAE-BRNS, UPE-Phase II, DST, CSIR, ICMR, UGC, DST-PURSE and DBT-CREBB is highly acknowledged.
- Financial support through CSIR-JRF and SRF is highly acknowledged.
- I am extremely grateful to my **parents** and my **Brothers** (Srihari, Ravidra, and Prasad) who has been my real strength and supporting, for their unconditional love, support and patience throughout my life.
- Above the all, I owe my thanks to **Almighty,** for associating these many great people around me.

Suresh Chava……..

Dedication

I dedicate this thesis to my parents to making me “who I am”

&

My Guru Dr. Bindu Madhava Reddy to shaping me into “what I am today”

Table of contents

Abbreviations

AD	Activation domain
AGEs	Advanced glycation end products
AICAR	5-Aminoimidazole-4-carboxamide ribonucleotide
Akt	Protein kinase B
ALP	Alkaline phosphatase
AM	Adipogenic media
AMPK	AMP-Activated serine threonine protein kinase
aP2	Adipocyte Protein 2
ATCC	American Type Culture Collection
ATF4	Activating transcription factor 4
ATP	Adenosine triphosphate
BM-MSCs	Bone marrow derived mesenchymal stem cells
BMP	Bone morphogenic protein
BMPC	Bone marrow progenitor cells
bp	Base pair
BS/TV	Bone surface density
BSA	Bovine serum albumin
BV/TV	Trabecular bone volume
C/EBP	CCAAT/enhancer-binding family of proteins
CaMKK	Calcium/calmodulin-dependent protein kinase kinase
CBFβ	Core binding factor β
CCD	Cleidocranial dysplasia
CD	Cluster of differentiation
Cdk1	Cyclin-dependent kinase 1
cDNA	Complimentary DNA
CEB	Cytoplasmic extraction buffer
CO_2	Carbon dioxide
CPCSEA	Control and Supervision of Experiments on Animals
CVD	Cardiovascular diseases
DAPI	4,6-diamidino-2-phenylindole

DBD	DNA Binding Domain
DEPC	Diethyl pyrocarbonate
DMEM	Dulbecco's modified essential Medium
DNA	Deoxy ribo nucleic acid
dNTPs	Deoxy nucleotide triphosphates
DPP-IV	Dipeptidyl peptidase IV
DTT	DL-Dithiothreitol
EDTA	Ethylene diamine tetraacetic acid
EGF	Epidermal growth factor
EMSA	Electrophoretic mobility shift assays
ER	Endoplasmic reticulum
ERK	Extracellular signal-regulated kinases
FACS	Fluorescence-activated cell sorting
FBS	Fetal bovine serum
FDA	Food and Drug Administration
FFA	Free fatty acids
FGF	Fibroblast growth factor
GFP	Green fluorescent protein
GIP	Glucose dependent insulinotropic polypeptides
GLP-1	Glucagon like peptide harmone-1
GLUT	Glucose transporters
GSK-3	Glycogen synthase kinase 3
GST	Glutathione S-transferase
H&E	Hematoxylin and Eosin staining
HbA1c	Hemoglobin A1c
HDACs	Histone deacetylases
HEK 293T	Human Embryonic Kidney cells
HEPES	2-hydroxyethyl)-1-piperazineethanesulfonic acid
HG	High glucose
HUVECs	Human Umbilical Vein Endothelial Cells
IAEC	Institutional Animal Ethics Committee

IBMX	3-isobutyl-1-methylxanthine
IDDM	Insulin dependent diabetes mellitus
IDF	International diabetic federation
IGF-1	Insulin-like growth factor 1
IMEM	Iscove's modified Dulbecco's Medium
IPDB	Immunoprecipitation dilution buffer
IPEB	Immunoprecipitation elution buffer
IPWB	Immunoprecipitation wash buffer
IRS-1	Insulin receptor substrate 1
JAK/STAT	Janus kinases /Signal Transducer and Activator of Transcription proteins
JNK	c-Jun N-terminal kinases
kb	Kilo base pairs
KD	Kinase domain
LiCl	Lithium chloride
LKB1	Liver kinase B1
LPS	Lipopolysaccharide
LSM	Laser scanning confocal microscope
MAPK	Mitogen-activated protein kinase
µCT	Micro-computed tomography
mM	Millimolar
mRNA	Messenger RNA
MSC	Mesenchymal stem cells
mTOR	Mammalian target of rapamycin
NAC	N-acetyl cysteine
NaCl	Sodium chloride
NEB	Nuclear extraction buffer
NFLD	Non-alcoholic fatty liver disease
ng	Nano gram
NM	Normal media
NPH-insulin	Neutral protamine Hagedorn insulin
OCN	Osteocalcin

OD	Optical density
Opti-MEM	Optimum minimum essential medium
PBS	phosphate-buffered saline
PCR	polymerase chain reaction
PEPCK	Phosphoenolpyruvate carboxy kinase
PFK-2	phosphorylating 6-phosphofructokinase 2
PGC1-α	Peroxisome proliferator-activated receptor gamma coactivator 1-alpha
PI3K	Phosphatidylinositol-4,5-bisphosphate 3-kinase
PKA	Protein kinase A
PMSF	Phenyl methyl sulfonyl fluoride
PPAR	Peroxisome proliferator-activated receptor
RD	Repression domain
RIPA buffer	Radio immunoprecipitation assay
RNA	Ribonucleic acid
RT	Room temperature
RT-PCR	Real Time Polymerase chain reaction
RUNX2	Runt related transcription factor 2
SD	Standard deviation
SDS-PAGE	Sodium dodecyl sulfate polyacrylamide gel electrophoresis
SEM	Standard error of the mean
STZ	Streptozotocin
T2D	Type 2 diabetes
TAE	Tris base, acetic acid-EDTA
Tb. N	Trabecular number
Tb.Th	Trabecular thickness
TBS	Tris buffer saline
TE	Tris EDTA
TGF-β	Transforming growth factor beta
TNF-α	Tumor necrosis factor alpha
Tris-HCl	Tris hydrochloride
TZDs	Thiazolidinediones

ULK1	Unc-51 like autophagy activating kinase
VEGF	Vascular endothelial growth factor
WHO	World Health Organization
YAP1	Yes-associated protein 1
^{0}C	Degrees Celsius
µg	Microgram
µl	Microliter
µM	Micrometer

Chapter 1

Review of Literature

1.1. Introduction

1.1.1. Diabetes: a global problem

In the 21st century, diabetes is considered as largest health emergencies in the world. According to the world health organization (WHO), globally the chronic hyperglycemia is the third most cause of premature death after high blood pressure and tobacco usage [1]. Although the prevalence and incidence of diabetes is consistently associated with reduced life expectancy [2], and it is increasing in the US adults because of the burden of diabetes among youngsters, particularly the joint pandemics of metabolic disorders (obesity & diabetes) continue to progress in the United States and globally [3].

The recent ICMR–INDIAB study reports shows that increasing the prevalence of diabetes around the world and to a greater extent in India followed by China. This largest epidemiological study reveals that 62.4 million people living with diabetes and 77.2 million people are with pre-diabetes in India. Undoubtedly these numbers demonstrate that diabetes has become an epidemic in the 21st century where India is leading as a diabetic capital of the world with the largest number of subjects [4]. Every year the people living with diabetes is increasing, which further results in life-changing complications. In 2017 International diabetic federation reports estimated that about 425 million are currently having diabetes in the world and there are 327 million adults with impaired glucose tolerance and it is expected to increase by 2045 to 629 million with diabetes among them 438 adults, which makes them to prone more risk of developing diabetes (IDF-2017)[5](Figure.1).

To prevent diabetes, timely diagnosis may avoid or delay the longstanding secondary complications. The education/awareness is needed to a greater extent to improve the disease management and diagnosis. It is also required to embed the contemporary lifestyle changes that may minimize the rise in type 2 diabetes.

1.1.2. History

Diabetes mellitus is apparently one of the earliest disorders known to man. The Egyptians are first stated about diabetes in ~1500 B.C [6]. The ancient Indian surgeons named it as Madhumeha (sweet urine), later aretaeus the Cappadocian, who coined the term Diabetes (In Greek 'siphon') and theoretically quoted that "no essential part of the drink is absorbed by the body while great

Figure 1: Global picture of diabetes: Number of people with diabetes worldwide and per region in 2017 and 2045 (image modified from International diabetic federation (IDF)-2017)

masses of the flesh are liquefied into urine" [7]. The Latin word mellitus ("sweet like honey") was named by John Rollo in 17th century, to differentiate the diabetes mellitus to diabetes insipidus (tasteless).

For the past 2000 years it has been considered that "Diabetes is a deadly and devastating disease". Around the 17th century a physician Dr. Thomas Willis, was practiced to diagnose his patients by

observing their urine since elevated sugar levels observed in blood and urine[8]. This method of diagnosis of blood/urine glucose levels continued until 20th century.

1.2. Diabetes

Diabetes mellitus is apparently one of the earliest disorders known to man. The Egyptians are the first stated about diabetes which was about 3000 years ago [9]. In 19th century people distinguished the clinical features of Type1 and Type 2 diabetes mellitus. Generally Type 1 DM results from genetic factors and Type 2 causes from genetic, environmental and lifestyle (sedentary, alcoholics and physical inactivity) [10]. The uncontrolled diabetic patients are more prone to various other complications which frequently associated with death[11]. The late diagnosis of the disease onset is shown to be more frequent and dangerous in developing countries [12].

1.2.1. Type 1 and Type 2 Diabetes

Insulin-dependent diabetes mellitus (Type1) is caused by damage of β-cell mass thus leads to severe deficiency of insulin secretion having an incidence of about 15-18% among diabetes cases. The onset of Type1 diabetes mellitus is mostly starts at early age and which also associated with genetically susceptible individuals of autoimmune degradation of pancreatic β-islet cells [13].

Insulin independent diabetes mellitus (Type2) is associated with glucose intolerance, insulin resistance and obesity which accounts of 80-85% of diabetic population. T2D patients fail to respond to insulin and clinically manifested with hyperglycemia and hyperlipidemia. The onset of T2D disease is mostly during adult age[14].

1.2.2. Pathophysiology

The pathogenesis of diabetes is similar in both Type I and Type II diabetes. It is majorly categorized by insulin resistance [15], decreased insulin secretion and gradual loss of pancreatic β-cell mass [16]. This further principals to decrease glucose uptake of various tissues in the body such as liver, muscles, and adipose tissues [17] [18]. The increased free fatty acids in circulation is also observed along with high glucose [19] [20]. This is further been identified with α-cell dysfunction as a consequence of decreased α-cell function, the hepatic blood glucose and glucagon hormone levels are elevated during fasting and are not controlled by food intake[21, 22] [23]. The

glucose homeostasis is regulated majorly two hormones insulin and glucagon [24]. The insulin resistance mainly caused due to the elevated levels of serum free fatty acids by decreasing insulin induced glucose uptake and glycogen synthesis [25]. Recent findings suggested that increased accumulation of lipid in skeletal muscle associated with insulin insensitivity[25] [26] [27]. The low levels of insulin and enhanced insulin insensitivity results hyperglycemia [28]. The metabolic hormones called incretins are also essential in insulin secretion and regulation [29]. One among them is a small peptide hormone Glucagon like peptide harmone-1 (GLP-1), increases the insulin secretion in glucose dependent manner [30, 31]. Considering it's importance, researchers are exploring GLP-1 as a potential therapeutic target to enhance insulinotropic effects. The analogues of GLP-1 with enhanced half-life and Dipeptidyl peptidase IV(DPP-IV) inhibitors have revealed to be a promising potential to normalize blood glucose levels [32] [33] [34]. It also has been observed recently that the impaired mitochondrial functions in the course of type 2 diabetes [35] [36]. Mitochondrial induced ROS (Reactive oxygen species) are the main source to give rise obesity mediated diabetes[37]. However, mitochondrial dysfunction in differentiated adipocytes has been associated with impaired fatty acid oxidation and glucose metabolism [38] [39] [40]. Many reports indicate that the obese people are more prone to diabetes with increased adipose tissue [41]. The increased non-esterified fatty acids (NEFA) in the circulations are the major cause of insulin resistance in obese patients [42] [43].

1.3. Treatment & Medication

The recent advancements in biologicals and clinical research lead to develop high quality, slow and controlled release of insulin resulted in supply of uninterrupted insulin for type 1 diabetes patients. But the systematic rapid acting human insulin and longer acting NPH-insulin yet to reach everybody around the world. There are several medications are present in the market for type 2 diabetic patients with different molecular actions as described below (Figure 2).

1.3.1. Metformin

Metformin ($C_4H_{11}N_5$) is a free base and it is the most commonly used anti-diabetic drug. It mainly exerts functions through the AMPK activation through the phosphorylation of LKB1 at T172 [44]. It inhibits the hepatic blood glucose production, elevates the glucose uptake by phosphorylating AMPK followed by activation of GLUTs [45] [46] [47]. It also enhances insulin

sensitivity [48]. Metformin promotes fatty acid oxidation thus reduces the levels of free fatty acids in circulation [49] [49]. It has less frequency of hypoglycemic concerns in contrast with other known drugs such as sulfonylureas. The most common side effect of metformin is gastrointestinal irritation, lactic acidosis. However long term use is associated with kidney damage although it is limited to pre-symptomatic cases [50].

1.3.2. Thiazolidinediones (TZDs)

Thiazolidinediones are also known as glitazones which are containing heterocyclic compounds. These are the most effective drugs to reduce the blood glucose by increasing insulin sensitivity, eliminating the free fatty acid from the circulation by activating peroxisome proliferator-activated receptors (PPARs), a group of transcription factors [51]. The mainly used thiazolidinediones in the market is pioglitazone where as another one is rosiglitazone which was stopped using regularly due to its increased incidence of cardiovascular side effects and the increased risk of bone fractures with prolonged use [52]. However this drug can be used in selected older individuals since it is not accompanying with hypoglycemia [53].

1.3.3. Meglitinides

These are a class of glinides drugs which acts as inducer of ATP-dependent potassium channel in β-cells of pancreas followed by increase insulin secretion [54]. Currently there are two drugs in the markets rapaglinide and neteglinide which are non-sulfonylurea drugs. Meglitinides lower blood glucose in very short duration (5 hrs.). The major limitation of Meglitinides increases the possibility of hypoglycemia in predialysis stage 5 diabetic nephropathy patients. As nephropathy itself increases the risk of hypoglycemia, recent outcomes furthermore recommend nephropathy patients taking short-acting meglitinides. Thus, parallel administration of meglitinide and insulin will increase the threat of hypoglycemia [55].

1.3.4. Sulfonylureas

These are the wide-range of well accepted drugs but they induce insulin secretion. Because of the endogenous insulin secretion, aged individuals with diabetes who are on sulfonylureas has enhanced risk (36%) of hypoglycemia. The major risk factors of sulfonylureas are hypoglycemia and kidney malfunctions. The long acting medication such as glyburide are avoided in old age patients whereas, short acting sulfonylureas (glipizide) are preferred [56].

1.3.5. Incretin based therapies

Incretins are the small peptide hormones such as glucose dependent insulinotropic polypeptides (GIP) and Glucagon like peptide 1 (GLP-1) which are secreted from gastrointestinal cells are shown to enhance the insulin secretion. They exist in the market with the name of Exenatide and Liraglutide. These incretin analogues does not show hypoglycemia, and many recent evidences suggest GLP-1 analogues reduces the liver metabolism inflammation and cardiovascular diseases [29].

1.3.6. Dipeptidyl-peptidase IV inhibitors

Dipeptidyl-peptidase IV is a ubiquitous enzyme that deactivates incretins (GLP-1 and GIP). The inhibitors of DPP-IV are an emerging class of anti-diabetic drugs due to their enhanced action of incretin's half-life. Thus these drugs are prescribed in combination with metformin, TZDs and insulin to increase glucose tolerance. These drugs show low risk to hypoglycemia [57].

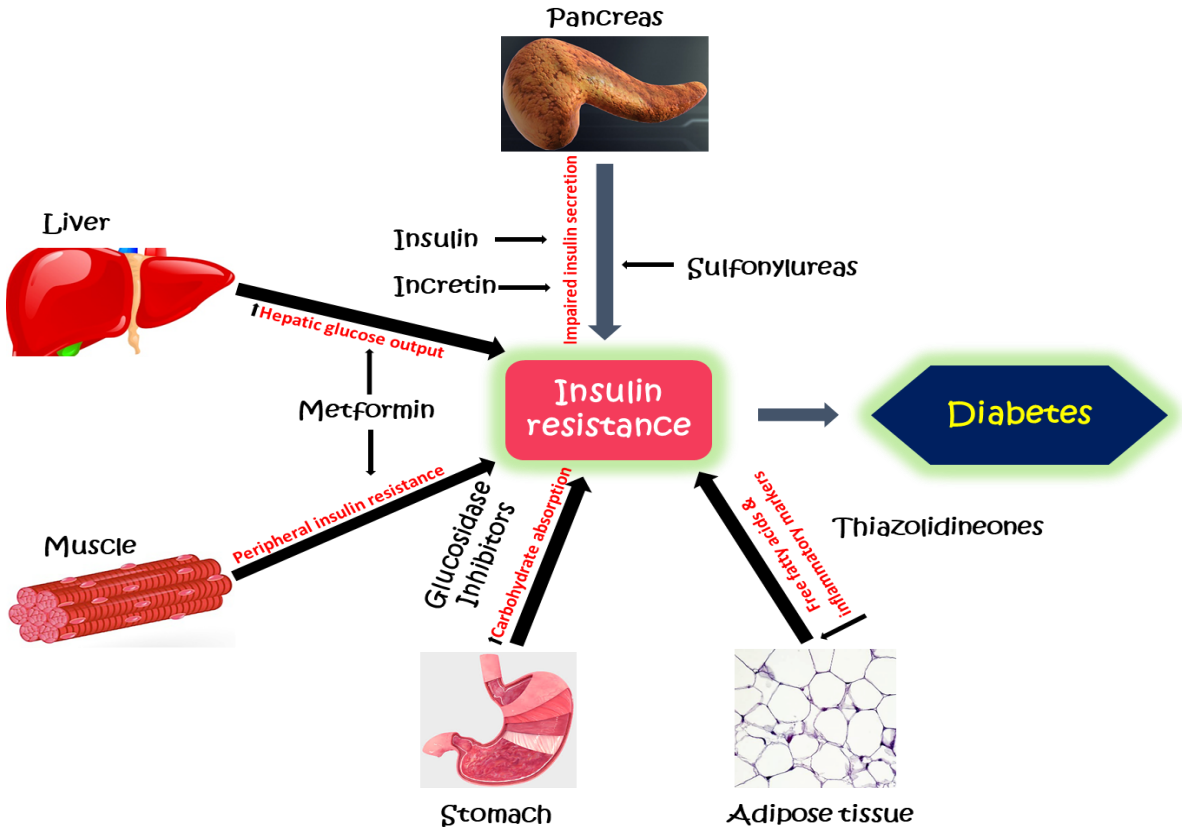

Figure 2: Anti-diabetic drugs and their mechanisms of action (image modified from http://wawvoid.com)

1.3.7. Insulin

Insulin an anabolic hormone secreted by pancreatic β-cells into the circulation. In diabetes mellitus the pancreatic β-cells exhaustion take place thus lowers the circulating levels of insulin and further glucose absorption. There are three types of insulin forms are available in the market, short acting, intermediate acting and long acting which provides effective levels of insulin to maintain glucose homeostasis [58].

1.4. Diabetic complications

Diabetes mellitus is a complex group of metabolic disorders and it is associated with the primary characteristic of chronic hyperglycemia. The Long term persistence hyperglycemia is the root cause for many micro as well as macrovascular complications, such as, nephropathy (renal failure) [59], neuropathy (nerve damage) [60], retinopathy (blindness) [61], diabetes accelerated cardiomyopathy (myocardial infractions) [62], osteoporosis (fragile bones) [63] and limb amputations (gangrene) [64]. These complications are equally reported in both type 1 and type 2 diabetes. The epidemiological reports reveals that the severity of the diabetes and its complications depends on age, ethnicity, gender, etc. Insulin deficiency also reduces the $Na^{+}K^{+}$- ATPase activity leads to obesity. Hyperglycemia induced glycation of proteins such as glycosylated hemoglobin and albumin and lipids produce various advanced glycation end products (AGEs) which results in chronic kidney diseases, arthritis and alzimers disease etc. [65]. In the diabetic patients the elevated level of HbA1c is associated with inflammation [66]. There some other long-lasting diabetic complications incorporates with depression, dementia and sexual inability [67].

1.4.1. Neuropathy

Neuropathy is one of the frequently reported complication in both types (Type I & II) diabetes patients. About 50-60% of diabetic patients develop neurological complications over the course of their disease. This disease is leading to substantial morbidity, depression, ulceration and limb amputations. The diabetic neuropathy is clinically characterized as axonopathy, which affects longest axons which are present in the feet: most often affect the knee and fingers. The mechanisms that cause diabetic neuropathy are complex. Biochemically the glucose intolerance is primarily associated with the disease development. The glycosylated hemoglobin is positively correlates with the intensity of neuropathy. The deregulated glucose uptake was more common in

neurons than endothelial cells which further leading to glucose mediated injury of diabetic neurons [60].

1.4.2. Nephropathy

Nephropathy is another leading cause of extensive morbidity and mortality associated with diabetes. As mentioned the long-term persistence of chronic hyperglycemia is the major risk factor for vascular complications, whereas, the patients who are on continues glycemic control reduced risk of complications. It is majorly characterized by proteinuria, hypertrophy and hypertension and uremic manifestations [59]. The histological observations shows renal fibrosis in patients that is due to increased extracellular matrix (ECM) proteins. Metabolic stress (oxidative stress, ER stress, AGE and TGF-β) is one of the reasons responsible for progression of diabetic nephropathy [68]. It has been reported that the risk of cerebral hemorrhage in severe nephropathic patients. Macroalbunuria causes high risk of cardiovascular diseases [69]. It has been identified that podocyte dysfunction is associated with glomerular hypertrophy and glomerulosclerosis, whereas the podocyte hypertrophy is associated with hyperglycemia mediated through angiotensin [70]. There are several signaling pathways for instance Wnt, JAK/STAT, P38 MAPK, PI3K/Akt, and TGF-β/Smad signaling are extensively studied and seen deregulated in diabetic nephropathy [71].

1.4.3. Retinopathy

Diabetic retinopathy is one of the major cause of blindness and is more prevalent in developed countries. Disease manifestations are mainly observed in aged patients. It is an alarming challenge to improve the quality of life. The major cause of diabetic retinopathy is retinal ischemia and capillary non-perfusion. The major known mechanisms that leads to diabetic retinopathy is by microangiopathy due to platelet derived growth factor, VEGF, IGF-1 and angiopoietin. In the clinical scenario the neurodegeneration is a primary manifestation of retinopathy. The chronic hyperglycemia, hypertension and dyslipidemia play substantial role in disease advancement. The standard diagnosis is eye examination and funduscopy. The systemic glycemic control and other factors such as lipids and blood pressure is required to prevent the development of retinopathy. The retinopathy affects neuronal glial cells, and vascular endothelial cells in response to hyperglycemia [72]. The loss of glial cells is associated with the detrimental effects on blood retinal barrier. The loss of blood vessels lead to ischemia and hypoxia. The retinopathy is also allied with, AGEs oxidative stress and inflammation [61, 68].

1.4.4. Bone adipogenesis

Bone marrow mesenchymal stem cells maintain bone homeostasis in healthy adults. Recently it has been established that the inverse relation between adipose and bone tissues in deregulated conditions [73]. For instance it has been observed bone resorption and osteoporosis during aging, steroidal intake, post menopause women [74] and Cushing's syndrome correlate with redistribution and deposition of adipocytes [75]. One major elucidation has been put front to clarify this the reciprocal relationship between osteocytes and adipocyte balance primary occurs in bone marrow by reprogramming of bone marrow stem cells in the direction of adipocytes rather osteocytes[73]. It has been reported that age induced progression of adipogenesis while inhibiting the osteogenesis in mice[76]. However, the signaling events at molecular level are not known clearly. Metabolic disorders such as diabetes and obesity are the highly wide spread disease in which bone adipogenesis is the major compliant. It is also evident that fragile bones are reported as diabetes induced secondary complications[77]. Recent *in vitro* studies shows that the incubation of bone marrow mesenchymal stem cells with serum of obese patients induces adipocyte differentiation and inhibits osteocytes [78]. High fat diet induced mice models reported to inhibit osteogenesis (bone resorption) with enhanced bone adipogenesis was observed [79]. Understanding the molecular mechanisms especially the deregulated pathways during chronic hyperglycemia is imperative.

1.5. Mesenchymal stem cell differentiation in diabetes

Mesenchymal stem cells are the self-renewing multipotent stromal stem cells, hold the maximum capacity to differentiate to various key lineages. MSCs can be differentiated into non-hematopoietic cell lineages such as osteocytes, adipocytes, chondrocytes, myocytes and neuronal differentiation. MSCs were first derived from bone marrow, later can be seen in various MSC originated tissues (skeletal muscles and fat depots, etc.). In the current era of medicine MSCs are explored actively in regenerative medicine because of their high differentiation potential, efficiency, and acceptance. Adult bone marrow mesenchymal stem cells majorly differentiate into adipocytes and osteocytes and the plasticity between these two cell types has been established over decades. In metabolic disorders the pathological local microenvironment may contribute to the fate of MSCs commitment towards adipocytes over osteocytes [80] [73] [81] (Figure 3).

Majorly MSCs are isolated from bone marrow tissues whereas off late adipose tissue become as an attractive source of MSC in regenerative medicine. MSCs can be differentiated by induction into specific cell types by shifting the gene expression of MSC towards that specific lineage. In adipogenesis, it is considered to be a two phase differentiation, the initial determination (preadipocytes) and terminal differentiation (adipocytes) with a stringent differentiation process regulated by complex signaling events converging at PPARγ transcriptional regulation[73].

Another face of MSCs is differentiation towards osteocytes for the formation of bone tissues. Similar to adipogenesis, the osteocyte differentiation initially commits to pre-osteocytes and eventually progress towards mature osteoblast and terminally osteocytes [73]. The MSCs commitment towards osteocyte primarily regulated by transcription factor Runt related transcription factor (RUNX2), however, there are reports that RUNX2 alone is not enough for complete osteocyte differentiation [82](Figure 4). So far all the identified signaling pathways regulating adipogenesis and osteogenesis signaling transductions intersect at the two important key transcription factors PPARγ (adipogenic) and RUNX2 (Osteogenic).

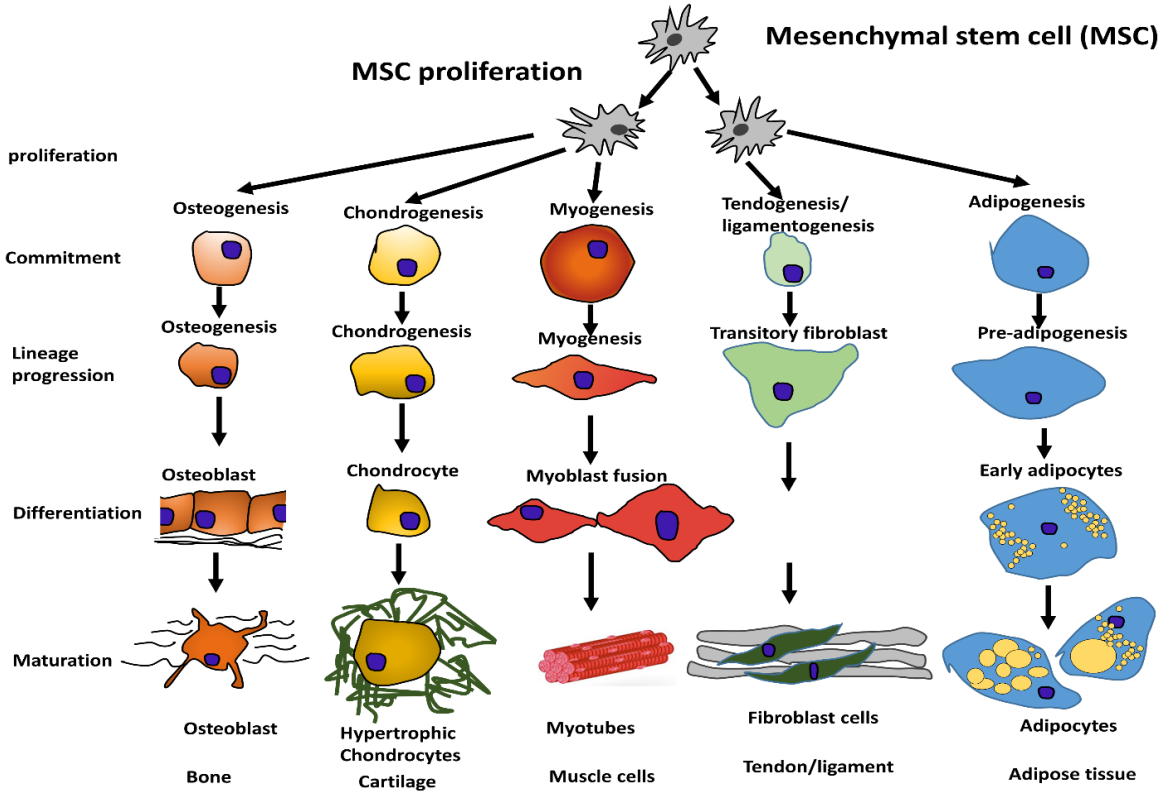

Figure 3: Mesenchymal stem cell (MSC) differentiation: MSCs are multipotent cells can differentiate into variety of cell lineages. The end-stage cell types are dependent on external cues. (Image modified from Arnold I. Caplan and Scott P. Bruder, 2001.)

In association with these transcription factors, CCAAT/enhancer-binding family of proteins (C/EBP) and Osterix are two important cofactors that play an auxiliary roles dealing with adipogenic and osteogenic events respectively [73]. However the process of adipogenesis at the cost of osteogenic phenotype during metabolic stress is still intriguing. Our study mainly focuses on the mechanistic events of MSCs differentiation in pathophysiological conditions especially under metabolic stress and diabetes.

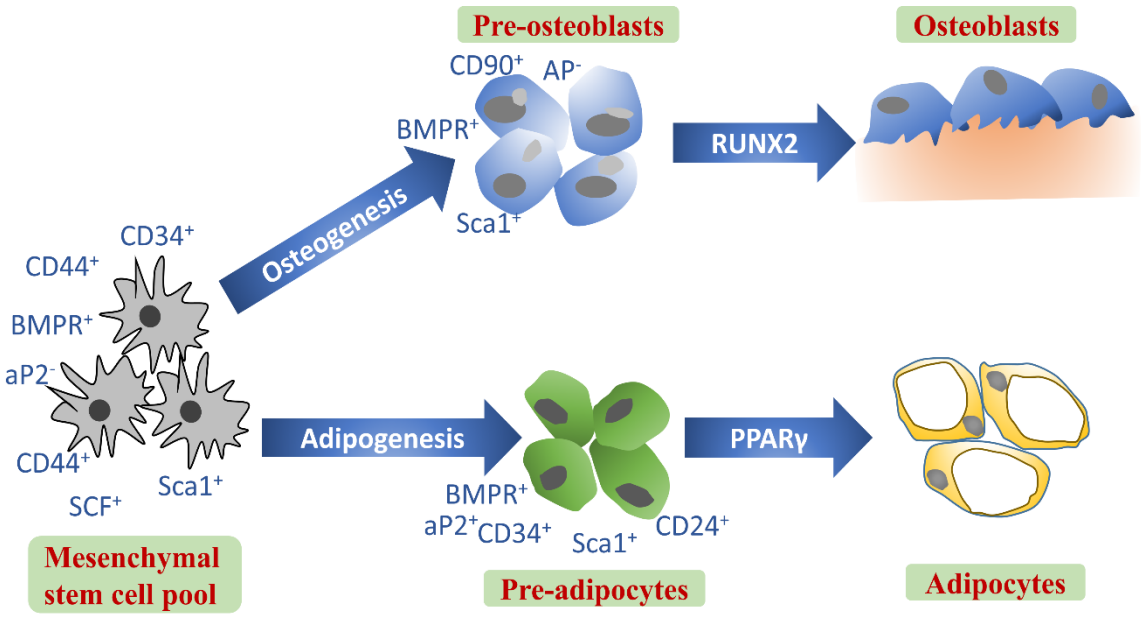

Figure 4: The balanced differentiation of adipocytes and osteoblasts: Mesenchymal stem cells differentiate into adipocyte or bone forming osteoblasts. This process is tightly regulated by transcription factors such as RUNX2 (osteoblasts) and PPARγ (adipocytes). (Image modified from Yen K Luu et. al. 2009)

1.5.1. Peroxisome proliferator-activated receptor gamma (PPARγ)

PPARγ is a class of transcription factor, known to regulate the adipogenesis, fatty acid metabolism and transport. PPARγ transcriptionally regulate adipogenic genes such as fatty acid transport protein, aP2, acetyl CoA carboxylase and lipoprotein lipase thus it is essential for the differentiation of pre-adipocytes to adipocytes (adipocyte maturation) [83]. Lacking PPARγ in embryonic stem cell fail to differentiate adipocytes reveals its involvement in adipogenesis. The genetic deletion studies of PPARγ in mice are shown to be embryonic lethal [84]. The agonist of PPARγ is associated with increased insulin sensitivity [85]. In contrast to these studies the heterozygous deletion of PPARγ is survived and are less susceptible to insulin resistance even on

high fat diet [86]. The overall functions of PPARγ is associated with glucose uptake and free fatty acid absorption and followed by conversion of triglycerides [87].

1.5.2. Runx family proteins

Runt DNA binding domain containing proteins are known to be as RUNX family proteins. RUNX family proteins are initially shown to be transcription factors involved in both transcriptional activation and repression. These transcription factors regulates gene expression of large number of genes by interacting with promoters and enhancers. It has been reported that Core binding factor β (CBFβ) heterodimerizes with RUNX family proteins and regulate the transcription activation and repression by interacting with promoters and enhancers [88].

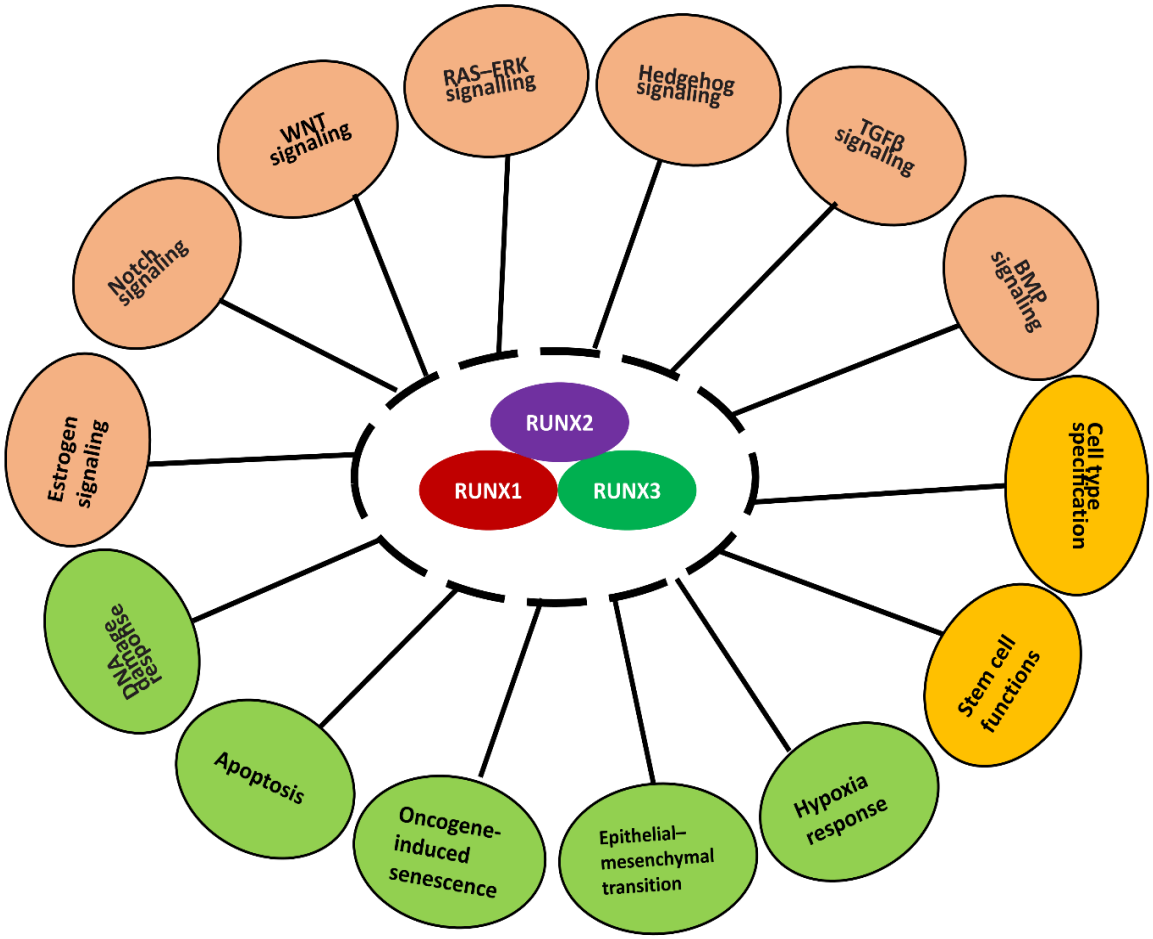

Figure 5: RUNX family transcription factors regulated by various signaling pathways.
(Image modified from Yoshiaki Ito et. al. 2015)

RUNX family proteins regulates divergent physiological processes which involved in lineage specific cellular differentiation, division, and apoptosis. RUNX genes were first identified in *Drosophila Melanogaster* located in chromosome 8adobe; 21 which known as *Runt* gene involved in segmentation during development [89]. In mammals RUNX family comprises three members of proteins such as RUNX1, RUNX2 and RUNX3. These are conserved across the evolution in both simple as well as complex organisms.

These genes observed to be differential tissue specific expression. The functions of these transcription factors regulated by various signaling pathways such as WNT, RAS-ERK, BMP, estrogen, Notch, MST-YAP1 and Hedgehog signaling etc. [90], (Figure 5)

1.5.3. RUNX2: Osteogenic transcription factor

RUNX2 is one of the three RUNX family proteins, which shares the common domain containing 128 amino acids sequence and it is homologues to Drosophila runt gene which is involved in

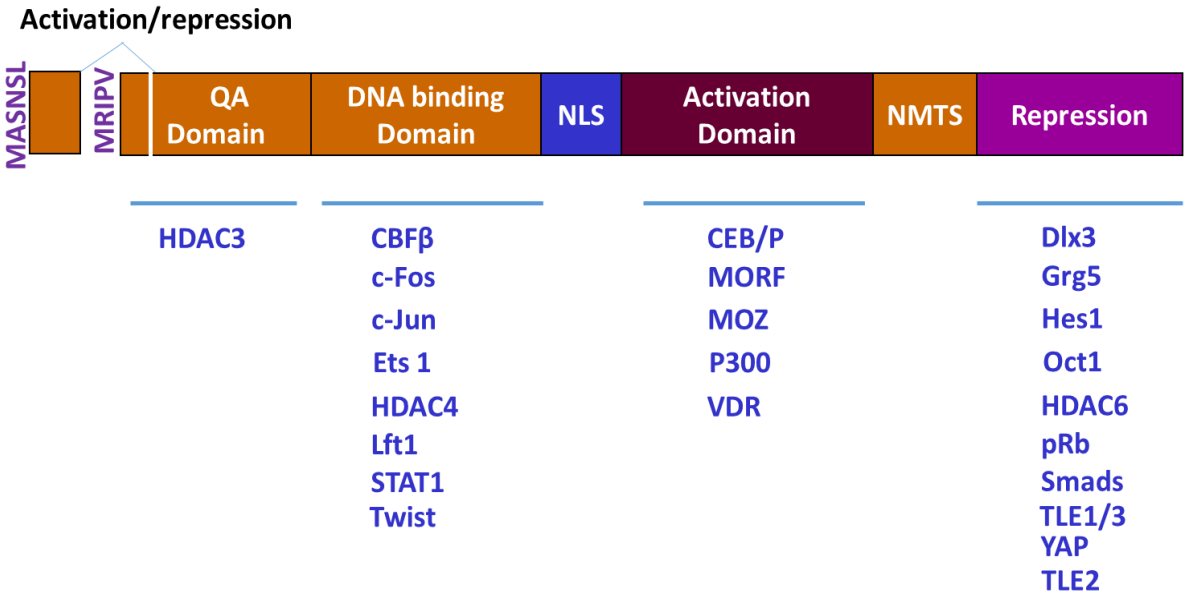

Figure 6: RUNX2 protein structure and its domains: Functional activities of RUNX2 domains are shown at the top of the figure. Alternative N-termini (MASNS and MRIPV) are generated from two promoters. Interaction domains for proteins listed below. (Image modified from Tania M. Schroeder et. al. 2005)

proper segmentation during development[89, 91]. RUNX2 is a transcription factor and interacts with a specific DNA motif 5'-PuACCPuCA-3', or its complement, 5'-TGPyGGTPy-3' [92] [93] RUNX2 involved in cell fate commitment of mesenchymal differentiation towards osteoblast cells, chondrocyte maturation and vascular invasions during skeletal development [94]. The

RUNX2 levels are tightly regulated during osteoblast lineage specification during development. Hence it also said as osteogenic factor.

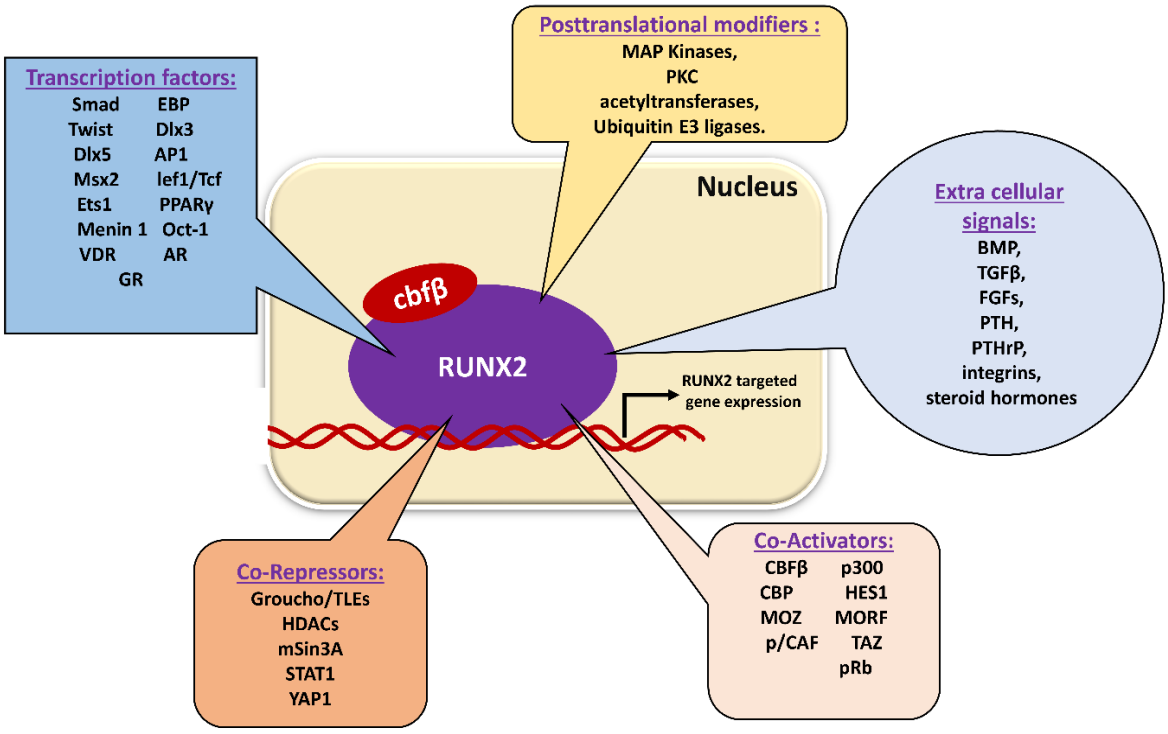

Figure 7: RUNX2 is a regulatory center for gene expression: RUNX2 interacts with specific DNA sequence to regulate gene expression. Localized in the nuclear matrix. RUNX2 interacts with CBFβ. The interacting partners are classified as corepressors, coactivators, or transcription factors. RUNX2 regulated by various extracellular signals and its posttranslational modifications. (Image modified from Tania M. Schroeder et. al. 2005)

1.5.4. Structure and functions

The RUNX2 gene has two alternative promoters which can encodes multiple functional mRNA with alternative splicing possibly can give rise to at least 12 different transcripts [95] [96]. However, there are only two RUNX2 distinct isoforms, Type I and Type II corresponds to two different promoters P2 (proximal) and P1 (distal) respectively. RUNX2 Type I isoform with 513 amino acids initiates with MRIPV motif, which is mostly observed in non-osteoblast mesenchymal and chondrocyte cells. Whereas, Type II RUNX2 Isoform starts with MASNSL motif with 528 amino acids was distinctly observed in mesenchymal stem cells and osteoblast cells [97] [98].

RUNX2 is a critical regulator of skeletal development and mutations in RUNX2 causes cleidocranial dysplasia (CCD). RUNX2 also predominantly expressed in chondrocytes [99] [100]. RUNX2 has various domains Such as DNA Binding Domain (DBD), QA domain (glutamine and alanine rich domain), Nuclear localization signal sequence (NLS) [93] [101], Nuclear matrix targeting signal (NMTS) and activation as well as repression domain (AD&RD) followed by

VWRPY region [95, 102]. Reports shows that the functional attributes of RUNX2 is mainly contributed by the highly conserved DNA binding domain (128 amino acids) [103]. RUNX2 also interacts with various proteins to exert its functions such as cbfβ. The interaction with cbfβ enhances its DNA binding affinity by promoting structural conformations which unfolds the DNA binding surface. Cbfβ also involved in protection of RUNX2 from ubiquitin mediated proteosomal degradation [104]. Thus the reports shows that Cbfβ plays a crucial role in osteoblast differentiation [105] [106] [107].

RUNX2 comprise activation and repression domains which is crucial for its transcriptional activation as well as repression. The activation domain of RUNX2 rich in proline, serine and threonine (PST) and it is primarily essential to interacts with its transcriptional co-activator proteins (p300, Hes1, MORF, MOZ and TAZ) and co-repressors (Groucho/TLE, HDACs, mSin3A, Stat1 and YAP1)(Figure 6). RUNX2 predominantly regulated by five different signaling pathways (Notch, BMP/TGFβ, FGF/EGF, Wnt and Hedgehog). These signaling pathways regulate RUNX2 functional activities through the activation of upstream signaling intermediators that posttranslationally modifies RUNX2 that affects the interaction with co-activators or co-repressors which regulate the RUNX2 transcriptional activity either positively or negatively [93](Figure 7).

1.5.5. RUNX2 in diabetes

In humans Type I & Type II diabetes is associated with skeletal disorders with decreased bone mass and delayed fracture healing was observed. Many reports shows that the diabetic patients has reduced bone formation by decreased osteoblast formation and simultaneously can increase osteoclast formation in contrast with normal individuals. It is clearly known that the detrimental effect of bone is accompanying with diabetes induced micro and macro vascular complications in association with chronic hyperglycemia[108]. RUNX2 promoter polymorphism is allied with high serum triglycerides[109]. Many recent studies in Streptozotocin induced diabetic mouse and rat models has extensively demonstrated the reduction of bone mass and decreased bone formation was restored by insulin supplement [110]. Different mechanisms have been proposed for decreased osteoblast activity in diabetic patients such as reduced IGF-1 expression or basic fibroblast growth factor [111]. Many questions concerning the molecular mechanisms of diabetes induced bone loss is remained to be unanswered.

For the first time Lu H et al., shows that the diabetic individuals produce adequate number of immature mesenchymal stem cells but they fails to differentiate towards osteoblast lineage by

reducing the osteoblast specific gene expression such as RUNX2, Dlx5, osteocalcin and collagen type I which in turn may lead to skeletal abnormalities [111]. Cheng SL et al shows that Msx2 regulates the osteogenesis vs adipogenesis in myofibroblasts and Msx2 induces the osteogenesis over the adipogenesis in synergy with BMP2 signaling [112]. Rzonca SO et al & Benvenuti S et al., seminal observation that rosiglitazone which is a FDA approved antidiabetic drug drive the mesenchymal stem cells towards adipocytes (by PPAR γ2, AP2, fatty acid binding protein upregulation) and inhibit the osteogenesis through the decreased expression of RUNX2, Dlx5 and alpha (1) collagen, integrin binding sialoprotein, Phex, metalloproteinase-9, Akp2, Dmp1, Col1a2, Vdr, and osterix, and osteocalcin in human mesenchymal stem cells [113, 114] [115]. In contrast metformin and Liraglutide (GLP-1 receptor agonists) increase bone formation by positively regulating osteogenic transcription factor RUNX2 through AMPK/USF-1/SHP pathway [116]. Botolin S et al showed increased bone adipogenesis is associated with elevated expression of PPARγ but the RNA of RUNX2 was not affected whereas, inhibition of PPARγ reduces the bone adiposity but not the bone loss in Streptozotocin induced type1 diabetic mice models [117]. Intriguingly Irwin R et al showed that decreased insulin receptor mediated signaling is not responsible in skeletal bone mass in type 1 diabetes [118].

Hyperinsulunemia also promotes BMP-2 induced osteogenic differentiation of ligament cells [119]. High glucose downregulates RUNX2 DNA binding activity mediated through the aldose reductase polyol pathway whereas, euglycemia supports RUNX2 transcriptional activity and promotes endothelial cell migration [120]. The anti-diabetic drug Metformin promotes the osteogenesis, which might be through the RUNX2/cbfa1and AMPK activation in bone marrow progenitor cells BMPCs [121]. Dose dependent glucose treatment down regulation of RUNX2 is reversed by metformin treatment at all glucose concentrations [122]. Hyperglycemia also promotes the adipogenesis and inhibits osteogenic differentiation through the activation of ERK/PKA/cAMP signaling in osteosarcoma cells (MG-63) [123]. Proinflamatory cytokine TNF-α also induces RUNX2 expression and promotes vascular calcification in vascular smooth muscle cells (VSMCs) [124]. Jang WG et al., demonstrated that metformin may induces the bone formation by increasing the transcriptional activity of RUNX2 through the AMPK/USF-1/SHP mediated pathway in MC3T3E1 cells [125]. Glucose intolerance is frequently associated with deregulation of insulin signaling network whereas Adhami M., showed that RUNX2 controls the gene network associated with glucose and energy metabolism in 3T3-L1 cells[126]. High glucose induced chronic inflammation down regulates RUNX2 expression which further leads to bone

resorption [127]. A study shows that high glucose induced reactive oxygen species inhibit the osteogenesis and induce the adipogenesis through PI3K/Akt pathway whereas, inhibition of ROS by N-acetyl cysteine (NAC) reversed the adipogenic phenotype[128]. Dong X et al identified that free fatty acids (FFA) released by adipocytes induced lipotoxicity affect the bone metabolism [129]. The diabetic patients serum factors affect osteoblast differentiation (e.g. TGF-β) [130]. Several studies also shows the over expression of RUNX2 mice severely develop arterial medial calcifications (AMC) which is another hallmark of diabetes, chronic kidney diseases [131]. The *in vitro* administration of vitamins K2 and D3 combination show promoting the bone formation by elevating anabolic bone markers (RUNX2, Dlx5, ATF4, OSX) [132]. High fat diet(HFD) and high-sucrose diet (HSD) reduce the bone markers genes (RUNX2, BMP2, ALP and OCN) and decreased bone mineral density was observed [133]. High glucose induced endoplasmic reticulum stress down regulates RUNX2 expression. The different osteoporosis models (ovariectomy, type 1 diabetes, excessive glucocorticoids and orchiectomy) provide a strong evidences that the mesenchymal progenitors differentiate adipocytes over osteoblast by down regulating RUNX2 and up regulating PPARγ in Bone marrow stromal cells (BMSCs) [134]. RUNX2 and PPARγ reciprocally regulated by Protein phosphatase (PP5) in mesenchymal stem cells [135]. The diabetes induced down regulation of bone mineral density is restored by AMPK activator Metformin by AMPK independent and dependent mechanisms [136]. Chronic leptin treatment also regulates the RUNX2 expression via the Akt and ERK dependent manner in human valualar intestitial cells (hVICs) [137].

1.5.6. AMP-activated serine/threonine protein kinase (AMPK)

AMP-activated serine/threonine protein kinase (AMPK) is a vital energy sensor of the cell, regulates the cellular energy homeostasis. AMPK is highly conserved across the evolution and express ubiquitously all over the body. AMPK a heterotrimeric protein complex, has three subunits α, β, and γ. The N-terminal of α-subunit consists Kinase domain (KD) and C-terminal consist regulatory region. The β-subunit is essential for the formation of structural scaffold between α and γ subunits and it also had a carbohydrate binding domain. The γ subunit is essential for nucleotide binding activity. The α-subunit has two isoforms and β and γ have two and three respectively. The AMPK is activated by phosphorylating at T172 α-subunit of kinase domain. It has been identified that AMPK is regulated by two upstream kinases, Calcium/calmodulin-dependent protein kinase kinase (CaMKK) b and LKB1 in the cascade. Metabolic stress activates

the AMPK by sensing AMP/ATP and AMP/ADP ratio. AMPK is activated in three phase mechanism 1) interaction increased AMP levels with γ-subunit of AMPK which further promote the phosphorylation of T172 Kinase domain of α-Subunit. 2) Interaction of AMP to γ-subunit of AMPK induce specific conformational changes to protect T172 phosphorylation from phosphatases 3) AMP interaction with γ-subunit induces 10 fold allosteric activation whereas ATP inhibits all these conformational changes of AMPK. Activated AMPK stimulate catalytic activity to synthesize ATP to restore the cellular energy requirements. Activated AMPK inhibits anabolic pathways and promote catabolic pathways. The AMPK regulate a wide array of metabolic processes such as glucose Uptake, mitochondrial biogenesis, fatty acid oxidation, protein synthesis and autophagy and also inhibits the fatty acid synthesis, cholesterol biosynthesis, and protein synthesis [138, 139]. MPK controls the glucose uptake by translocating GLUT4 to plasma membrane [140]. AMPK positively regulates mitochondrial biogenesis through the phosphorylation of PGC1α [141]. AMPK can also trigger the autophagy by phosphorylating ULK1[142] (Figure 8).

1.5.7. AMPK deregulation in metabolic disorders

The regulation of AMPK draw enormous attention in the study of metabolic disorders [143]. The dysregulation of AMPK play a critical role in diabetes induced pathogenesis, insulin insensitivity in humans and rodent animal models. The various animal models diabetic and obesity reported to exhibit decreased AMPK activity in liver, adipose tissue and skeletal muscle [144]. Hyperglycemia and hyperlipidemia plays a vital role in progression of diabetes and obesity. High hepatic glucose production, insulin resistance and deregulated lipid metabolism was seen in in the liver of diabetes or obesity and atherosclerosis patients [145]. Many recent studies shows loss of AMPK activity in type II diabetes resulted in deregulated white adipose tissue and brown adipose tissue metabolism thus causes insulin resistance in humans and rodent animal models [146] [147] [148, 149] [150, 151]. AMPK activation inhibits insulin resistance by activating PI3K or by negative feedback mechanisms of IRS1 through the downregulation of mTOR/S6K activity [152]. AMPK is abundantly expressed in kidney and it is also demonstrated that AMPK is involved in physiological functions such as ion transport. Recent reports shows reduced AMPK activity in various rodent animal models including *fa/fa* (leptin receptor knockout) rats*, ob/ob* (leptin knockout) mice [153] and Interlukin-6 knockout mice [154], streptozotocin induced diabetic mice models, indicate

decrease AMPK activity associated with metabolic disorders. Regulation of AMPK mediated phosphorylation of AS160 and TBC1D1 is essential for interaction with 14-3-3, which further regulates GLUT4 vesicle recycling and translocation which further enhances glucose uptake [155]. Exercise induced activation of AMPK regulates the insulin sensitivity through the phosphorylation of IRS1 (Ser-789). The chronic AMPK activation by AICAR shown to be transcriptionally regulate GLUT4 and Hexokinase II (HK II) in skeletal muscle cells. AMPK increase the glycolysis by phosphorylating 6-phosphofructokinase 2(PFK-2) in heart tissues [156]. In response to chronic hyperglycemia the AMPK down regulate the rate limiting gluconeogenic enzymes such as PEPCK, Pyruvate kinase and glucose 6 phosphatase. Osteoporosis of osteopenia are the most prevalent

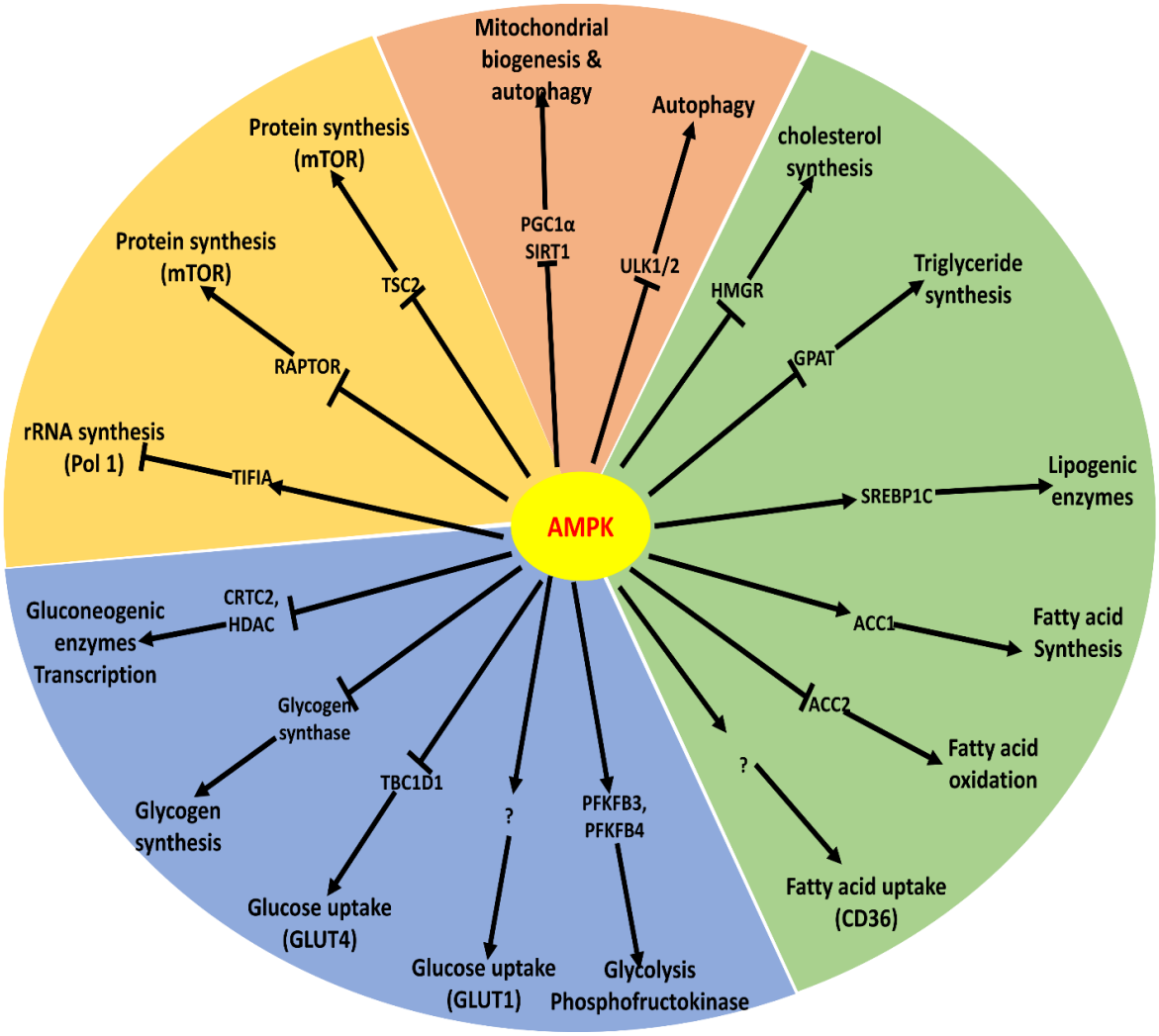

Figure 8: AMPK activation on various metabolic events: The proteins that are mediate various metabolic effects of AMP-activated protein kinase (AMPK), as well as the final metabolic outcomes, are depicted. Catabolic pathways (GLUT4, GLUT1, PFKFB3, PFKFB4, CD36 PGC1α, SIRT1, ULK1/2 and ACC2) are activated by AMPK. Anabolic pathways ACC1, SREBP1C, GPAT, HMGR, CRTC2, HDACs, RAPTOR, TIFIA, TSC2 and Glycogen synthase are inhibited by AMPK. (Image modified from D. Grahame Hardie et, al. 2012)

diabetic complication with increased risk of fractures in type 1 and type 2 diabetic individuals [157] [158] [159]. Xi et al demonstrated that AMPK activation is essential for the pro-osteogenic effect of IGF-1 during osteogenesis [160]. Metformin shows pro osteogenic effect through AMPK and RUNX2 activation in bone marrow progenitor cells (BMPCs) [121]. These evidences considered bone metabolism is closely associated with glucose metabolism. Very few recent studies shows that AMPK activation may induce the bone formation, but there are gaps in understanding the intricate molecular mechanisms connecting bone metabolism vs glucose metabolism.

Since the strategies that modulate AMPK activity are chosen for the prevention and management of metabolic disorders, the regular physical activity was shown to be activate AMPK. Certain evidences shows that the diseases associated with metabolic disorders (e.g. diabetes, obesity, hypertension, atherosclerosis, CVD and few cancers) are shown to be less progressed in physically active people by correlating with insulin action. These findings may suggest that AMPK might be a potential metabolic target to study for the improved therapies in diabetes and its associated complications.

Objectives

RUNX2 (Osf2/Cbfa1, AML3 or Pebp2αA) is a transcription factor which has a pivotal role in regulation of cartilage and osteoblastic differentiation. Loss of bone mass in RUNX2-/- mice associated with decreased mature osteoblast. It has been shown that RUNX2 and osteoblast specific gene expression is down regulated in diabetic patients as well as in animal models. Although it is known that specific transcription factors (RUNX2 & PPARγ) are important in mesenchymal fate determination, however, the mechanisms that lead to deregulation of RUNX2 is not yet clear. In the current study, we explored to understand some of these mechanisms by formulating the following objectives.

- Identifying the novel upstream regulators of RUNX2 by *in silico* analysis.
- Characterization and demonstration of physiological significance of putative post translational modifications of RUNX2 by cellular differentiation and transdifferentiation models and diabetic-induced bone adipogenesis mouse model.

Materials and Methods

2.1. Materials and methods

2.1.1. *In silico* analysis

AMPK-dependent phosphorylation prediction was done with PhosphoMotif Finder (http://www.hprd.org/PhosphoMotif_finder/), and its prediction efficiency was measured by NetPhos 3.1 tool (http://www.cbs.dtu.dk/services/NetPhos/) by following the instructions provided. RUNX2 protein sequence alignments were done by ClustalW2 (http://www.ebi.ac.uk/Tools/clustalw2/index.html). All the sequences were taken from NCBI from human data base and numbering also corresponds to human RUNX2 (NM_001024630.3).

2.1.2. Cell culture and reagents

The multipotent murine mesenchymal stem cells (C3H10T1/2), murine 3T3-L1 pre-adipocytes, murine skeletal muscle cells (C2C12) and Human Embryonic Kidney (HEK) cells were procured from American Type Culture Collection (ATCC, Manassas, VA, USA). All the cells were maintained in DMEM except C3H10T1/2 in MEM supplemented with 10% FBS and 50 U/ml penicillin and 50 mg/ml streptomycin. The C3H10T1/2 cells were maintained in α-MEM supplemented with 10% FBS 50 U/ml penicillin and 50 mg/ml streptomycin. Cultures were maintained in a humidified chamber at 37°C and 5% CO_2, and the culture medium was replaced every 2–3 days. AMPK activators (Metformin), AICAR and inhibitors (Compound C) were procured from Sigma, USA. All the cell culture reagents were obtained from Invitrogen, USA, unless mentioned otherwise.

2.1.3. Bone marrow derived mesenchymal stem cells (BM-MSC) isolation

BALB/c male mice (6-8 weeks) was sacrificed by cervical dislocation and the whole mice were wiped with 70% ethanol for 5 minutes. BM-MSCs were isolated as described earlier[161]. In brief, the fore limbs and hind limbs were dissected at the ankle and carpel joints before removing the soft tissues associated with tibias and femur. The ends of marrow cavity was excised followed by flushing with 5ml of IMEM medium using 23G needle. For culturing BM-MSCs, the collected cells were rinsed IMEM contains 1X antibiotics before plating in 100mm tissue culture dish and incubated in 37^0c and in 5% CO_2 for 5 days. The culture medium was replaced every 72 hours. The cultures were passaged (0.25% trypsin for 2 min) after reaching the 70-80% confluence. After

the third passage the cells were characterized by FACS analysis by staining with CD44, CD90 (positive MSC markers) and CD45 (negative MSC Marker) (Abcam, Cambridge, MA) (Figure S1). Well characterized BM-MSCs were used for all experiments. RNA and protein expression analysis on bone marrow flush cells in normal, diabetic and metformin treated mice, the collected cells were directly subjected for Trizol or RIPA lysis respectively.

2.1.4. Plasmids

Full length RUNX2 cDNA (NM_001024630.3) was commercially obtained from Genecopoeia, USA (H5214). WT, site-specific S118A, R115A and deletion mutants; 1-140, 1-140 S118A, 141-521 of RUNX2 were generated and sub-cloned into GST-tagged vector pGEX-4T1(GE Health Care) for bacterial expression using primers listed in Table.no.1. The proteins were expressed in *E. coli* (BL21-De3) strain and purified by using GST beads (GE Healthcare). For eukaryotic expression, WT, site-directed mutants of S118A, S118D and R115A were sub-cloned in to pDsRed1-N1 (Clonetech, USA) containing RFP for mammalian expression. The primers used for overlap PCR to generate mutants and deletions are listed Table.no.1. 6XOSE (six tandem repeats of 5'-CCGGGCTGCAATCACCAACCACAGCATC-3') oligonucleotides was synthesized and sub-cloned into pGL3-basic vector for luciferase assays.

2.1.5. Site directed mutagenesis

The cDNA encoding full length Human RUNX2 (NP_001019801.3) mutants were created by overlap extension PCR method. The primers were synthesized corresponding to the particular mutants (Table no.1). During the first PCR cycles the AB was amplified with the help of A and B primers which will be considered as smaller fragment followed bye I have amplified the other fragment with CD considered as larger fragment. Both the fragments were gel extracted and column purified and these two fragments used as templates for further amplification of full length clone, since both the fragments exhibit terminal complementarity and the reaction mixture have PCR primers which leads to hybridization and extension to full length (Figure 9).

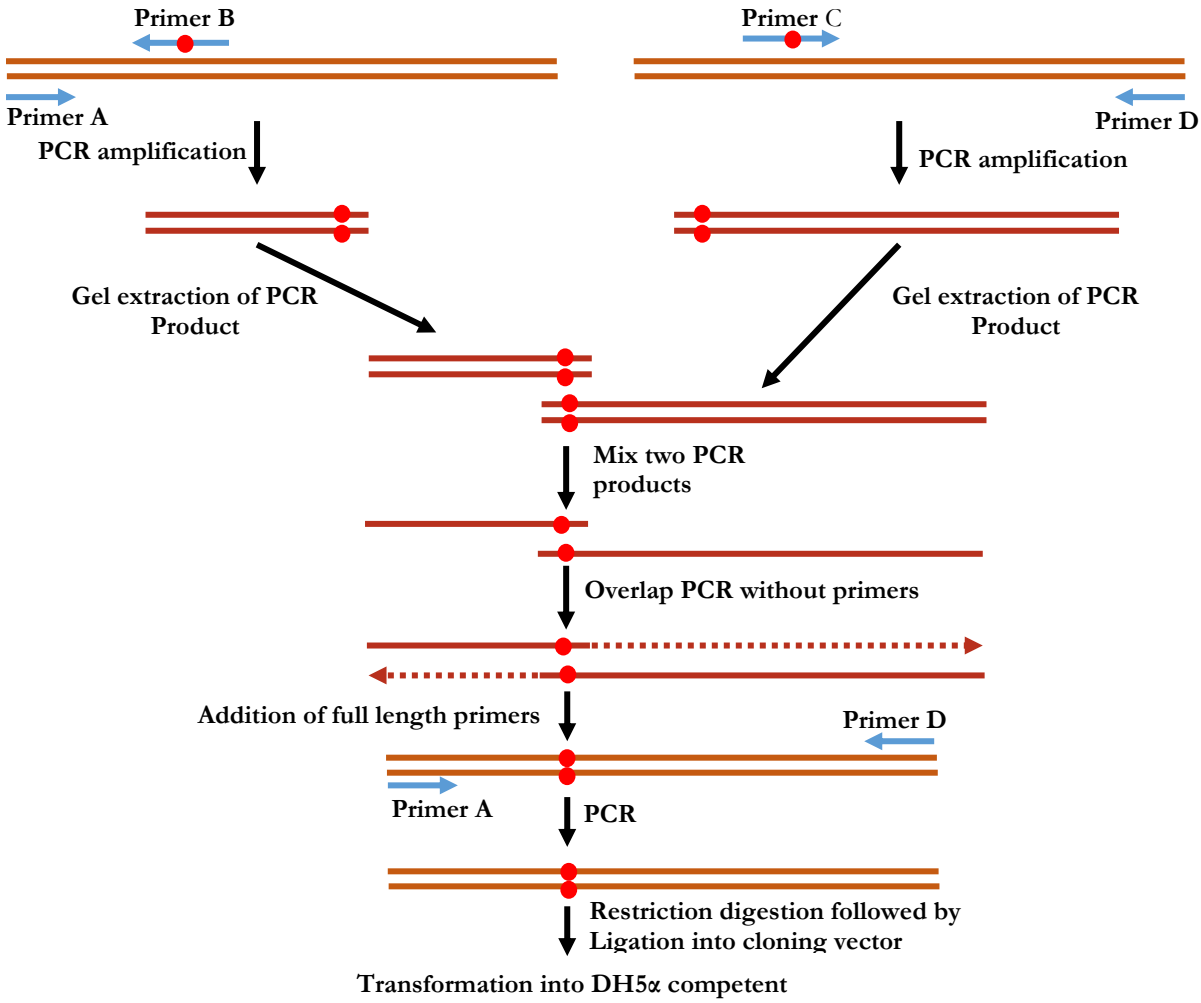

Figure 9: Schematic representation of site directed mutagenesis by overlap PCR method

2.1.6. Agarose gel electrophoresis

To run the DNA and RNA samples based on their size and charge we have used 0.8% (DNA) & 2% (RNA) agarose gel prepared in in TAE (Tris, acetate and EDTA) buffer. Ethidium bromide (EtBr) (0.5µg/ml) was added in agarose to visualize loaded nucleic acids and 6X loading dye used for tracking. The DNA marker (NEB) ranging from 500 bp to 10 kb was used for size comparison. The gel images were taken in BioRad gel doc machine and documented.

2.1.7. Transfection

The adherent cells (HEK293T) cells were procured from ATCC. Cells were seeded with about 5X 10^5 cell density in 60mM culture dish with nutrients medium of DMEM 10% FBS (fetal bovine serum) and 100U/ml of pen/strep. The cells were cultured until 50% confluency at 37^0C with 5% CO_2 in a humidified chamber. The cells were transfected with Lipofectamine2000 in Opti-MEM media containing 3µg of each plasmid and the medium was replaced with complete medium (DMEM 10% FBS with 100U penstrep) after 12hrs of transfection. The cells were maintained for 24-48 hours and observed the transgene/ reporter expression.

2.1.8. Recombinant protein expression and purification

GST-fused RUNX2-WT, RUNX2-S118A, RUNX2-R115A, RUNX2Δ(1-140), RUNX2Δ(1-140)-S118A recombinant proteins were expressed in *E. coli* (BL21-De3) strain along with vector control (pGEX-4T1) by inducing with 1mM IPTG at 16°C overnight. Cells were harvested and sonicated in ice-cold bacterial cell lysis buffer (50mM Tris-HCl, 300mM NaCl, 1mM PMSF and 1mM DTT) at 35% amplitude with pulse of 15sec ON / 45sec OFF, for 15-20 times on ice. Sonicated cell-free extract was centrifuged at 11000 rpm for 20 min and supernatant was allowed to bind onto an equilibrated column packed GST beads, washed with cold column wash buffer and eluted with 25mM reduced glutathione. Eluted protein fractions were loaded onto 10% SDS-PAGE gel and investigated by coomassie brilliant blue staining for recombinant protein expression.

2.1.9. *In vitro* AMP-activated serine threonine protein kinase assay

The reaction mixture containing protein (5ug of GST-RUNX2-WT, RUNX2-S118A, RUNX2-R115A, RUNX2 (1-140), RUNX2 (1-140) S118A or GST protein) kinase assay buffer (20mM HEPES, pH 7.4, 50µM cold ATP, and 5µCi [γ-^{32}P] ATP for auto radiograms, 1mM dithiothreitol, 10mM magnesium acetate) along with 100 ng of AMPK purified enzyme (Cat #14-840 – EMD Millipore) were incubated at 30°C for 30 min and the assay was stopped by adding 4X Laemmli sample preparation buffer before loading on to SDS-PAGE gel. The gels were dried and exposed to autoradiography. Non-radiography reactions were subjected to Western blot analysis using AMPK substrate specific antibody (Cat# 5759, Cell Signaling, USA).

2.1.10. Diabetic animal models

BALB/c, 6–8 week-old male mice were procured from National Animal Resource Facility for Biomedical Research (NARFBR), National Institution of Nutrition (NIN), Hyderabad, India and housed at Animal Resource Facility at University Of Hyderabad, India, for acclimatization before beginning of the experiments. All the animal procedures were performed adhering the norms of Institutional Animal Ethics Committee (IAEC) regulated by the Committee for the Purpose of Control and Supervision of Experiments on Animals (CPCSEA) of India with due approvals.

Diabetes was induced by daily intraperitoneal injections of streptozotocin (40mg/kg body weight, IP in citrate buffer pH 4.5 for five days and controls were injected with citrate buffer alone. After a week of the last dose, the blood glucose (non-fasting) level was measured with the glucometer (Accu-Check instant, Roche Molecular Biochemicals Corp. Indianapolis, IN) and the mice having more than 300 mg/dl were classified as the diabetic group. Mice were sacrificed after 10 weeks after confirmation of diabetes. Metformin control and diabetes treated with metformin group mice received 60 mg/kg b.w. of metformin daily by intra peritoneal for 10 weeks. All the mice were sacrificed and subjected to further analysis.

2.1.11. Tissue and bone histology and histology

Proximal tibiae were collected from all the mice after appropriate treatments and subjected to histology as described earlier. In brief, the fixed samples were decalcified in 5% nitric acid followed by tissues were embedded in paraffin blocks and slides were prepared. Hematoxylin and Eosin (H&E) staining were performed to observe the histology. Detectable adipocytes, greater than 30μm, were observed in the trabecular region ranging from the growth plate to 2 mm away at distal end.

2.1.12. Micro-computed tomography (μCT) analysis

Femurs and tibias from normal, diabetic, diabetic treated with metformin were scanned (n=3/group), with a Skyscan 1176 system (Bruker, Billerica, MA), at a pixel size of 12.34 μm, with a source voltage and current of 50 kV, 500 μA, correspondingly. A 0.5mm Al Filter was used to reduce the beam hardening from the polychromatic nature of the covered X-ray source. Subsequent scanning, three-dimensional (3D) microstructural images of the sagittal and axial

planes of the tibia metaphysis and diaphysis were created and recreated using SkyScan CTvox, CTAn softwares. Volumes of interest were distinct and structural indices considered using Skyscan CT Analyzer software. The region of interest for trabecular micro-architectural parameters to quantify percent of trabecular bone volume (BV/TV), mean trabecular number (Tb. N), mean trabecular thickness (Tb.Th), and bone surface density (BS/TV).

2.1.13. Adipogenic differentiation

For adipogenic differentiation from either mesenchymal stem (C3H10T1/2) cells or pre-adipocytes (3T3-L1), the 85–90% confluent cells were induced with regular growth medium supplemented with 10% FBS, 0.5mM IBMX, 20nM Insulin and 5 mM Dexamethasone (Sigma) for 48 hours and the medium was changed with fresh medium comprising 10% FBS and 20nM insulin for an additional 8 days by replacing with fresh medium for every alternate day.

2.1.14. Transdifferentiation

Osteoblast cells (U2OS) were induced with charcoal stripped FBS (10%), and rosiglitazone (1μM) (Sigma) was added starting post confluent day 4 and maintained for the next 14 days. Adipogenesis was confirmed by Oil Red O staining. Cell lysates from different sets/time points were collected and subjected to Western blotting.

2.1.15. Oil Red O Staining

Oil Red O staining solution was prepared by diluting with distilled water (6:4) from stock solution of 0.5% Oil Red O (Sigma–Aldrich) dissolved in isopropanol overnight. After appropriate incubations, cells were washed thrice with phosphate-buffered saline (PBS) and fixed with 4% formaldehyde in PBS for 1 hr at room temperature. The excess stain was taken out and washed with PBS followed by 60% isopropanol before drying. For quantitative measurements, the stain was eluted after washes with 100% isopropanol and quantified with spectrophotometer at 500nm.

2.1.16. Immunoprecipitation and Western blotting

Equal amounts (750μg) of cell lysates obtained after the indicated treatments were incubated with anti-RUNX2 or anti-p-AMPK (cell Signaling) in 600μl of TBS having 0.1% Triton X-100,

phosphatase and protease inhibitor cocktails(PIC), for binding samples were kept on rotator at 4°C O/N. Protein A-Sepharose beads (GE Healthcare) (2.5 mg/sample) were added to the samples, followed by incubation for another 3 hr at 4°C and washed thrice with TBS containing 0.1% Triton X-100 (Sigma). Pellet-containing immunoprecipitated protein complexes with beads were boiled in 1X loading dye followed by loaded on to 10% SDS-PAGE and subjected to Western blotting. Where immunoprecipitation was not done, samples were directly subjected to Western blotting and incubated with respective specific antibodies, rabbit monoclonal anti-RUNX2, rabbit monoclonal Anti-β-Actin rabbit monoclonal Anti-p-AMPK, rabbit monoclonal anti-Bip1, goat monoclonal anti-p-GSK3β, mouse polyclonal anti-p-JNK, rabbit monoclonal anti-p-AMPK substrate motif specific antibodies, HRP-enzyme-linked secondary antibodies (anti-mouse, anti-rabbit) were obtained from Cell signaling technology, USA. Mouse monoclonal Anti-PPAR-γ and mouse polyclonal anti-PGC1α were acquired from Santa Cruz Biotechnology, Santa Cruz, CA, USA. The signal was sensed by the Amersham ECL prime Western blotting detection reagent, and images were documented by Bio-Rad chemidoc MP system. The same membranes were used after stripping between each specific antibody application were re-probed.

2.1.17. Isolation of mouse bone marrow cells

The mice were euthanized using CO_2, the skin covering hind legs was removed, the muscle cut off, acetabulum was carefully dislocated from the hip joint and the femur was separated from tibiae at the knee joint without breaking femur ends and the bones were placed in ice cold PBS (pH7.5). Bone marrow cells were flushed and collected from both the ends of the bone shafts using ice cold PBS with 25 gauge needle fitted syringe. Cells were separated by centrifuging for 10 min at 1300rpm at 4°C. The red blood cells were lysed by re-suspending the whole cell pellet in 15-20 ml of 0.2% NaCl solution for around 20 sec before stopping the lysis by adding 1.6% NaCl and the reaction mixture was separated by centrifugation for 10 min at 1300 rpm at 4°C. The cell lysates were prepared by adding RIPA lysis buffer with protease inhibitor cocktail to the pellet, followed by Western blotting and immunoprecipitation analysis. Trizol was added for RNA extraction in the place of RIPA lysis buffer.

2.1.18. Confocal microscopy analysis

Confluent (80%) cells, cultured on coverslips, were treated with indicated agents and time points

and were washed with PBS before fixing in 4% formalin for 10 min at RT. The slides were blocked using 5% BSA for 30 min at RT to avoid non-specific binding. The cells were covered with primary antibodies anti- RUNX2 and anti-p-AMPK antibody overnight at 4°C, followed by washing with PBS prior to incubating with secondary antibody (anti-rabbit (Alexa Flour 488) and anti-mouse (Alexa Flour 546)) for RUNX2 and Ubiquitin respectively) for 2 hours at RT. Cells were counterstained with 4, 6-diamidino-2-phenylindole (DAPI) to visualize the nuclei. After mounting, the cells were sealed with clear finger nail polish and the images were taken using a laser scanning confocal microscope (LSM 780, Carl Zeiss).

2.1.19. Electrophoretic mobility shift assay (EMSA)

HEK 293T cells were seeded in 100mm dish at density $1.5X10^6$. Once cells reached to 70-80% confluency cells were transiently transfected with 10μg of RUNX2-WT, RUNX2-S118A, RUNX2-S118D mammalian expression plasmids with lipofectamine2000 (Invitrogen, USA). The cells were also treated with and without Metformin, or Compound C for 6 hrs. Cytoplasmic extracts were separated using cytoplasmic extraction buffer(CEB) comprising 10 mM HEPES (pH-7.4), 10 mM KCl, 0.1mM EDTA(pH-8),0.1M EGTA and 1% NP-40 and nuclear lysates was prepared with nuclear extraction buffer (NEB) comprising 20 mM HEPES (pH-7.4), 0.4mM NaCl, 1mM EDTA(pH-8),0.1M EGTA and protease inhibitor cocktail. The 5' end labelling of Osteocalcin promoter RUNX2 consensus sequence at -140 (5'-CGAGTATTGTGGTTAATACG-3') was done with 20 fmol of [γ32p] and unlabeled probe was removed with illustra Microspin-G-50 columns. 5μg of protein was incubated with 10pmol of probe at 37^0C for 30 min in 1X binding buffer (200mM HEPES (pH 7.4), 40mM dithiothreitol, 4mM EDTA (pH-8.0) and 50% glycerol). The nuclear protein complexes were loaded on 7.5% agarose gel (45 min pre-run gel) with 6X DNA loading dye.

2.1.20. Chromatin immunoprecipitation assay

RUNX2 overexpressed HEK 293T cells were washed with PBS and fixed with 1% formaldehyde for 10 min to crosslink DNA-protein complexes. The crosslinking was quenched using 125mM glycine in 5 min. The crosslinked cells were washed with cold PBS, centrifuged at 2000 rpm 4^0C. Resuspended the cells in 1.5X cytoplasmic extraction buffer (CEB)(Tris-Cl(10 mM), (pH 8), Nacl (10 mM), NP-40 (0.2%) and protease inhibitor cocktail) incubated on ice for 10 min by pipetting

up and down. Pelleted the nuclei at 2500 rpm for 5 min and was resuspended the collected nuclei in nuclei lysis buffer (NLB)(Tris-Cl (50 mM), EDTA (10 mM), SDS (1%), and protease inhibitor cocktail) and kept on ice for 10 min followed by dilution with 2 ml immunoprecipitation dilution buffer (IPDB)(Tris-Cl (20 mM), NaCl (150 mM), EDTA (2 mM), Triton-X100 (1%), SDS (0.01%) and protease inhibitor cocktail. The isolated nuclei were sonicated (15 sec burst with 45 sec interval and 45% amplitude for 10 min) using a sonicator to obtain sheared chromatin. The sheared chromatin was run on 1% agarose gel to verify the range of DNA in 0.3 kb to 1 kb. The Sheared chromatin was snap frozen and stored in -80°C. The chromatin was pre-cleared with protein-G sepharose resin beads on upright rotator for 3 hours and spin down beads at 3000rpm for 2 min at 4^0C and the supernatant was separated into a fresh tube. The immunoprecipitation was initiated by adding 2 μg of RUNX2 antibody (Cat. No. 12556 Cell Signaling technology) or 2 μg immunoglobulin G (IgG) (Cat. No. 2729 Cell Signaling) followed by mixing by rotation on upright rotator for 12-16 hrs. The complexes were enriched using Protein-G beads (Sigma). The protein bead complexes were washed by adding IPWB1(Tris-Cl (20 mM), Nacl (50 mM), EDTA (2 mM), Triton X100 (1%), and SDS (0.1%)) and IPWB2(Tris-Cl (10 mM), LiCl (250 mM), EDTA (1 mM), NP-40 (1%) and Deoxycholate (1%)) with increasing salt concentrations and spinning at 1000g for 5 min each. The immune complexes were eluted with IPEB ($NaHCO_3$ (100mM, 1% SDS) and successively reverse crosslinked at with proteinase K (10μg/ml) NaCl (500mM) and EDTA (12.5mM) at 65°C overnight. DNA was isolated by phenol chloroform extraction followed by ethanol precipitation. The DNA precipitates were washed with 70% ethanol and air dried the pellet and resuspended in 50μl of nuclease free water.

2.1.21. Polymerase chain reaction

Full length RUNX2 was amplified by polymerase chain reaction using cDNA clone (from genecopiea) as a template. The reaction mixture contains 10 μM of each forward primer RUNX2-Fwd: 5' -3' (*BglII*) and RUNX2-Rev: 5'--3' (*XhoI*) specific for Human *RUNX2*, 10mM dNTPs, 1 U of taq DNA polymerase enzyme(New England Biologicals, USA). The reaction was setup with an initial denaturation at 95^0C for 3 min, followed by 95^0C for 30 sec, 63^0C for 30 sec and 68^0C for 2 min of 30 cycles and a final extension at 68^0C for 10 min. The enriched PCR product was ran on 0.8% agarose gel electrophoresis and purified using gel purification method (Invitrogen).

2.1.22. RNA isolation

The total RNA was isolated using trizol reagent (Invitrogen). After harvesting the bone marrow cells from mice tibia, 1 ml of trizol reagent was added and stored in 80^0C RNA extraction was initiated by separating aqueous phase by after adding 200 µl of chloroform/ 1ml of trizol and vigorous shaking followed by incubation on ice for 10 min. The samples were subjected to centrifigation at 13000 rpm for 10 min. The aqueous phase was separated to a new tube and RNA was precipitated by adding 1 volume of isopropanol followed by incubation at -80^0C for an hour. The samples were centrifuged at 13000 rpm for 10 min at 4^0c. The RNA pellet was washed with 75% ethanol followed by air-dry in room temperature for 10 min and resuspended in RNAse free DEPC treated water. The RNA was quantified with Nanodrop against blank. About 1 µg of RNA was used for cDNA preparation (iScript™ cDNA Synthesis Kit, BioRad, CA, USA).

2.1.23. RT-PCR

The RT-PCR reaction was set per well containing 5 µl of SYBR green master mix (2X) (iTaq Universal SYBR Green Supermix), 10 µM of each primer (forward and reverse), and 50ng of cDNA. Each reaction was set in triplicates along with template alone and other controls. The PCR conditions was used according to manufactures protocol along with 60^0c annealing temperature. β-actin was used as internal loading control to normalize the CT values. All the reactions were performed using CFX96 Touch™ Real-Time PCR Detection System.

2.1.24. Statistical analysis

The data values are articulated as mean ±. SEM statistical analysis were accomplished using student T-Test. The differences between the mean values were analyzed using student T-Tests When P value lesser than 0.05 was considered as statistically significant. For all cell culture studies, a minimum of three independent experiments were carried out. For all mice-related work, each mouse was considered as an experimental component.

2.1.25. Table 1: List of primers

S.No	Primer Name	Primer Sequence
1	RUNX2-WT-Fwd	5'-CCGCTCGAGACCATGGCATCAAACAGCCTCTTCAGC-3'
2	RUNX2-WT-Rev	5'-GGAAGATCTCGATATGGTCGCCAAACAGATTCATC-3'
3	RUNX2-S118A-Fwd	5'-GTCCGCACCGACGCCCCCAACTTCCTG-3'
4	RUNX2- S118A -Rev	5'-CAGGAAGTTGGGGGGCGTCGGTGCGGAC-3'
5	RUNX2-Fwd-RT	5'-CCGGTCTCCTTCCAGGAT-3'
6	RUNX2-Rev-RT	5'-GGGAACTGCTGTGGCTTC-3'
7	Osteocalcin-Fwd-RT	5'-CCAAGCAGGAGGGCAATA-3'
8	Osteocalcin-Rev-RT	5'-TCGTCACAAGCAGGGTCA-3'
9	ALP-Fwd-RT	5'-CCCCATGTGATGGCGTAT-3'
10	ALP-Rev-RT	5'-CGGTAGGGAGAGCACAGC-3'
11	PPARγ-Fwd-RT	5'-GGAAGACCACTCGCATTCCTT-3'
12	PPARγ-Rev-RT	5'-TCGCACTTTGGTATTCTTGGAG-3'
13	AdipoQ-Fwd-RT	5'-TGTTCCTCTTAATCCTGCCCA-3'
14	AdipoQ-Rev-RT	5'-CCAACCTGCACAAGTTCCCTT-3'
15	XBP1-Fwd-RT	5'-TGAGAACCAGGAGTTAAGAACACGC-3'
16	XBP1-Rev-RT	5'-CCTGCACCTGCTGCGGAC-3'
17	Actin-Fwd	5'-AGTACCCCATTGAACGC-3'
18	Actin-Rev	5'-TGTCAGCAATGCCTGGGTAC-3'

Results

3.1. Results:

3.1.1. RUNX2 is novel substrate of AMPK *in silico*

RUNX2 is a transcription factor involved in skeletal development and also essential in self-renewal of mesenchymal stem cells[162]. Recent studies on 3T3L1 demonstrated that knockdown of RUNX2 significantly altered gene networks associated with insulin signaling and energy homeostasis[126]. As AMPK is a master regulator of energy homeostasis[163], to check the functional correlation between RUNX2 and AMPK, so as to exert its signaling, we first performed *in silico* analysis using PhosphoMotif Finder tool[164] to predict putative kinase motif on RUNX2. The algorithm of this tool predicted an AMPK-binding motif at 113 to 122 aa with target of serine 118 having the highest motif homology sequence conservation (Table 2). The motif consists with strongly preferred basic amino acids at –3 and –4 positions, which act as phosphoacceptor site, and other consensus hydrophobic residues including leucine and methionine at –5 and +4 positions are shown to be important for strong substrate selectivity demonstrated by site-directed mutagenesis studies and molecular modeling studies[165]. This prediction was further supported by NetPhos 3.1 tool analysis showing a significant score (Table 3). However, the other predicted kinases at the same motif targeting serine 118 by PhosphoMotif do not show any homology consensus/conservation, and the scores are also not significant (Table 4 & 5).

3.1.2. *In vitro & In vivo* validation of AMPK mediated RUNX2 phosphorylation & its functional interaction

To validate our *in silico* observations, we performed AMP-activated kinase assay in a cell-free system using partially purified site-specific motif mutants (S118A and R115A) of GST-RUNX2 along with wild-type protein as described in Methods section. Western blot analysis of *in vitro* kinase assayed proteins using p-AMPK substrate specific antibody shows that AMPK efficiently phosphorylated GST-RUNX2-WT but no phosphorylation was observed in serine 118 mutant of RUNX2 (GST-RUNX2-S118A)(Figure 10a), which was further confirmed by autoradiography. The results showed, the phosphorylation is seen in both RUNX2 WT and RUNX2-Δ1-140 , but reduced phosphorylation in RUNX2-S118A, RUNX2-Δ1-140-S118A, and the R115A mutant at –3 position of conserved residue in AMPK motif site [165], emphasizing that the motif is highly specific (Figure 10b).

S. No	position	Sequence	corresponding kinase consensus motif	predicted motif specific kinase
1	3-8	SNS	pSX[E/pS*/pT*]	Casein Kinase II substrate motif
2	4-9	NSLFST	X[pS/pT]XXX[A/P/S/T]	G protein-coupled receptor kinase 1 substrate motif
3	5-8	SLFS	[pS/pT]XX[S/T]	Casein Kinase I substrate motif
4	5-8	SLFS	pSXX[E/pS*/pT*]	Casein Kinase II substrate motif
5	5-8	SLFS	[pS/pT]XX[E/D/pS*/pY*]	Casein Kinase II substrate motif
6	5-9	SLFST	pSXXX[pS/pT]	MAPKAPK2 kinase substrate
7	5-10	SLFSTV	[pS/pT]XXX[S/T][M/L/V/I/F]	Casein Kinase I substrate motif
8	10-12	VTP	X[pS/pT]P	GSK-3, ERK1, ERK2, CDK5 substrate motif
9	20 - 23	DPST	[E/D]XX[pS/pT]	Casein Kinase I substrate motif
10	21 - 23	PST	P[pS/pT]X	DNA dependent Protein kinase substrate motif
11	22 - 24	STS	pSX[E/pS*/pT*]	Casein Kinase II substrate motif
12	23 - 25	TSR	[pS/pT]X[R/K]	PKA kinase substrate motif
13	23 - 25	TSR	[pS/pT]X[R/K]	PKC kinase substrate motif
14	23 - 28	TSRRFS	X[pS/pT]XXX[A/P/S/T]	G protein-coupled receptor kinase 1 substrate motif
15	24 - 28	SRRFS	pSXXX[pS/pT]	MAPKAPK2 kinase substrate
16	24 - 28	SRRFS	pSXXXpS*	GSK3 kinase substrate motif
17	25 - 28	RRFS	RXXpS	Calmodulin-dependent protein kinase II substrate motif
18	25 - 28	RRFS	RXXpS	PKA kinase substrate motif
19	25 - 28	RRFS	RXX[pS/pT]	Calmodulin-dependent protein kinase II substrate motif
20	25 - 28	RRFS	[R/K]XX[pS/pT]	PKC kinase substrate motif
21	25 - 28	RRFS	[R/K][R/K]X[pS/pT]	PKA kinase substrate motif
22	25 - 28	RRFS	RRXpS	PKA kinase substrate motif
23	25 - 28	RRFS	RRXpS	PKA kinase substrate motif
24	25 - 28	RRFS	R[K/E/R]XpS	PKC epsilon kinase substrate motif
25	25 - 28	RRFS	[R/K][R/X]X[pS/pT]	PAK2 kinase substrate motif
26	26 - 28	RFS	RXpS	PKA kinase substrate motif
27	26 - 28	RFS	[R/K]X[pS/pT]	PKA kinase substrate motif
28	26 - 28	RFS	[R/K]X[pS/pT]	PKC kinase substrate motif
29	26 - 29	RFSP	XXpSP	GSK-3, ERK1, ERK2, CDK5 substrate motif
30	27 - 29	FSP	X[pS/pT]P	GSK-3, ERK1, ERK2, CDK5 substrate motif
31	28 - 29	SP	pSP	ERK1, ERK2 Kinase substrate
32	28 - 31	SPPS	[pS/pT]XX[S/T]	Casein Kinase I substrate motif
33	28 - 31	SPPS	pSXX[E/pS*/pT*]	Casein Kinase II substrate motif
34	28 - 31	SPPS	[pS/pT]XX[E/D/pS*/pY*]	Casein Kinase II substrate motif
35	28 - 32	SPPSS	pSPXX[pS*/pT*]	Casein Kinase I substrate motif
36	30 - 32	PSS	P[pS/pT]X	DNA dependent Protein kinase substrate motif
37	31 - 33	SSS	pSX[E/pS*/pT*]	Casein Kinase II substrate motif
38	31 - 36	SSSLQP	X[pS/pT]XXX[A/P/S/T]	G protein-coupled receptor kinase 1 substrate motif
39	38 - 40	KMS	[R/K]X[pS/pT]	PKA kinase substrate motif
40	38 - 40	KMS	[R/K]X[pS/pT]	PKC kinase substrate motif
41	39 - 44	MSDVSP	X[pS/pT]XXX[A/P/S/T]	G protein-coupled receptor kinase 1 substrate motif

42	40 - 43	SDVS	[pS/pT]XX[S/T]	Casein Kinase I substrate motif
43	40 - 43	SDVS	pSXX[E/pS*/pT*]	Casein Kinase II substrate motif
44	40 - 43	SDVS	[pS/pT]XX[E/D/pS*/pY*]	Casein Kinase II substrate motif
45	41 - 44	DVSP	XXpSP	GSK-3, ERK1, ERK2, CDK5 substrate motif
46	42 - 44	VSP	X[pS/pT]P	GSK-3, ERK1, ERK2, CDK5 substrate motif
47	43 - 44	SP	pSP	ERK1, ERK2 Kinase substrate
48	98 - 101	DNRT	[E/D]XX[pS/pT]	Casein Kinase I substrate motif
49	101 - 104	TMVE	[pS/pT]XX[E/D]	Casein Kinase II substrate motif
50	101 - 104	TMVE	[pS/pT]XX[E/D/pS*/pY*]	Casein Kinase II substrate motif
51	101 - 104	TMVE	[pS/pT]XX[E/D]	Casein Kinase II substrate motif
52	113 - 118	LVRTDS	[M/I/L/V]X[R/K]XX[pS/pT]	Chk1 kinase substrate motif
53	113 - 118	LVRTDS	[M/I/L/V/F/Y]XRXX[pS/pT]	Calmodulin-dependent protein kinase IV substrate motif
54	113 - 120	LVRTDSPN	[M/V/L/I/F]X[R/K]XX[pS/pT]XX	Calmodulin-dependent protein kinase II substrate motif
55	113 - 122	LVRTDSPNFL	[M/V/L/I/F]XRXX[pS/pT]XXX[M/V/L/I/F]	Calmodulin-dependent protein kinase I substrate motif
56	114 - 122	VRTDSPNFL	[M/L/V/I/F][R/K/H]XXSXXX[M/L/V/I/F]	HMGCoA Reductase kinase substrate motif
57	114 - 122	VRTDSPNFL	[M/V/L/I/F][R/K/H]XX[pS/pT]XXX[M/V/L/I/F]	AMP-activated protein kinase substrate motif
58	115 - 118	RTDS	RXXpS	Calmodulin-dependent protein kinase II substrate motif
59	115 - 118	RTDS	RXXpS	PKA kinase substrate motif
60	115 - 118	RTDS	RXX[pS/pT]	Calmodulin-dependent protein kinase II substrate motif
61	115 - 118	RTDS	[R/K]XX[pS/pT]	PKC kinase substrate motif
62	116 - 119	TDSP	XXpSP	GSK-3, ERK1, ERK2, CDK5 substrate motif
63	117 - 119	DSP	X[pS/pT]P	GSK-3, ERK1, ERK2, CDK5 substrate motif
64	117 - 121	DSPNF	[E/D][pS/pT]XXX	b-Adrenergic Receptor kinase substrate motif
65	118 - 119	SP	pSP	ERK1, ERK2 Kinase substrate motif
66	123 - 128	CSVLPS	X[pS/pT]XXX[A/P/S/T]	G protein-coupled receptor kinase 1 substrate motif
67	124 - 128	SVLPS	pSXXX[pS/pT]	MAPKAPK2 kinase substrate
68	124 - 128	SVLPS	pSXXXpS*	GSK3 kinase substrate motif
69	127 - 129	PSH	P[pS/pT]X	DNA dependent Protein kinase substrate motif
70	134 - 139	KTLPVA	X[pS/pT]XXX[A/P/S/T]	G protein-coupled receptor kinase 1 substrate motif
71	152 - 155	TVVT	[pS/pT]XX[S/T]	Casein Kinase I substrate motif
72	162 - 165	ENYS	[E/D]XX[pS/pT]	Casein Kinase I substrate motif
73	165 - 167	SAE	pSX[E/pS*/pT*]	Casein Kinase II substrate motif
74	169 - 172	RNAS	RXXpS	Calmodulin-dependent protein kinase II substrate motif
75	169 - 172	RNAS	RXXpS	PKA kinase substrate motif
76	169 - 172	RNAS	RXX[pS/pT]	Calmodulin-dependent protein kinase II substrate motif
77	169 - 172	RNAS	[R/K]XX[pS/pT]	PKC kinase substrate motif
78	191 - 193	SGR	[pS/pT]X[R/K]	PKA kinase substrate motif
79	191 - 193	SGR	[pS/pT]X[R/K]	PKC kinase substrate motif

80	193 - 196	RGKS	RXXpS	Calmodulin-dependent protein kinase II substrate motif
81	193 - 196	RGKS	RXXpS	PKA kinase substrate motif
82	193 - 196	RGKS	RXX[pS/pT]	Calmodulin-dependent protein kinase II substrate motif
83	193 - 196	RGKS	[R/K]XX[pS/pT]	PKC kinase substrate motif
84	195 - 198	KSFT	KXX[pS/pT]	PKA kinase substrate motif
85	195 - 200	KSFTLT	X[pS/pT]XXX[A/P/S/T]	G protein-coupled receptor kinase 1 substrate motif
86	196 - 198	SFT	pSX[E/pS*/pT*]	Casein Kinase II substrate motif
87	196 - 200	SFTLT	pSXXX[pS/pT]	MAPKAPK2 kinase substrate motif
88	196 - 201	SFTLTI	[pS/pT]XXX[S/T][M/L/V/I/F]	Casein Kinase I substrate motif
89	202 - 205	TVFT	[pS/pT]XX[S/T]	Casein Kinase I substrate motif
90	211 - 216	ATYHRA	X[pS/pT]XXX[A/P/S/T]	G protein-coupled receptor kinase 1 substrate motif
91	218 - 220	KVT	[R/K]X[pS/pT]	PKA kinase substrate motif
92	218 - 220	KVT	[R/K]X[pS/pT]	PKC kinase substrate motif
93	219 - 224	VTVDGP	X[pS/pT]XXX[A/P/S/T]	G protein-coupled receptor kinase 1 substrate motif
94	233 - 237	KLDDS	KXXX[pS/pT]	PKA kinase substrate motif
95	236 - 240	DSKPS	[E/D][pS/pT]XXX	b-Adrenergic Receptor kinase substrate motif
96	237 - 240	SKPS	[pS/pT]XX[S/T]	Casein Kinase I substrate motif
97	237 - 240	SKPS	pSXX[E/pS*/pT*]	Casein Kinase II substrate motif
98	237 - 240	SKPS	[pS/pT]XX[E/D/pS*/pY*]	Casein Kinase II substrate motif
99	238 - 240	KPS	[R/K]X[pS/pT]	PKA kinase substrate motif
100	238 - 240	KPS	[R/K]X[pS/pT]	PKC kinase substrate motif
101	239 - 241	PSL	P[pS/pT]X	DNA dependent Protein kinase substrate motif
102	242 - 247	FSDRLS	X[pS/pT]XXX[A/P/S/T]	G protein-coupled receptor kinase 1 substrate motif
103	243 - 245	SDR	[pS/pT]X[R/K]	PKA kinase substrate motif
104	243 - 245	SDR	[pS/pT]X[R/K]	PKC kinase substrate motif
105	243 - 247	SDRLS	pSXXX[pS/pT]	MAPKAPK2 kinase substrate motif
106	243 - 247	SDRLS	pSXXXpS*	GSK3 kinase substrate motif
107	244 - 247	DRLS	[E/D]XX[pS/pT]	Casein Kinase I substrate motif
108	245 - 247	RLS	RXpS	PKA kinase substrate motif
109	245 - 247	RLS	[R/K]X[pS/pT]	PKA kinase substrate motif
110	245 - 247	RLS	[R/K]X[pS/pT]	PKC kinase substrate motif
111	255 - 257	PSM	P[pS/pT]X	DNA dependent Protein kinase substrate motif
112	256 - 258	SMR	[pS/pT]X[R/K]	PKA kinase substrate motif
113	256 - 258	SMR	[pS/pT]X[R/K]	PKC kinase substrate motif
114	267 - 269	RPS	RXpS	PKA kinase substrate motif
115	267 - 269	RPS	[R/K]X[pS/pT]	PKA kinase substrate motif
116	267 - 269	RPS	[R/K]X[pS/pT]	PKC kinase substrate motif
117	268 - 270	PSL	P[pS/pT]X	DNA dependent Protein kinase substrate motif
118	268 - 273	PSLNSA	X[pS/pT]XXX[A/P/S/T]	G protein-coupled receptor kinase 1 substrate motif
119	269 - 272	SLNS	[pS/pT]XX[S/T]	Casein Kinase I substrate motif
120	269 - 272	SLNS	pSXX[E/pS*/pT*]	Casein Kinase II substrate motif
121	269 - 272	SLNS	[pS/pT]XX[E/D/pS*/pY*]	Casein Kinase II substrate motif
122	273 - 276	APSP	XXpSP	GSK-3, ERK1, ERK2, CDK5 substrate motif

123	274 - 276	PSP	X[pS/pT]P	GSK-3, ERK1, ERK2, CDK5 substrate motif
124	274 - 276	PSP	P[pS/pT]X	DNA dependent Protein kinase substrate motif
125	274 - 279	PSPFNP	X[pS/pT]XXX[A/P/S/T]	G protein-coupled receptor kinase 1 substrate motif
126	275 - 276	SP	pSP	ERK1, ERK2 Kinase substrate motif
127	282 - 284	QSQ	XpSQ	DNA dependent Protein kinase substrate motif
128	283 - 284	SQ	pSQ	ATM kinase substrate motif
129	283 - 286	SQIT	[pS/pT]XX[S/T]	Casein Kinase I substrate motif
130	283 - 286	SQIT	pSXX[E/pS*/pT*]	Casein Kinase II substrate motif
131	292 - 295	QSSP	XXpSP	GSK-3, ERK1, ERK2, CDK5 substrate motif
132	293 - 295	SSP	X[pS/pT]P	GSK-3, ERK1, ERK2, CDK5 substrate motif
133	293 - 298	SSPPWS	X[pS/pT]XXX[A/P/S/T]	G protein-coupled receptor kinase 1 substrate motif
134	294 - 295	SP	pSP	ERK1, ERK2 Kinase substrate motif
135	294 - 298	SPPWS	pSXXX[pS/pT]	MAPKAPK2 kinase substrate motif
136	294 - 298	SPPWS	pSPXX[pS*/pT*]	Casein Kinase I substrate motif
137	294 - 298	SPPWS	pSXXXpS*	GSK3 kinase substrate motif
138	302 - 305	SYPS	[pS/pT]XX[S/T]	Casein Kinase I substrate motif
139	302 - 305	SYPS	pSXX[E/pS*/pT*]	Casein Kinase II substrate motif
140	302 - 305	SYPS	[pS/pT]XX[E/D/pS*/pY*]	Casein Kinase II substrate motif
141	304 - 306	PSY	P[pS/pT]X	DNA dependent Protein kinase substrate motif
142	307 - 309	LSQ	XpSQ	DNA dependent Protein kinase substrate motif
143	307 - 312	LSQMTS	X[pS/pT]XXX[A/P/S/T]	G protein-coupled receptor kinase 1 substrate motif
144	308 - 309	SQ	pSQ	ATM kinase substrate motif
145	308 - 311	SQMT	[pS/pT]XX[S/T]	Casein Kinase I substrate motif
146	308 - 311	SQMT	pSXX[E/pS*/pT*]	Casein Kinase II substrate motif
147	308 - 312	SQMTS	pSXXX[pS/pT]	MAPKAPK2 kinase substrate motif
148	308 - 312	SQMTS	pSXXXpS*	GSK3 kinase substrate motif
149	310 - 313	MTSP	XXpSP	GSK-3, ERK1, ERK2, CDK5 substrate motif
150	311 - 313	TSP	X[pS/pT]P	GSK-3, ERK1, ERK2, CDK5 substrate motif
151	311 - 314	TSPS	[pS/pT]XX[E/D/pS*/pY*]	Casein Kinase II substrate motif
152	312 - 313	SP	pSP	ERK1, ERK2 Kinase substrate motif
153	312 - 314	SPS	pSX[E/pS*/pT*]	Casein Kinase II substrate motif
154	313 - 315	PSI	P[pS/pT]X	DNA dependent Protein kinase substrate motif
155	313 - 318	PSIHST	X[pS/pT]XXX[A/P/S/T]	G protein-coupled receptor kinase 1 substrate motif
156	314 - 317	SIHS	[pS/pT]XX[S/T]	Casein Kinase I substrate motif
157	314 - 317	SIHS	pSXX[E/pS*/pT*]	Casein Kinase II substrate motif
158	314 - 318	SIHST	pSXXX[pS/pT]	MAPKAPK2 kinase substrate motif
159	317 - 319	STT	pSX[E/pS*/pT*]	Casein Kinase II substrate motif
160	318 - 320	TTP	X[pS/pT]P	GSK-3, ERK1, ERK2, CDK5 substrate motif
161	319 - 322	TPLS	[pS/pT]XX[S/T]	Casein Kinase I substrate motif
162	319 - 322	TPLS	[pS/pT]XX[E/D/pS*/pY*]	Casein Kinase II substrate motif

163	322 - 324	SST	pSX[E/pS*/pT*]	Casein Kinase II substrate motif
164	322 - 327	SSTRGT	X[pS/pT]XXX[A/P/S/T]	G protein-coupled receptor kinase 1 substrate motif
165	323 - 325	STR	[pS/pT]X[R/K]	PKA kinase substrate motif
166	323 - 325	STR	[pS/pT]X[R/K]	PKC kinase substrate motif
167	323 - 327	STRGT	pSXXX[pS/pT]	MAPKAPK2 kinase substrate motif
168	324 - 327	TRGT	[pS/pT]XX[S/T]	Casein Kinase I substrate motif
169	325 - 327	RGT	[R/K]X[pS/pT]	PKA kinase substrate motif
170	325 - 327	RGT	[R/K]X[pS/pT]	PKC kinase substrate motif
171	335 - 340	VPRRIS	[M/I/L/V]X[R/K]XX[pS/pT]	Chk1 kinase substrate motif
172	335 - 340	VPRRIS	[M/I/L/V/F/Y]XRXX[pS/pT]	Calmodulin-dependent protein kinase IV substrate motif
173	335 - 342	VPRRISDD	[M/V/L/I/F]X[R/K]XX[pS/pT]XX	Calmodulin-dependent protein kinase II substrate motif
174	337 - 340	RRIS	RXXpS	Calmodulin-dependent protein kinase II substrate motif
175	337 - 340	RRIS	RXXpS	PKA kinase substrate motif
176	337 - 340	RRIS	RXX[pS/pT]	Calmodulin-dependent protein kinase II substrate motif
177	337 - 340	RRIS	[R/K]XX[pS/pT]	PKC kinase substrate motif
178	337 - 340	RRIS	[R/K][R/K]X[pS/pT]	PKA kinase substrate motif
179	337 - 340	RRIS	RRXpS	PKA kinase substrate motif
180	337 - 340	RRIS	RRXpS	PKA kinase substrate motif
181	337 - 340	RRIS	R[K/E/R]XpS	PKC epsilon kinase substrate motif
182	337 - 340	RRIS	[R/K][R/X]X[pS/pT]	PAK2 kinase substrate motif
183	338 - 340	RIS	RXpS	PKA kinase substrate motif
184	338 - 340	RIS	[R/K]X[pS/pT]	PKA kinase substrate motif
185	338 - 340	RIS	[R/K]X[pS/pT]	PKC kinase substrate motif
186	339 - 344	ISDDDT	X[pS/pT]XXX[A/P/S/T]	G protein-coupled receptor kinase 1 substrate motif
187	339 - 345	ISDDDTA	XpSXXDXX	Pyruvate dehydrogenase kinase substrate motif
188	340 - 343	SDDD	pSXX[E/D]	Casein kinase II substrate motif
189	340 - 343	SDDD	pS[E/D][E/D][E/D]	Casein Kinase II substrate motif
190	340 - 343	SDDD	[pS/pT]XX[E/D]	Casein Kinase II substrate motif
191	340 - 343	SDDD	[pS/pT]XX[E/D/pS*/pY*]	Casein Kinase II substrate motif
192	340 - 343	SDDD	[pS/pT]XX[E/D]	Casein Kinase II substrate motif
193	340 - 344	SDDDT	pSXXX[pS/pT]	MAPKAPK2 kinase substrate motif
194	341 - 344	DDDT	[E/D]XX[pS/pT]	Casein Kinase I substrate motif
195	343 - 347	DTATS	[E/D][pS/pT]XXX	b-Adrenergic Receptor kinase substrate motif
196	344 - 347	TATS	[pS/pT]XX[S/T]	Casein Kinase I substrate motif
197	344 - 347	TATS	[pS/pT]XX[E/D/pS*/pY*]	Casein Kinase II substrate motif
198	353 - 355	PST	P[pS/pT]X	DNA dependent Protein kinase substrate motif
199	354 - 357	STLS	[pS/pT]XX[S/T]	Casein Kinase I substrate motif
200	354 - 357	STLS	pSXX[E/pS*/pT*]	Casein Kinase II substrate motif
201	354 - 357	STLS	[pS/pT]XX[E/D/pS*/pY*]	Casein Kinase II substrate motif
202	357 - 359	SKK	[pS/pT]X[R/K]	PKA kinase substrate motif
203	357 - 359	SKK	[pS/pT]X[R/K]	PKC kinase substrate motif
204	358 - 360	KKS	[R/K]X[pS/pT]	PKA kinase substrate motif
205	358 - 360	KKS	[R/K]X[pS/pT]	PKC kinase substrate motif
206	359 - 361	KSQ	XpSQ	DNA dependent Protein kinase substrate motif

207	359 - 364	KSQAGA	X[pS/pT]XXX[A/P/S/T]	G protein-coupled receptor kinase 1 substrate motif
208	360 - 361	SQ	pSQ	ATM kinase substrate motif
209	363 - 366	GASE	XX[pS/pT]E	G protein-coupled receptor kinase 1 substrate motif
210	377 - 379	PSI	P[pS/pT]X	DNA dependent Protein kinase substrate motif
211	378 - 380	SIS	pSX[E/pS*/pT*]	Casein Kinase II substrate motif
212	378 - 381	SISS	[pS/pT]XX[S/T]	Casein Kinase I substrate motif
213	378 - 381	SISS	pSXX[E/pS*/pT*]	Casein Kinase II substrate motif
214	378 - 381	SISS	[pS/pT]XX[E/D/pS*/pY*]	Casein Kinase II substrate motif
215	380 - 385	SSLTES	X[pS/pT]XXX[A/P/S/T]	G protein-coupled receptor kinase 1 substrate motif
216	381 - 383	SLT	pSX[E/pS*/pT*]	Casein Kinase II substrate motif
217	381 - 384	SLTE	pSXX[E/D]	Casein kinase II substrate motif
218	381 - 384	SLTE	XX[pS/pT]E	G protein-coupled receptor kinase 1 substrate motif
219	381 - 384	SLTE	[pS/pT]XX[E/D]	Casein Kinase II substrate motif
220	381 - 384	SLTE	[pS/pT]XX[E/D]	Casein Kinase II substrate motif
221	381 - 385	SLTES	pSXXX[pS/pT]	MAPKAPK2 kinase substrate motif
222	381 - 385	SLTES	pSXXXpS*	GSK3 kinase substrate motif
223	384 - 388	ESRFS	[E/D][pS/pT]XXX	b-Adrenergic Receptor kinase substrate motif
224	385 - 388	SRFS	[pS/pT]XX[S/T]	Casein Kinase I substrate motif
225	385 - 388	SRFS	pSXX[E/pS*/pT*]	Casein Kinase II substrate motif
226	385 - 388	SRFS	[pS/pT]XX[E/D/pS*/pY*]	Casein Kinase II substrate motif
227	386 - 388	RFS	RXpS	PKA kinase substrate motif
228	386 - 388	RFS	[R/K]X[pS/pT]	PKA kinase substrate motif
229	386 - 388	RFS	[R/K]X[pS/pT]	PKC kinase substrate motif
230	396 - 401	ATFTYT	X[pS/pT]XXX[A/P/S/T]	G protein-coupled receptor kinase 1 substrate motif
231	397 - 400	TFTY	[pS/pT]XX[E/D/pS*/pY*]	Casein Kinase II substrate motif
232	398 - 400	FTY	FpTY	mTOR kinase substrate motif
233	400 - 402	YTP	X[pS/pT]P	GSK-3, ERK1, ERK2, CDK5 substrate motif
234	404 - 409	VTSGMS	X[pS/pT]XXX[A/P/S/T]	G protein-coupled receptor kinase 1 substrate motif
235	405 - 410	TSGMSL	[pS/pT]XXX[S/T][M/L/V/I/F]	Casein Kinase I substrate motif
236	406 - 409	SGMS	[pS/pT]XX[S/T]	Casein Kinase I substrate motif
237	406 - 409	SGMS	pSXX[E/pS*/pT*]	Casein Kinase II substrate motif
238	406 - 409	SGMS	[pS/pT]XX[E/D/pS*/pY*]	Casein Kinase II substrate motif
239	409 - 413	SLGMS	pSXXX[pS/pT]	MAPKAPK2 kinase substrate motif
240	409 - 413	SLGMS	pSXXXpS*	GSK3 kinase substrate motif
241	413 - 415	SAT	pSX[E/pS*/pT*]	Casein Kinase II substrate motif
242	413 - 416	SATT	[pS/pT]XX[S/T]	Casein Kinase I substrate motif
243	413 - 416	SATT	pSXX[E/pS*/pT*]	Casein Kinase II substrate motif
244	415 - 418	TTHY	[pS/pT]XX[E/D/pS*/pY*]	Casein Kinase II substrate motif
245	415 - 419	TTHYH	XpTXpY*X	PP2C delta substrate motif
246	415 - 420	TTHYHT	X[pS/pT]XXX[A/P/S/T]	G protein-coupled receptor kinase 1 substrate motif
247	416 - 418	THY	pTXpY*	Dual specificity protein phosphatase 6 substrate motif
248	429 - 431	SSQ	XpSQ	DNA dependent Protein kinase substrate motif
249	429 - 432	SSQS	[pS/pT]XX[S/T]	Casein Kinase I substrate motif

250	429 - 432	SSQS	pSXX[E/pS*/pT*]	Casein Kinase II substrate motif
251	429 - 432	SSQS	[pS/pT]XX[E/D/pS*/pY*]	Casein Kinase II substrate motif
252	429 - 434	SSQSQS	X[pS/pT]XXX[A/P/S/T]	G protein-coupled receptor kinase 1 substrate motif
253	430 - 431	SQ	pSQ	ATM kinase substrate motif
254	430 - 432	SQS	pSX[E/pS*/pT*]	Casein Kinase II substrate motif
255	430 - 434	SQSQS	pSXXX[pS/pT]	MAPKAPK2 kinase substrate
256	430 - 434	SQSQS	pSXXXpS*	GSK3 kinase substrate motif
257	432 - 433	SQ	pSQ	ATM kinase substrate motif
258	438 - 443	QTSSTP	X[pS/pT]XXX[A/P/S/T]	G protein-coupled receptor kinase 1 substrate motif
259	439 - 442	TSST	[pS/pT]XX[S/T]	Casein Kinase I substrate motif
260	440 - 442	SST	pSX[E/pS*/pT*]	Casein Kinase II substrate motif
261	441 - 443	STP	X[pS/pT]P	GSK-3, ERK1, ERK2, CDK5 substrate motif
262	441 - 444	STPY	[pS/pT]XX[E/D/pS*/pY*]	Casein Kinase II substrate motif
263	441 - 445	STPYL	XpTXpY*X	PP2C delta substrate motif
264	442 - 444	TPY	pTXpY*	Dual specificity protein phosphatase 6 substrate motif
265	442 - 444	TPY	pT[G/P/E]pY*	MAPK 11, 13, 14 Kinase substrate
266	448 - 453	GTSSGS	X[pS/pT]XXX[A/P/S/T]	G protein-coupled receptor kinase 1 substrate motif
267	450 - 453	SSGS	[pS/pT]XX[S/T]	Casein Kinase I substrate motif
268	450 - 453	SSGS	pSXX[E/pS*/pT*]	Casein Kinase II substrate motif
269	450 - 453	SSGS	[pS/pT]XX[E/D/pS*/pY*]	Casein Kinase II substrate motif
270	451 - 453	SGS	pSX[E/pS*/pT*]	Casein Kinase II substrate motif
271	463 - 466	DRSP	XXpSP	GSK-3, ERK1, ERK2, CDK5 substrate motif
272	464 - 466	RSP	X[pS/pT]P	GSK-3, ERK1, ERK2, CDK5 substrate motif
273	464 - 466	RSP	[R/K][pS/pT]P	Growth associated histone HI kinase substrate motif
274	464 - 467	RSPS	RXXpS	Calmodulin-dependent protein kinase II substrate motif
275	464 - 467	RSPS	RXXpS	PKA kinase substrate motif
276	464 - 467	RSPS	RXX[pS/pT]	Calmodulin-dependent protein kinase II substrate motif
277	464 - 467	RSPS	[R/K]XX[pS/pT]	PKC kinase substrate motif
278	465 - 466	SP	pSP	ERK1, ERK2 Kinase substrate
279	465 - 467	SPS	pSX[E/pS*/pT*]	Casein Kinase II substrate motif
280	465 - 468	SPSR	[pS/pT]PX[R/K]	CDK1, 2, 4, 6 kinase substrate
281	465 - 468	SPSR	[pS/pT]PX[R/K]	Growth associated histone HI kinase substrate motif
282	465 - 468	SPSR	[pS/pT]PX[R/K]	Cdc2 kinase substrate motif
283	465 - 469	SPSRM	pSPX[R/K]X	CDK kinase substrate motif
284	466 - 468	PSR	P[pS/pT]X	DNA dependent Protein kinase substrate motif
285	466 - 471	PSRMLP	X[pS/pT]XXX[A/P/S/T]	G protein-coupled receptor kinase 1 substrate motif
286	474 - 477	TTTS	[pS/pT]XX[S/T]	Casein Kinase I substrate motif
287	474 - 477	TTTS	[pS/pT]XX[E/D/pS*/pY*]	Casein Kinase II substrate motif
288	475 - 480	TTSNGS	X[pS/pT]XXX[A/P/S/T]	G protein-coupled receptor kinase 1 substrate motif
289	477 - 480	SNGS	pSXX[E/pS*/pT*]	Casein Kinase II substrate motif
290	477 - 481	SNGST	pSXXX[pS/pT]	MAPKAPK2 kinase substrate

291	477 - 482	SNGSTL	[pS/pT]XXX[S/T][M/L/V/I/F]	Casein Kinase I substrate motif
292	498 - 503	GSHSSS	X[pS/pT]XXX[A/P/S/T]	G protein-coupled receptor kinase 1 substrate motif
293	499 - 501	SHS	pSX[E/pS*/pT*]	Casein Kinase II substrate motif
294	499 - 502	SHSS	[pS/pT]XX[S/T]	Casein Kinase I substrate motif
295	499 - 502	SHSS	pSXX[E/pS*/pT*]	Casein Kinase II substrate motif
296	499 - 502	SHSS	[pS/pT]XX[E/D/pS*/pY*]	Casein Kinase II substrate motif
297	499 - 503	SHSSS	pSXXX[pS/pT]	MAPKAPK2 kinase substrate
298	499 - 503	SHSSS	pSXXXpS*	GSK3 kinase substrate motif
299	501 - 504	SSSP	XXpSP	GSK-3, ERK1, ERK2, CDK5 substrate motif
300	501 - 506	SSSPTV	[pS/pT]XXX[S/T][M/L/V/I/F]	Casein Kinase I substrate motif
301	502 - 504	SSP	X[pS/pT]P	GSK-3, ERK1, ERK2, CDK5 substrate motif
302	503 - 504	SP	pSP	ERK1, ERK2 Kinase substrate
303	503 - 505	SPT	pSX[E/pS*/pT*]	Casein Kinase II substrate motif
304	504 - 506	PTV	P[pS/pT]X	DNA dependent Protein kinase substrate motif
305	504 - 509	PTVLNS	X[pS/pT]XXX[A/P/S/T]	G protein-coupled receptor kinase 1 substrate motif
306	510 - 512	SGR	[pS/pT]X[R/K]	PKA kinase substrate motif
307	510 - 512	SGR	[pS/pT]X[R/K]	PKC kinase substrate motif
308	515 - 519	ESVWR	[E/D][pS/pT]XXX	b-Adrenergic Receptor kinase substrate motif

Table 2: *In silico* prediction of AMPK substrate motif in RUNX2 protein: (a) List of corresponding putative motif-specific kinases along with AMPK predicted by phospho motif finder in the N-terminal region (DNA-binding domain) of RUNX2.

S.No	Position	Motif	Score	Significance	Kinase
1	3	--M A S N S L F	0.002	-	CDC2
2	5	--M A S N S L F S T	0.061	-	PKA
3	8	N S L F S T V T P	0.627	S*	UNSP
4	22	F W D P S T S R R	0.191	-	GSK3β
5	24	D P S T S R R F S	0.841	S**	UNSP
6	28	S R R F S P PS S	0.998	S***	UNSP
7	31	F S P P S S S L Q P	0.904	S***	UNSP
8	32	S P P S S S L Q P	0.274	-	CDC2
9	33	P P S S S L Q P	0.356	-	CDC2
10	40	P G K M S L V S P	0.220	-	PKA
11	43	M S D V S P V V A	0.961	S***	UNSP
12	118	V R T D S P N F L	0.928	S***	AMPK
13	124	N F L C S V I P S	0.574	-	PKC
14	128	S V L P S H W R C	0.593	-	PKC
15	165	DE N Y S A E L R	0.011	-	CKII
16	172	L R N A S A V M K	0.061	-	CAMII
17	191	F V G R S G R G K	0.897	S**	UNSP
18	196	G R G K S F T L T	0.881	S**	UNSP
19	237	K L D D S K P S L	0.412	-	CDC2
20	240	D S K P S L F S D	0.900	S***	UNSP

Table 3: *In silico* prediction of AMPK substrate motif in RUNX2 protein: (a) List of corresponding putative motif-specific kinases along with AMPK predicted by Netphos3.1 in the N-terminal region (DNA-binding domain) of RUNX2.

S.No	Name of the AMPK Substrate	Position	-5	-4	-3	-2	-1	0	+1	+2	+3	+4
1	HMG-CoA Reductase	Ser862	M	T	H	N	R	S	K	I	N	L
2	p300	Ser89	L	L	R	S	G	S	S	P	N	L
3	ACC1	ser1216	M	T	H	V	A	S	V	S	D	V
4	CRCT2 / TORC2	ser171	L	N	R	T	S	S	D	S	A	L
5	iPFK2	ser461	L	M	R	R	N	S	V	T	P	L
6	Glycogen Synthase 1	Ser8	L	N	R	T	L	S	M	S	S	L
7	FOXO3A	Ser413	M	Q	R	S	S	S	F	P	Y	T
8	Harmone Sens. Lipase	Ser554	M	R	R	S	V	S	E	A	A	L
9	ACC1 / ACC2	Ser79/80	I	R	S	S	M	S	G	L	H	L
10	IRS1	Ser789	L	R	L	S	S	S	S	G	R	L
11	TSC2(Tuberin)	Ser1387	L	S	K	S	S	S	S	P	E	L
12	MED1	Ser671	L	E	R	Q	N	S	S	S	G	S
13	RAG1	Ser531	L	K	N	V	S	S	R	T	D	V
14	Runx2	Ser118	L	V	R	T	D	S	P	N	F	L

Table 4: (**a)** The predicted corresponding putative AMPK substrate motif of RUNX2 significantly aligned with all the important residues of known and validated AMPK substrate motifs in other proteins.

S. No	Species	Position	-5	-4	-3	-2	-1	0	+1	+2	+3	+4
1	Homo sapiens	Ser118	L	V	R	T	D	S	P	N	F	L
2	Mus musculus	Ser125	L	V	R	T	D	S	P	N	F	L
3	Rattus norvegicus	Ser126	L	V	R	T	D	S	P	N	F	L
4	Pan troglodytes	Ser188	L	V	R	T	D	S	P	N	F	L
5	Macaca mulatta	Ser187	L	V	R	T	D	S	P	N	F	L
6	Bos taurus	Ser183	L	V	R	T	D	S	P	N	F	L
7	Gallus gallus	Ser91	L	V	R	T	D	S	P	N	F	L
8	Danio rerio	Ser79	L	V	R	T	D	S	P	N	F	L
9	Xenopus tropicalis	Ser92	L	V	R	T	D	S	P	N	L	L

Table 5: Cross-Species conservation of AMPK substrate motif in RUNX2 protein: The ClustalW2 sequence alignment showing cross-species conservation with predicted optimal AMPK substrate motif of RUNX2.

Follow-up immunoprecipitation experiments in myoblasts cells (C2C12) showed that the pharmacological activation of AMPK using metformin or AICAR resulted in co-precipitation of p-AMPK with RUNX2 , and this was not observed in AMPK inhibitor (compound C) treated cells (Figure 10c & d). We characterized these observations further by immunofluorescence studies where co-localization of AMPK and RUNX2 were identified in metformin treated cells (Figure 10e & f). Overall, these findings confirm our *in silico* prediction of RUNX2 as a physiological substrate of AMPK. Since the identified AMPK binding motif (S118) was present in DNA binding domain of RUNX2, we have assayed to check the effect of S118 phosphorylation on DNA binding activity of RUNX2 by EMSA. The results demonstrated that metformin induced and phosphomimetic S118D mutant overexpressed lysates showed an enhanced binding activity of RUNX2 to its consensus DNA sequence (Figure 10g).

3.1.3. Adipogenesis is associated with AMPK-mediated loss of RUNX2-S118 phosphorylation differentiation models

Recent studies have established that AMPK may have a role in MSC differentiation; however, the mechanistic association and downstream signaling events remain unclear [166]. As our *in silico* and *in vitro* analyses confirm that RUNX2 is a substrate for AMPK, we have made an attempt to understand the significance and relationship between AMPK activation and RUNX2-S118

phosphorylation during the differentiation process. To demonstrate the same, we utilized various well-characterized differentiation models to study downstream signaling mediators in the osteogenesis *vs* adipogenesis process. Our data show that phosphorylated (active) form of AMPK (T172), RUNX2-S118 phosphorylation and expression of RUNX2 downstream target, increased mRNA level of Osteocalcin is associated throughout the differentiation of osteoblasts from myoblasts (C2C12) upon induction with BMP2 (Figure 11a & b). We then examined the physiological functions of AMPK-induced RUNX2 phosphorylation and its downstream effects in pre-adipocyte to adipocyte differentiation using 3T3-L1 as described in the methods section. By the eighth day from the induction of differentiation, RUNX2 protein level and AMPK activity were decreased whereas other adipogenic markers such as PPARγ, AdipoQ and C/EBPβ were increased as shown in Oil Red O staining, Western blot and RT-PCR analysis (Figure 11c, d & e). These results demonstrated that adipogenesis is associated with loss of RUNX2 protein level and active AMPK.

3.1.4. AMPK activity regulates adipogenesis through RUNX2 phosphorylation at S118

As it is evident from the above results, the loss of AMPK activity and RUNX2 expression are associated with adipocyte differentiation in both MSC and 3T3-L1 pre-adipocyte models, we then further examined the effects of pharmacological activation of AMPK in adipogenesis in MSC differentiation model (C3H10T1/2). Accumulation of triglycerides by Oil Red O staining (Figure 12a) and quantification of intracellular triglyceride content (Figure 12c) explain that AMPK activator (Metformin) delayed the differentiation to adipocytes even in the presence of adipogenic inducers, which is further clarified by Western blot analysis showing the expression of other adipogenic marker, PPARγ (Figure 12b). Real time PCR analysis confirmed the expression of markers such as RUNX2, PPARγ and AdipoQ (Figure 12e). To determine whether RUNX2 serine 118 residue was indeed phosphorylated by AMPK during differentiation, we differentiated normal MSCs (C3H10T1/2) with and without metformin, and immunoprecipitated the cell lysates with RUNX2 antibody. Results from the pulled immunocomplexes were probed with AMPK substrate antibody, suggesting that p-AMPK mediated RUNX2- S118 phosphorylation is the key regulator of MSC differentiation process (Figure 12d).

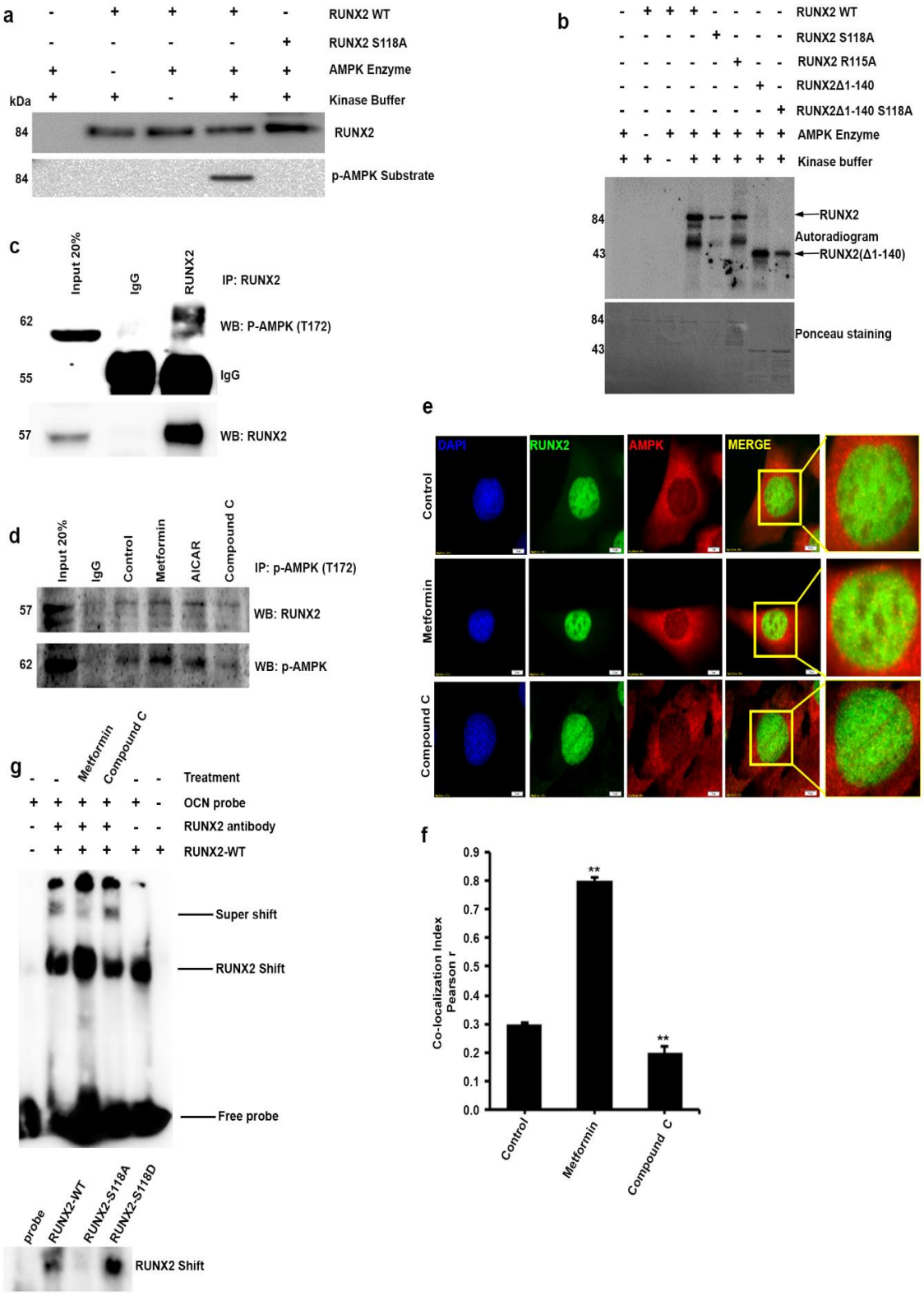
a
RUNX2 WT
RUNX2 S118A
AMPK Enzyme
Kinase Buffer
kDa
84
RUNX2
84
p-AMPK Substrate
b
RUNX2 WT
RUNX2 S118A
RUNX2 R115A
RUNX2Δ1-140
RUNX2Δ1-140 S118A
AMPK Enzyme
Kinase buffer
84
43
RUNX2
Autoradiogram
RUNX2(Δ1-140)
84
43
Ponceau staining
c
Input 20%
IgG
RUNX2
IP: RUNX2
62
WB: P-AMPK (T172)
55
IgG
57
WB: RUNX2
d
Input 20%
IgG
Control
Metformin
AICAR
Compound C
IP: p-AMPK (T172)
57
WB: RUNX2
62
WB: p-AMPK
e
DAPI
RUNX2
AMPK
MERGE
Control
Metformin
Compound C
f
Co-localization Index
Pearson r
0.9
0.8
0.7
0.6
0.5
0.4
0.3
0.2
0.1
0.0
**
**
Control
Metformin
Compound C
g
Metformin
Compound C
Treatment
OCN probe
RUNX2 antibody
RUNX2-WT
Super shift
RUNX2 Shift
Free probe
probe
RUNX2-WT
RUNX2-S118A
RUNX2-S118D
RUNX2 Shift

Figure 10: S118 Phosphorylation of RUNX2 is AMPK-Specific: (**a**) GST-RUNX2 WT, RUNX2 S118A, and GST purified proteins were incubated with active AMPK purified enzyme in presence and absence of kinase assay buffer. After performing AMPK kinase assay, the samples were loaded into SDS-PAGE and subsequent western blotting and probed with anti-p-AMPK substrate antibody. The loading control of RUNX2 was confirmed by anti-RUNX2 antibody. (**b**) GST-RUNX2 WT, RUNX2 S118A, RUNX2 R115A, RUNX2 (1-140), RUNX2 (1-140) S118A and GST purified proteins were incubated with active AMPK purified enzyme in presence and absence of kinase assay buffer. After performing AMPK kinase assay, the samples were loaded into SDS-PAGE and subsequent to autoradiography. The loading control of RUNX2 was confirmed by ponceau staining. (**c**) Whole cell lysates were incubated with RUNX2 antibody overnight. The immunoprecipitates were subjected to immunoblotting with anti-AMPK, anti-RUNX2 antibody. (**d**) C2C12 cells were treated with AMPK activators (metformin, AICAR) and inhibitors (compound C) and the cell lysates were prepared, and incubated with anti-p-AMPK antibody. Immunoprecipitates were loaded on SDS-PAGE and probed with RUNX2 and p-AMPK specific antibodies. (**e**) The immunofluorescence staining carried out on myoblast cells treated with AMPK activators (Metformin) in presence and absence of Inhibitors (compound C) against RUNX2 (Alexa Fluor 488) AMPK(Alexa Fluor 546) and DAPI(nuclei staining). **(f)** Quantification of colocalization of figure e with image J software. **(g)** Electrophoretic mobility shift assay was performed using nuclear lysates from RUNX2 full length overexpressed followed by metformin (5mM) and compound C (20μM) treatment in HEK 293T cells. The subsequent nuclear extracts of over expressed (RUNX2-WT, S118A and S118D) cells was incubated with osteocalcin promoter specific probe with and without RUNX2 antibody.

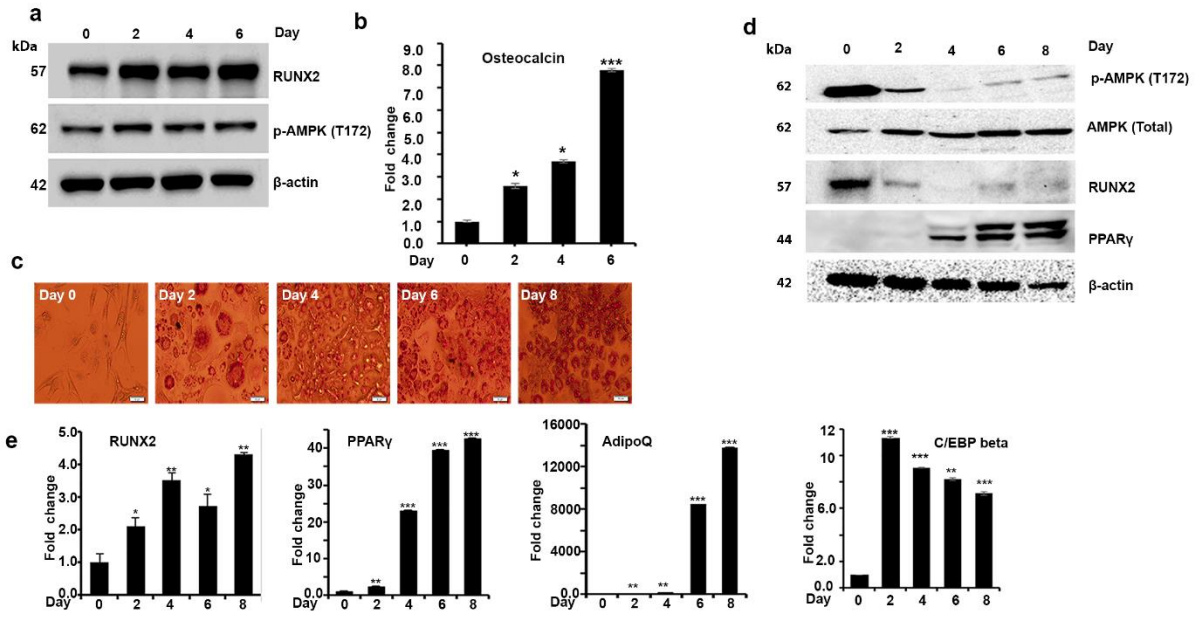

Figure 11: The correlation between active AMPK and RUNX2 in adipogenic vs osteogenic differentiation: **(a)** Myoblasts (C2C12) were differentiated to osteocytes with BMP-2 (300ng/ml) for 6 days and the RUNX2 and p-AMPK expression was analyzed. (b) RNA level of osteocalcin was measured in differentiated C2C12 Cells. Pre-adipocytes (3T3-L1) were treated with adipogenic inducers 0.5mM IBMX, 20nM Insulin and 5 mM Dexamethasone (Sigma) for 48 hrs and were incubated with growth medium having 20nM insulin for another 8 days. **(c)** The adipogenesis was determined at each day intervals by the Oil Red O staining. (**c**) The protein levels of p-AMPK, RUNX2, PPARγ, and PGC1α was measured. (**d**) The mRNA levels of RUNX2, AdipoQ, PPARγ and CEBP beta were quantified. Mean ± S.E.M.; n=3, *p<0.1 versus 0 day control, **p<0.05 versus 0 day control; ***p<0.001 0 day control.

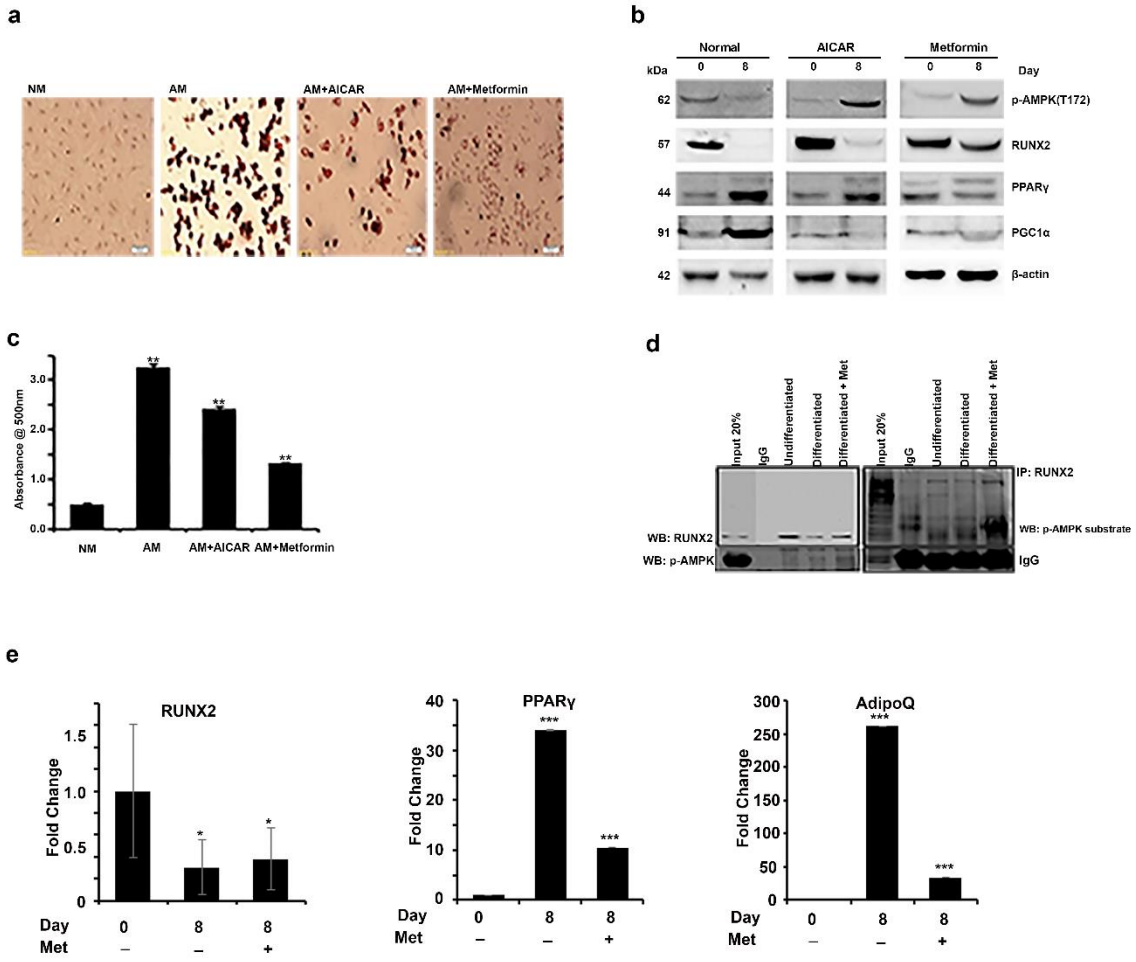

Figure 12: AMPK activators (metformin) delayed adipogenesis by RUNX2 phosphorylation (S118): (a) Mesenchymal stem cells (C3H10T1/2) were treated with adipogenic inducers 0.5mM IBMX (sigma), 20nM insulin, 5 mM dexamethasone (Sigma) in the presence and absence of AMPK activators (metformin (Sigma), AICAR (Sigma)) for 48 hrs and then they were incubated with growth medium having 20nM insulin, AMPK activators (metformin, AICAR) for another 8 days. On day 8 the adipogenesis was measured by Oil Red O staining. (**b**) The expression of

p-AMPK, RUNX2, PPARγ and PGC1α was measured (**c**) The Oil Red O stain was eluted with 100% Isopropanol and measured absorbance at 510nm. (d) MSCs (C3H10t1/2) were differentiated to adipocytes with and without metformin and cell lysates were subjected to immunoprecipitation with RUNX2 antibody and probed with AMPK substrate specific antibody. The IP analysis showing the reduced levels of RUNX2 phosphorylation (S118), and is the same was restored upon metformin treatment. (e) The mRNA expression levels of RUNX2, PPARγ, and AdipoQ (Adiponectin) were quantified. Mean ± S.E.M.; n=3, *p<0.1 versus 0 day, ***p<0.001 versus 0 day.

3.1.5. Adipogenesis is associated with AMPK activity in bone marrow derived mesenchymal stem cells (BM-MSC) differentiation models

Since it is shown that from the above studies, the loss of AMPK activity and RUNX2 expression are associated with in *in vitro* adipocyte differentiation in both MSC(C3H10T1/2) and 3T3-L1 pre-adipocyte models, we then further isolated the bone marrow derived mesenchymal stem cells(BM-MSC) from BALB/c male mice and characterized various positive surface markers ($CD44^+$(81.8%) & $CD\ 90^+$(89.9%)) and negative markers ($CD45^+$(4.81%)) FACS analysis, (Figure

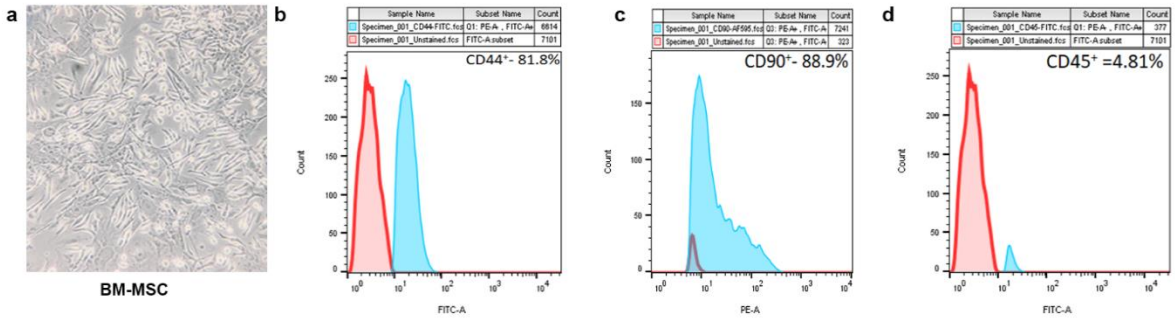

Figure 13: Characterization of BM-MSCs by using surface antigens: a) morphological characteristics of BM-MSCs at passage 3. Flow cytometry analysis showed 81.8% positive for (b) CD44 (c) 88.9% for CD90 and 4.81% for CD45.

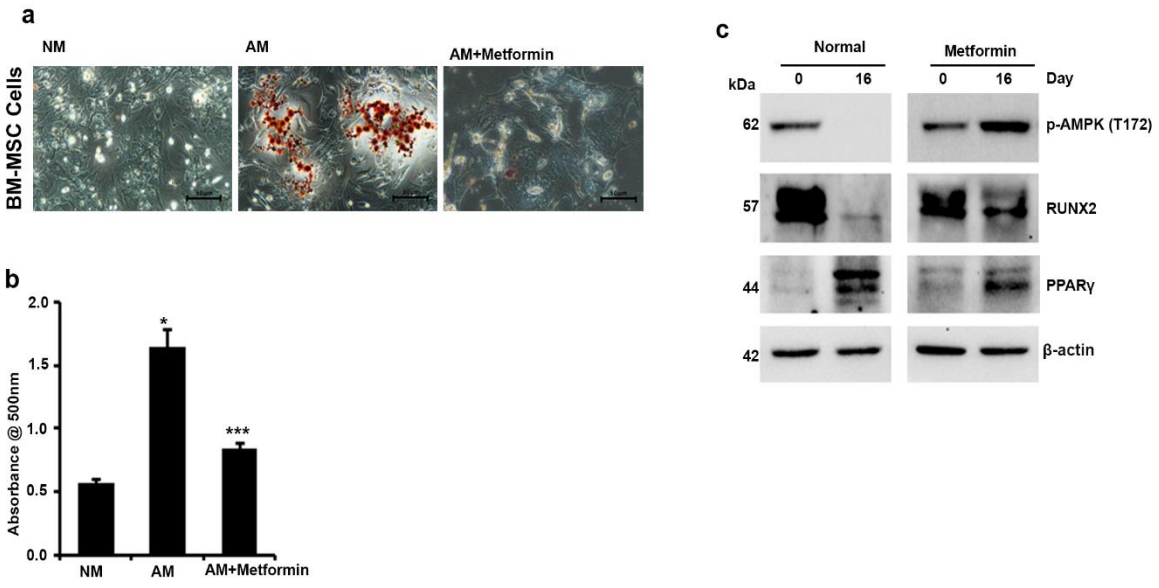

Figure 14 : Activation of AMPK by metformin for 48 hr before treating with adipogenic differentiation medium abrogated the effects of adipogenic inducers when compared with control (NM), and adipogenic medium (AM) alone in MSCs was evident from the reduced oil droplets (dark brown)**(a)**. Representative picture of quantitative measurements of eluted Oil Red O stain precipitates. **(b)**. Western blot analysis for p-AMPK, RUNX2 and PPARγ, expression**(c)**.

13) and the effects of pharmacological activation of AMPK in adipogenesis in BM-MSC differentiation model.

Accumulation of triglycerides by Oil Red O staining (Figure 14a) and quantification of intracellular triglyceride content (Figure 14b) explain that AMPK activator (Metformin) delayed the differentiation to adipocytes even in the presence of adipogenic inducers, which is further clarified by Western blot analysis showing the expression of other adipogenic marker, PPARγ (Figure 14c).

3.1.6. AMPK activity regulates transdifferentiation (osteocytes to adipocytes) through RUNX2

It is known that terminally differentiated osteocytes and myocytes can also dedifferentiate to adipocytes upon altered external stimuli, and that could be seen in the modified metabolic conditions [167]. In order to check the existence of similar relationship of AMPK and RUNX2 even in this transdifferentiation process, we used transdifferentiation of U2OS (osteoblasts) to adipocytes, upon treatment with rosiglitazone showed a loss of AMPK activity and reduced RUNX2 levels during differentiation process (Figure 15). Collectively, these findings suggest that AMPK-mediated RUNX2 phosphorylation is essential for maintaining the osteocytes, and loss of its activity could potentially lead to adipogenesis.

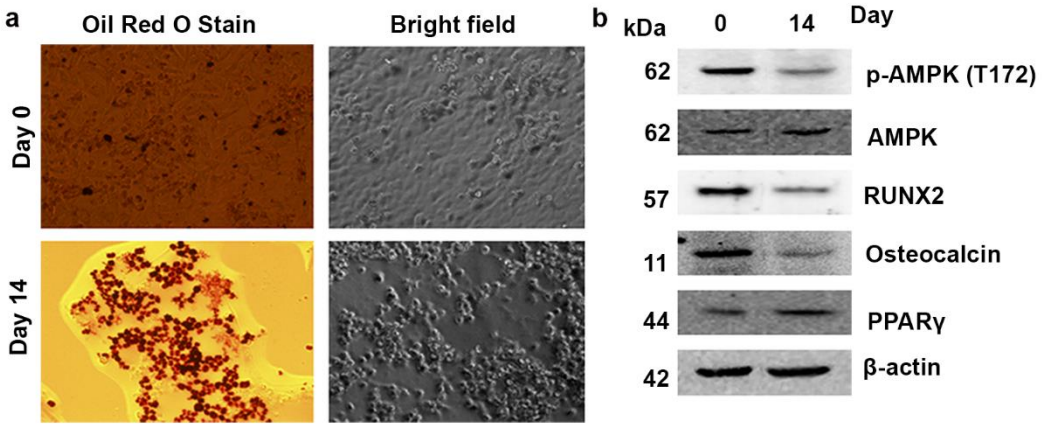

Figure 15: Transdifferentiation of osteocytes to adipocytes: The differentiation of osteocytes (U2OS) to adipocytes after induction with adipogenic medium containing charcoal stripped FBS (10%) and rosiglitazone (1μM) for 14 days, **(a)** the Oil Red O staining confirms the adipogenesis. **(b)** The differentiated and undifferentiated adipocyte lysates were subjected to western blotting and probed with p-AMPK, AMPK (total), RUNX2, PPARγ, and osteocalcin antibodies.

3.1.7. High glucose-induced loss of RUNX2 phosphorylation is associated with loss of active AMPK

Reduced AMPK activity is associated with elevated levels of glucose in various cells and tissues[168]. As results from our earlier study suggest that AMPK activity is associated with RUNX2 protein level, here we investigated the effects of high glucose (HG) on RUNX2-S118 phosphorylation and its effects on adipogenic model. MSCs were exposed to low glucose (5.5mM), standard adipogenic-induced medium with 25mM glucose and high glucose (44mM) conditions as described in methods and observed for triglyceride formation and adipogenesis. Oil Red O staining (Figure 16a - b) revealed that MSC exposed to high glucose (25 and 44 mM) became more adipogenic with high levels of triglycerides as compared to low glucose with adipogenic induction medium (5.5 mM glucose). The p-AMPK and RUNX2 protein level were decreased in high glucose induced (25 mM) differentiation when compared with normal level of glucose (5.5 mM) (Figure 16c). The mRNA levels of RUNX2, PPARγ and AdipoQ were also correlated with adipogenesis (Figure 16e). Which shows that chronic hyperglycemia favoring the adipogenesis. Further immunoprecipitation with RUNX2 on lysates of MSCs (C3H10T1/2), differentiated with normal (5.5mM) *vs* high (25mM) glucose blots probed with phosphor-specific AMPK substrate antibody suggested that AMPK-mediated RUNX2-S118 phosphorylation is the key modulator of differentiation process during diabetes (Figure 16d). Thus these results suggest that exposure to physiological glucose levels maintains optimal AMPK activity and RUNX2 stabilization, which favors the homeostasis of osteogenesis *vs* adipogenesis.

3.1.8. High glucose microenvironment favors adipogenesis through RUNX2 & AMPK activity in BM-MSCs

Our previous study suggest that AMPK activity & RUNX2 protein levels is closely associated glucose concentration, here we further investigated the effects of high glucose (HG) on RUNX2 and its effects on BM-MSC adipogenic model. BM-MSCs were exposed to low glucose (5.5mM), standard adipogenic-induced medium with 25mM glucose and high glucose (44mM) conditions as

described in methods and observed for triglyceride formation and adipogenesis. Oil Red O staining (Figure 17a & b) revealed that BM-MSCs exposed to high glucose (25 and 44mM) became more adipogenic with high levels of triglycerides as compared to low glucose with adipogenic induction medium (5.5mM glucose). The p-AMPK and RUNX2 protein level were decreased in high glucose induced (25mM) differentiation when compared with normal level of glucose (5.5mM) (Figure 17c). Which shows that chronic hyperglycemia favoring the adipogenesis. Thus these results suggest that exposure to physiological glucose levels maintains optimal AMPK activity and RUNX2 stabilization, which favoring the homeostasis of osteogenesis *vs* adipogenesis

Figure 16: The effect of high glucose on adipogenic differentiation: Mesenchymal stem cells (C3H10T1/2) were

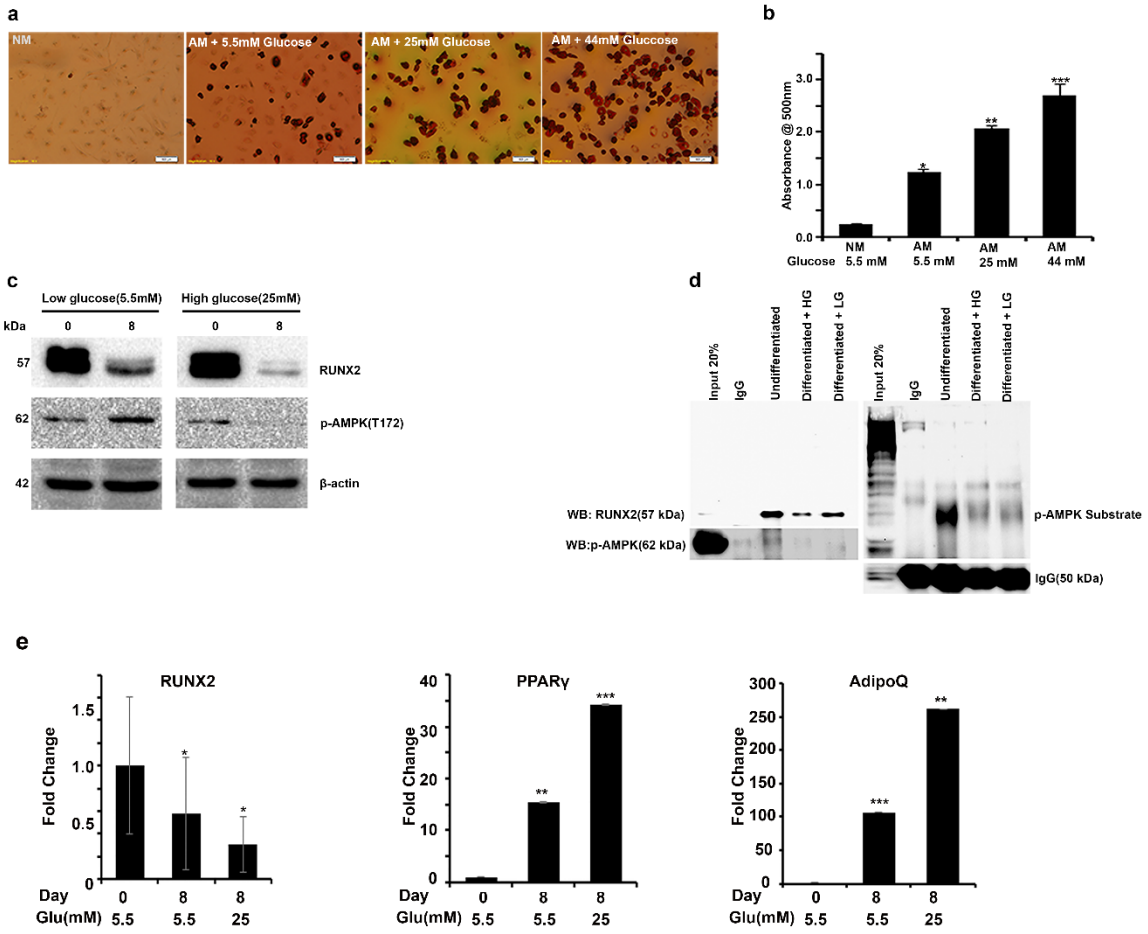

exposed to various indicated concentrations of D (+) glucose along with adipogenic inducers 0.5mM IBMX, 20nM insulin, 5mM dexamethasone (Sigma) for 48 hrs and then they were incubated with growth medium having 20nM insulin, D (+) glucose continued for 8 days. (**a**) On day 8 the adipogenesis was measured by Oil Red O staining. (**b**) The Oil Red O stain was eluted with 100% isopropanol and estimated absorbance at 510nm (**c**) The protein levels of p-AMPK, RUNX2, was analyzed by western blotting. (d) The RUNX2 was immunoprecipitated from the lysates of

differentiated with 5.5mM (normal) and 25mM (high glucose) glucose variables vs undifferentiated and the immunocomplexes were probed with AMPK substrate specific antibody. (e) The RNA levels of RUNX2, PPARγ and AdipoQ were quantified. Mean ± S.E.M.; n=3, *p<0.1 versus 0 day, **p<0.05 versus 0 day; ***p<0.001 versus 0 day

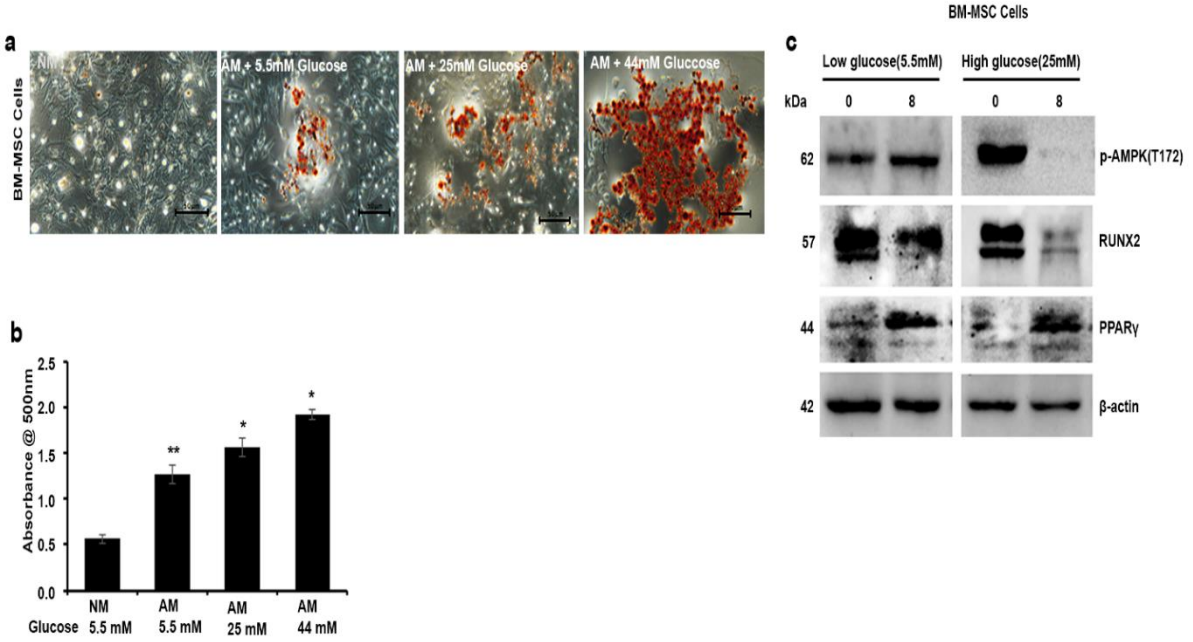

Figure 17: MSCs (BM-MSCs) were exposed to various indicated concentrations of D (+) Glucose along with adipogenic inducers. (**a**) Oil Red O stain shows glucose concentration (25 & 44mM) dependent increased adipogenesis compared with normal glucose (5mM) and without adipogenic-induced medium (NM). **(b)** Representative picture showing the quantitative measurement of Oil Red O stain eluted with 100% Isopropanol (n=3). (**e &f**) Western blot analysis of p-AMPK and RUNX2 shows loss of AMPK activation and RUNX2 protein stability in high glucose-treated cells.

3.1.9. Streptozotocin-induced diabetic bone adipogenesis is abrogated by pharmacological activation of AMPK by metformin

Many recent studies demonstrated that diabetic animal models generate adequate amount of mesenchymal stem cells whereas they fail to differentiate towards to osteogenesis due to down regulation of RUNX2 and Dlx5 which leads to skeletal disorders such as bone adipogenesis[117, 121]. Defect in insulin secretion in IDDM is associated with bone loss through the blocking of Wnt signaling and Akt inactivation [169].

Our previous studies shoes that upon exposure to high glucose favors adipogenesis by modulating RUNX2 protein level by AMPK. In line with these observations, long-term treatment with AMPK activators, metformin in chronic diabetic patients were shown to be less adipogenic and had healthy bones as compared to diabetic patients who are on other treatments[170]. Next, we

explored the correlation between RUNX2 protein level and AMPK activity upon pharmacological exposure to metformin in streptozotocin-induced diabetic mice to reinstate their association *in vivo*. Histological sections of tibiae from streptozotocin-induced diabetic animals showed high levels of adipogenic as compared to control mice, whereas 10 weeks exposure of metformin

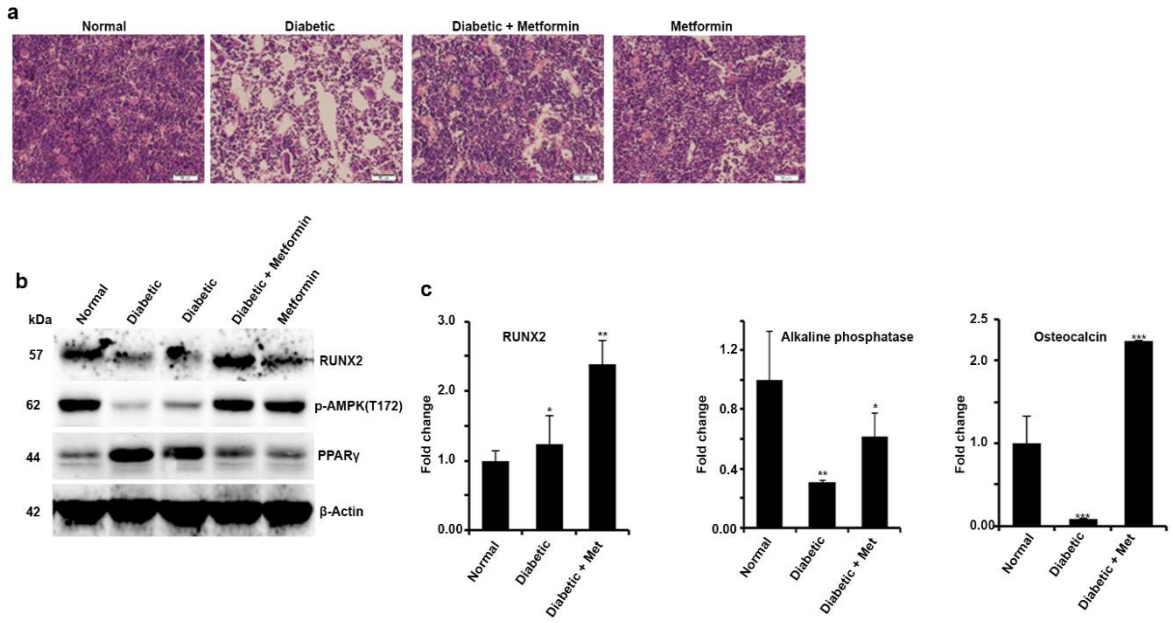

abrogated diabetes induced bone adipogenesis (Figure 18a).

Figure 18: Diabetes was induced in 6-8 weeks old BALB/c male mice with streptozotocin followed by a group of diabetic mice were treated with AMPK activator (metformin) remaining control mice and diabetic mice were given with saline (N=5) (a) Histological images of normal, diabetic and metformin treated, bone adipogenesis was observed by H&E staining . (b) (c) Isolated bone marrow mesenchymal cells and the cell lysates probed with indicated specific antibodies. (d) The RNA was isolated, measured RUNX2, PPARγ and AdipoQ, Osteocalcin RNA expression levels. Mean ± S.E.M.; n=3, *p<0.1 versus normal control, **p<0.05 versus normal control; ***p<0.001 versus normal control.

Western blot and real time PCR analysis of cells isolated from bone marrow showed that metformin treatment stabilized RUNX2 protein level and correlated with p-AMPK and other adipogenic *vs* osteogenic markers (Figure 18b). The gene expression (mRNA) of osteocalcin and alkaline phosphatase levels in bone marrow cells explained the decreased osteogenic markers in diabetes except RUNX2 (Figure 18c). To further explore these observations, micro-computed tomography analysis of limb bones of mice treated with metformin for 10 weeks were visualized, which revealed that longitudinal and cross sectional tibias shows increased bone health in metformin treated animals (Figure 19a-d). Collectively, these findings for the first time conclude

that correlation of healthy bones in patients who are on metformin is through stabilization of RUNX2 via active AMPK and loss of this balance leads to bone adipogenesis.

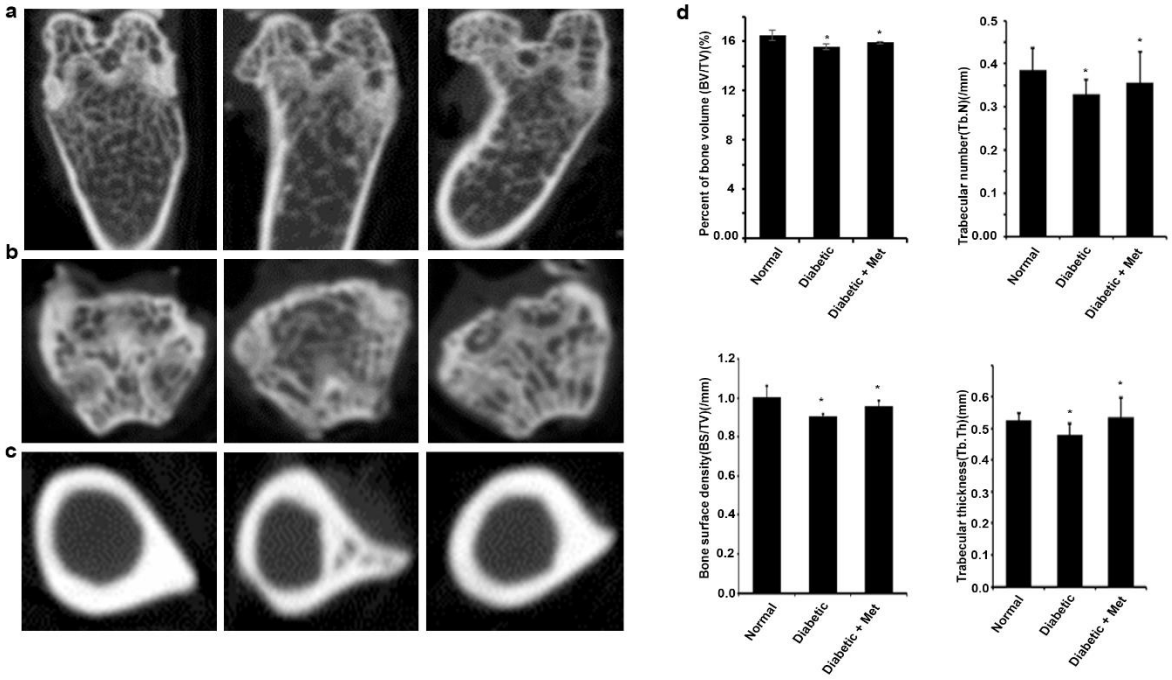

Figure 19: μ-CT image analysis showing (b) longitudinal (c) transaxial and (d) cortical midshaft on tibia of hind limbs. The histomorphometric parameters are expressed as (e) the change in percentage of bone volume (BV/TV), trabecular number (Tb.N), bone surface density (BS/TV) and trabecular thickness (Tb.Th). Mean ± S.E.M.; n=3, *p<0.1 versus normal control, **p<0.05 versus normal control; ***p<0.001 versus normal control.

Discussion

4.1. Discussion

RUNX2 (Osf2/Cbfa1, AML3 or Pebp2αA) is a transcription factor has shown a pivotal role in regulation of cartilage and osteoblastic differentiation. RUNX2 induces the expression of osteocyte lineage specific genes such as alkaline phosphatase, osteocalcin, osteopontin, and type1 collagen by binding to its osteocyte specific responsive elements (OSE) on their promoters[90] [99]. Loss of bone mass in $RUNX2^{-/-}$ mice is associated with decreased mature osteoblast [171]. It has been shown that RUNX2 and osteoblast specific gene expression is down regulated in diabetic patients as well as in animal models [113]. However, the mechanisms for RUNX2 down regulation are not known. In the current study, we have demonstrated a distinct mechanism employed by RUNX2 and its post translational modifications during osteogenic vs adipogenic differentiation, where AMPK acts as a key kinase that has major influence on mesenchymal stem cell differentiation.

The worldwide prevalence of diabetes is enormously increasing as a consequence of ageing and modern lifestyle. The epidemiology of the diabetic patients around the globe over past three decades witnessed two fold increase of disease burden. According to international diabetic federation (IDF) based on reports in year 2017, it is been estimated that world diabetic burden will increase to 439 million people by 2045[172]. Surprisingly, the numbers have reached to 451 million by recent reports of IDF-2017. It is also reported that about 79% of are from low and middle income countries. That means that about 727 billion USD are spending on diabetic health care globally (IDF-2017). Diabetes is mainly described as hyperglycemia with chronic and relative insulin resistance. This chronic hyperglycemic microenvironment is associated with many complications, which results in microvascular (retinopathy, nephropathy, and neuropathy) as well as macrovascular complications (cardiovascular complications). Apart from these vascular complications, hyperglycemia also induces bone anomalies such as bone adipogenesis, osteoporosis.

The mesenchymal stem cells (MSC) are multipotent stromal cells that reside in bone marrow microenvironment. MSCs differentiates to various cell types such as adipocytes, osteocytes, chondrocytes, myoblasts, skin cells, etc. Each lineage specific MSC differentiation is regulated by set of transcription factors and signal mediators. Among them osteocytes and adipocytes are two major important cell types that are been well studied in relevance with physiological context. It

has been reported that osteocyte and adipocyte differentiation is reciprocally regulated by two specific transcription factors RUNX2 and PPARγ respectively, however the molecular mechanisms are not defined clearly [73]. In the current study we have explored to understand how RUNX2 is regulating the osteogenic vs adipogenic differentiation in normal as well as diabetic animal models.

AMP-activated serine threonine protein kinase (AMPK) is a master regulator of cellular energy metabolism, ubiquitously expressed throughout the body. AMPK is a hetero trimeric protein with three subunits α, β, and γ that regulate various physiological functions. . The AMPK is activated by phosphorylating at T172 α-subunit of kinase domain. It has been identified that AMPK is regulated by two upstream kinases, calcium/calmodulin-dependent protein kinase kinase (CaMKK) b and LKB1 in the cascade. The AMPK regulate a wide array of metabolic processes such as glucose uptake, mitochondrial biogenesis, fatty acid oxidation, protein synthesis and autophagy and also inhibits the fatty acid synthesis, cholesterol biosynthesis, and protein synthesis [138]. The dysregulation of AMPK play a critical role in diabetes induced pathogenesis and insulin resistance in humans and rodent animal models. AMPK modulators (metformin) are widely used in treatment for diabetes [139]. In this report we have demonstrated that AMPK mediated deregulation of RUNX2 protein stability is responsible for bone adipogenesis in diabetic animal models.

Using an *in silico* methodologies we have identified RUNX2 is a novel substrate of AMPK (Table 2 & 3), having highly conserved kinase motif across RUNX family proteins, species (Table 5) and also with other known substrates of AMPK (Table 4). So far, its been reported that AMPK activation (phosphorylation (T172) by LKB1 significantly inhibits the adipogenesis in 3T3-L1 pre-adipocytes [173]. AMPK phosphorylation of ACC down regulates the lipogenesis by increasing the energy metabolism there by inhibits the lipid accumulation in 3T3-L1 cells [174]. Activation of AMPK also promotes the development of brown and beige adipose phenotype of C3H10T1/2 cells [175, 176]. Haploinsufficiency of AMPKα1 intimidated the brown adipogenesis [177]. However, the molecular targets of AMPK signaling is not clear. Based on cited literature, we hypothesized that AMPK might be regulating RUNX2 there by inhibiting adipogenesis by promoting osteogenesis. Based on this hypothesis and our *in silico* predictions, our *in vitro* phosphorylation (Figure 10a & b), immunoprecipitation assays confirmed the RUNX2 is the substrate of AMPK and phosphorylates by physical interaction (Figure 10c & d). The same has been confirmed by visualizing of colocalization in our immunofluorescence studies (Figure 10e).

In addition, the pharmacological activation of AMPK and its upstream kinases with metformin and AICAR showed increased interaction of AMPK with RUNX2 in contrast to AMPK inhibitor (Compound C). We further observed increase in RUNX2 protein levels upon pharmacological activation of AMPK indicates that AMPK activity is essential to maintain RUNX2 protein levels. Our results strongly supports the earlier observations where AMPK activation promotes osteogenesis [178]. The basal activity might be essential for adipogenesis whereas the activation of AMPK with metformin can inhibit adipogenesis by promoting osteogenesis through AMPK-dependent and independent mechanisms[179].

Years of research has made it clear that the osteogenic and adipogenic processes from MSC are reciprocally regulated[73]; for instance, BMP2 at high concentration induces osteogenesis whereas low concentrations induces adipogenesis[180]. AMPK is sufficient to stimulate osteogenesis of MC3T3-E1 cells at the cost of adipogenesis; but lack of AMPK leads to adipogenesis [178]. However, the exact molecular mechanisms underlying the reciprocal relationship in cell fate commitment and transdifferentiation during altered metabolic (pathogenic) conditions are yet to be elucidated. Our findings mechanistically demonstrate that the identified AMPK specific phosphorylation of RUNX2 (S118) is driving the mesenchymal stem cells into osteocytes over adipocytes. We have shown the down regulation of RUNX2 and AMPK activity synergistically correlates in preadipocyte to adipogenic differentiation (Figure 11b & c). Whereas, the same synergistic up regulation of AMPK and RUNX2 was seen during osteogenic differentiation (Figure 11a), which indicates that AMPK modulating the RUNX2 expression during osteogenesis as well as adipogenesis. However, the total AMPK levels and RUNX2 RNA level were unchanged (Figure 11d). These results indicated us that the regulation of RUNX2 might be at post translational level. Further we also observed that presence of AMPK activators (AICAR & metformin) inhibits the adipogenesis by maintaining the RUNX2 protein levels in *in vitro* MSCs (C3H10T1/2 & BM-MSCs) to adipogenic differentiation models (Figure 12 & 14). Further our immunoprecipitation results shows that RUNX2 phosphorylation at S118 in metformin treated samples indicates that AMPK induced phosphorylation maintains RUNX2 protein levels (Figure 12d). It is reported that terminally differentiated osteocytes and myocytes can also dedifferentiate to adipocytes upon altered external stimuli, and that could be seen in the modified metabolic conditions such hyperglycemia [167]. Similar correlation was evident in transdifferentiation models, viz. myocytes to adipocytes, osteocytes to adipocytes and pre-adipocytes to adipocytes. These studies correlate with our hypothesis that active AMPK helps in reducing adipogenesis and

maintaining healthy bone, and also explains that RUNX2 being a substrate of AMPK may act as a regulatory connection between energy homeostasis and osteoblast development. The transdifferentiation studies confirm the adipogenic process in altered metabolic conditions; however, it should be carefully considered that metformin and compound C studies have revealed AMPK may maintain a homeostasis of osteocytes *vs* adipocytes where low levels of AMPK may favor adipogenesis, whereas high levels of AMPK may lead to osteocytes by stabilizing RUNX2 protein. This was evident from the fact that there was minimal activity of p-AMPK (T172) at all times as seen from our studies as well as by other investigators[136]. As mRNA levels of RUNX2 are maintained in both the differentiation processes, there is an indication that dynamic and sequential regulation at translational or post-translational levels may exist. The transdifferentiation of osteocytes to adipocytes with rosiglitazone which is another well-known antidiabetic drug from thiazolidinedione class, showed down regulation of RUNX2 protein along with loss of active AMPK (Figure 15). Together these data demonstrates that RUNX2 expression might be modulating through the AMPK activity, where as in metabolic disorders loss AMPK activity and energy homeostasis, resulted in clinical observations of fragile bones and bone marrow adipogenesis. Our results correlates with clinical reports where patients who are thiazolidinedione for antidiabetic therapy reported shown fragile bones and more bone adipogenic than metformin.

RUNX2 and PPARγ are two critical transcription factors involved in osteogenesis and adipogenesis from mesenchymal stem cells respectively [181, 182]. $RUNX2^{-/-}$ mice failed to differentiate into osteocytes but spontaneously committed towards adipose tissue[181], whereas, $PPAR\gamma^{-/-}$ mice showed impaired adipogenesis but formed osteocytes [84]. Differentiation models explained that PPARγ is expressed early in the adipocyte differentiation program similarly, RUNX2 expression is seen all through mesenchymal condensation representing the common precursors of osteoblasts and chondrocytes. However, the RUNX2 expression is maintained in cells derived from osteoblastogenesis but lost in chondrocytes-derived cells, thus RUNX2 may not be critical for later stage maturation of osteoblasts to osteoclasts. These demonstrations indicate that regulatory signals are involved in the differential commitment process. It is known that increased PPARγ activity is observed during decreased levels of AMPK expression and favors fat cell development. Our results further showed that active AMPK is responsible for stability of RUNX2 by regulating at post-translational level, and these observations are correlated with commitment of osteogenesis. Thus, these results give us a hint that AMPK senses the cellular

metabolic energy and regulates the homeostasis of RUNX2 *vs* PPARγ, which directs the MSCs into osteoblasts *vs* adipogenic commitment.

Earlier reports shows that AMPK is minimally functional in diabetic individuals and loss of AMPK activity is associated with chronic hyperglycemia. Signaling integrations of AMPK regulate the energy nutrients (amino acids, free fatty acids and glucose) and metabolic stress to control the cellular metabolism [144]. Further we have studied the adipocyte differentiation varying with glucose concentrations. Surprisingly we have observed that enhanced adipogenesis with increasing glucose (high glucose) concentration. Indicating that diabetes induced hyperglycemia drive the mesenchymal stem cells more towards adipocytes. Further we have also observed that hyperglycemic (25mM) induced downregulation of RUNX2 compared to normal glucose (5.5mM)(Figure 16 & 17) in C3H10T1/2 and BM-MSCs. Whereas, the RNA levels of RUNX2 is not altered (Figure 16e). Indicating that protein levels are modulated at post translational level. Thus we show that hyperglycemia mediated RUNX2 down regulation is responsible for progression of adipogenesis rather osteogenesis of mesenchymal stem cells.

From a clinical perspective, hyperglycemia positively regulates adipogenic differentiation by inhibiting osteogenic variation in muscle-derived stem cells [183] and it is also shown to activate polyol pathway and decreasing the DNA-binding affinity of RUNX2 [120]. Metformin-induced osteogenesis and mineralization in OCT-1 expressing iPSC derived MSCs demonstrated its potential use for enhanced bone and periodontal regeneration in diabetic patients [184]. Epidemiological clinical data suggests that long-term administration of metformin reduces bone adipogenesis and resorption [170], similarly use of thiazolidinediones (TDZ) has been reported to show reduced bone mineral density and activation of PPARγ induced osteoclastogenesis [185]. Based on above clinical and experimental evidences, we investigated role of AMPK and bone adipogenesis in connection with RUNX2 phosphorylation using streptozotocin-induced diabetic mice model.

μCT image analysis of hind limbs shows comparatively better healthy bone architecture in the metformin group compared to the diabetic controls (Figure 19). This analysis correlated with the active AMPK and RUNX2 protein levels in bone marrow cells and further with bone adipogenesis in sections of tibia (Figure 18). Our studies are associated with earlier observations that *in vitro* model of bone formation using primary osteoblasts shows metformin, and AICAR treatments stimulated bone nodule formation whereas compound C ameliorated the mineralization. It has

been demonstrated that RUNX2 expression is controlled by both transcriptional as well as translational levels. Our real-time PCR experiments highlight the maintenance of RNA levels in both *in vitro* adipogenic differentiation as well as in diabetes-induced Streptozotocin model of bone marrow cells. Significantly low levels of RUNX2 protein gives us an indication of the existence of regulation at translational level during this differentiation process.

RUNX2 is also known to be regulated by GSK3β [186] [187], JNK[188], Cdk4[189], Cdk1[190] and cdc2 [120]. Although GSK3 β and JNK share the same serine118 as the kinase target for phosphorylation, but do not demonstrated its functional consequences in relation with differentiation [188]. However, genetic knockdown of GSK3 β has shown that RUNX2 phosphorylation by GSK3 β inhibits the transcriptional activity and osteogenesis [186]. These studies have shown that specific phosphorylation occurs in inhibitory transactivation domain rather than DNA-binding domain where S118 is sited. Similarly studies have shown that metformin suppresses adipogenesis by both AMPK-dependent and independent mechanisms, whereas in exercise-induced model, mTORC2 has shown to be critical in muscle glucose uptake independent of AMPK [136]. These findings demonstrate that interpretation of metformin actions on osteogenesis *vs* adipogenesis needs to be taken into consideration; however, AMPK has proven critical in maintaining the homeostasis.

In conclusion, our results demonstrated that RUNX2 is a novel substrate of AMPK and RUNX2-S118 phosphorylation, which also protects it from ubiquitination. Stress (tunicamycin, hyperglycemia) induced degradation of RUNX2 depends upon active levels of AMPK. Clinical correlation of metformin restricts diabetes-induced bone adipogenesis, might be due to stabilization of RUNX2. (Figure 24) Overall, AMPK plays a critical role in maintaining the RUNX2 and PPARγ expression and cellular energy levels thereby regulating the differentiation of osteogenesis *vs* adipogenesis.

Chapter 2

Introduction

5.1. Introduction

5.1.1. Understanding the Role of RUNX2 in metabolic stress

In diabetes the insulin deficiency (Type1) or insulin resistance (Type 2) cause hyperglycemia. The chronic hyperglycemia constant stimulation of pancreatic β-cells leads continual downregulation of insulin secretion. As the consequence of chronic diabetic hyperglycemia, glucose serves as a precursor for many harmful metabolites of pancreatic β-cells [191]. Glucotoxicity is one of the major cause for the generation of Reactive oxygen species in various metabolic reactions such as glucose oxidation, mitochondrial oxidative phosphorylation and sorbitol metabolism [192]. Cellular metabolism is majorly depends on the endoplasmic reticulum homeostasis, whereas in metabolic disorders accumulation of Advanced glycation end products (AGEs) which are the primary cause of unfolded protein response and its pathological mechanisms contribute various secondary complications[193]. However the majority of these disorders are containing a classical feature is endoplasmic reticulum stress.

Many clinical and preclinical studies reveals that endoplasmic reticulum and oxidative stress have significant implication on the pathophysiology of metabolic disorders such as insulin resistance(IR), diabetes, atherosclerosis, non-alcoholic fatty liver disease (NFLD) and obesity[194-196]. A recent understanding of the molecular mechanisms clarified that β-cell dysfunction in diabetes is associated with ER stress induced by glucotoxicity [196]. Still some controversies persist in the field weather chronic hyperglycemia are the major cause of ER stress by inducing PERK phosphorylation [197]. Recent growing evidences shows that β-cell dysfunction and death by unresolvable ER stress [198]. However, additional studies is crucial to understand how the chronic hyperglycemia and free fatty acids disrupt ER functions and how it affect the cellular events. Recent studies sows that RUNX2 is critical in the course of H2O2 mediated oxidative stress induced osteocyte specific lineage progression and calcification through Akt signaling in VSMC cells[199]. In contrast Chia Hua Lin et.al. shown that H2O2 induced oxidative stress favors adipogenesis through SIRT1 mediated regulation of specific transcriptional cofactors[200].
In the current study we explored that bone morphogenic protein RUNX2 sensitizes to ER stress and we also shown an essential role of AMPK activation in restoration of RUNX2 protein levels in ER stress C2C12 myoblast as well as C3H10T1/2 cells. AMPK induced RUNX2 S118

phosphorylation (RUNX2-S118D) protects from stress induced RUNX2 degradation in ectopically expressed HEK 293T cells.

Objectives

Many clinical and preclinical studies reveals that endoplasmic reticulum and oxidative stress have significant implication on the pathophysiology of metabolic disorders such as insulin resistance(IR), diabetes, atherosclerosis, non-alcoholic fatty liver disease (NFLD) and obesity. It has been established that RUNX2 and osteoblast specific gene expression is down regulated in diabetic patients as well as in animal models. Our studies in Chapter-1 showed that, energy homeostasis plays a critical role in regulation of RUNX2 through AMPK modulation. There are several reports that under physiological stress due to various factors including diabetes, alters the activity of AMPK, however the mechanisms of stress response on AMPK mediated RUNX2 and it's significance in adipogenesis is still elusive. In this chapter to address the significance of physiological stress on adipogenesis, the following objectives were designed.

- Investigating the role of RUNX2 in metabolic stress (ER stress).
- Deciphering the role of AMPK mediated RUNX2 phosphorylation (S118) and its regulation in ER stress models.

Materials and Methods

6.1. Materials and methods

6.1.1. Reagents and antibodies

The antibodies used in this study were: RUNX2, Bip1, p-AMPK and β-Actin were procured from Cell Signaling technology, USA. Ubiquitin (Santa Cruz Biotechnology, USA). The reagents used in this study are: tunicamucin, thapsigargin, rotenone, metformin, compound C and AICAR are procured from sigma Aldrich, USA. All the media, antibiotics, transfection reagent (Lipofectamine2000) and other cell culture supplements are procured from Invitrogen USA. All the restriction enzymes used in cloning were purchased from New England Biolabs, UK.

6.1.2. Plasmids

The full length RUNX2 was amplified using the ORF as a templet, obtained from genecopiea ((H5214) by polymerase chain reaction using specific primers (Table 1). The RUNX2 gene was cloned into a RFP-reporter mammalian expression vector, Ds-Red-N1 inserting the restriction sites *XhoI* and *BglII* in Forward and reverse primers respectively. The RUNX2 mutants (RUNX2-S118A & RUNX2 S118D) were generating using the overlap PCR method (described in methods chapter 1) with site specific mutational primers (Table 1).

6.1.3. Cell culture & treatments

The experiments were conducted using C2C12, HEK 293T and C3H10T1/2 cell lines procured from American Type Culture Collection (ATCC), USA. Cells were cultured in DMEM (HEK 293T & C2C12) and Alpha-MEM (C3H10T1/2) growth medium supplemented with 10% FBS, L-Glutamine (2mM) 100 U/ml Penicillin (100 U/ml) and streptomycin (100 U/ml) in 5% CO_2 at 37^0C in humidified incubator. All the Transfections was done at 60% confluency along with specific expression plasmids using lipofectamine2000 (Invitrogen USA) as per the manufacturer's guidelines.

6.1.4. Confocal microscopy

C2C12 cells were seeded on coverslips treated with tunicamycin (5μg/ml), metformin (5mM), AICAR (0.5mM) and compound C (20μM) with indicated time points. Control were treated with vehicle. Post treatment the cells were fixed with 4% formalin followed by washed with phosphate

buffer saline (PBS) thrice. The permeabilization was done using 0.1% Triton X-100 for 10 min followed by washed the cells with PBS thrice. The blocking was done for 30 min using 3% bovine Serum albumin (BSA) to avoid the non-specific interaction of antibodies. Later removed the blocking solution the primary antibody was added on the coverslip covered by parafilm to evenly distribute the antibody for 2 hours. After primary antibody incubation the cells were washed using PBS, cells were stained with corresponding secondary antibodies conjugated with Alexa flour 488(green) and alexa flour 594(red) for 2 hours having different excitation wavelengths. Followed by washed with PBS thrice to remove the non-specific interaction of antibody and to minimize the background fluorescence. Finally the coverslips were mounted using antifade DAPI followed by sealed with nail polish to prevent drying. Analyzed the slides using confocal laser scanning microscopy (ZEISS LSM 800).

6.1.5. Western blotting

For immunoblotting analysis, the cells were lysed in RIPA buffer (pH-7.4 Tris-HCl (50mM), NaCl (150mM), deoxycholic acid (1%), Triton X-100 (1%), EDTA (0.25mM) and SDS (0.1%) along with Protease and phosphatase cocktail inhibitor(Roche, Switzerland). The protein estimation was done by using Bradford assay reagent. The equal amount of protein was loaded on SDS-PAGE. The resolved proteins were transferred into nitrocellulose membrane followed by probed with indicated antibodies. The immunoblots were developed and documented by using Bio-Rad ChemiDoc touch imaging system.

6.1.6. Transfection

The adherent cells (HEK293T) cells were procured from ATCC. Cells were seeded with about 5 X 10^5 cell density in 60mM culture wells and the cells were cultured in DMEM 10% FBS (fetal bovine serum) and 100U/ml of penstrep. The cells were cultured until 50% confluency at 37^0C with 5% CO_2 in a humidified chamber. The cells were transfected with Lipofectamine2000 in Opti-MEM media containing 3µg of each plasmid. After 6 hrs the medium was replaced with complete medium (DMEM 10% FBS with 100U penstrep). The cells were maintained for 24-48 hours and observed the reporter expression.

6.1.7. RNA isolation

The total RNA was isolated using trizol reagent (Invitrogen). Post treatments the cells were harvested in 1 ml of trizol reagent. Followed by aqueous phase was separated by using 200 µl of chloroform/ 1ml of trizol by vigorous shaking followed by 10 min incubation on ice. Spin the samples at 13000 rpm for 10 min the aqueous phase was separated into a new tube and RNA was precipitated by addition 1 volume of 100% isopropanol keeping at -80 for an hour. After an hour centrifuged at 13000 rpm for 10 min at 4^0c. The RNA pellet was washed with 75% ethanol. Followed by the pellet was air-dried in room temperature for 10 min and resuspended in RNAse free DEPC treated water. The RNA was quantified with Nanodrop against blank. About 1 µg of RNA used for cDNA preparation. The cDNA was synthesized using iScript™ cDNA Synthesis Kit (BioRad, CA, USA.) as per the manufactures protocol.

6.1.8. RT-PCR

The RT-PCR reaction was set per well containing 5 µl of SYBR green master mix (2X) (iTaq Universal SYBR Green Supermix), 10 µM of each primer (forward and reverse), and 50ng of cDNA was used. Set up each reaction in triplicates along with no templet control and the PCR program was used according to manufactures protocol along with 60^0c annealing temperature. β-actin used as internal loading control to normalization of CT values. All the reactions was performed using CFX96 Touch™ Real-Time PCR Detection System.

6.1.9. Statistical Analysis

The data values are articulated as mean ±. SEM statistical analysis was performed using student T-Test. The differences between the mean values were analyzed using student T-Tests when P value lesser than 0.05 was considered as statistically significant. For all cell culture studies, a minimum of three independent experiments were carried out.

Results

7.1. Results:

7.1.1. RUNX2 down regulates in ER stress and oxidative stress

Exposure to high glucose and Streptozotocin-induced diabetes models show that stabilization of RUNX2 depends upon AMPK activation, and our *in vitro* kinase assays showed that AMPK phosphorylates RUNX2 at S118. However, the role of serine 118 on the synergistic correlation of AMPK and stabilization of RUNX2 is still uncertain. It is well established that impaired glucose tolerance and T2DM induces Endoplasmic Reticulum (ER)[201] and oxidative stress[202]. Here, we examined the effects of ER and oxidative stress on RUNX2 protein levels and the mechanisms involved in RUNX2 stabilization. We first studied the effect of tunicamycin; an ER stress inducer on myoblast cells (C2C12) & Mesenchymal stem cells(C3H10T1/2) and observed that RUNX2 protein levels are decreased in time (Figure 20a & f) and dose (Figure 20b & g) dependent manner. We have also observed the consistent results with the thapsigargin (ER stress inducer) (Figure 20c & h). However, RNA levels were unchanged with tunicamycin treatment (Figure 20d & i) Similar results were obtained when we treated with oxidative stress inducers (Rotenone) (Figure 20e & j). Consistently, these data suggest that tunicamycin and thapsigargin induced ER stress downregulates RUNX2 protein levels. Whereas, the RUNX2 transcripts levels are unchanged (Figure 20d & i).

7.1.2. AMPK activation inhibits RUNX2 degradation

Since RUNX2 protein levels are getting down regulated but not RNA levels, this may be due to the post translational regulation of RUNX2. To address this question we have treated the cells with proteosomal degradation inhibitors (MG132). Where we have observed that ER stress induced RUNX2 downregulation was restored upon proteosomal inhibitor treatment (Figure 21a & 22a). Which indicating that RUNX2 is undergoing proteosomal degradation through ubiquitination machinery. Since it is well known that AMPK has significant role in ER stress. AMPK activation suppresses the ER stress through the Tgf-β, aldosterone and high glucose. Metformin also can reduces the ER stress in mouse models [203]. These evidences lead us to study AMPK activation on RUNX2 regulation in ER stress (tunicamycin). We further investigated the Effects of AMPK activation on ER tress and RUNX2 down regulation. To test whether ubiquitin-mediated RUNX2 degradation is in agreement with active AMPK, cells were treated with AMPK activators along with and without proteosomal inhibitors and subjected to Western blot analysis.

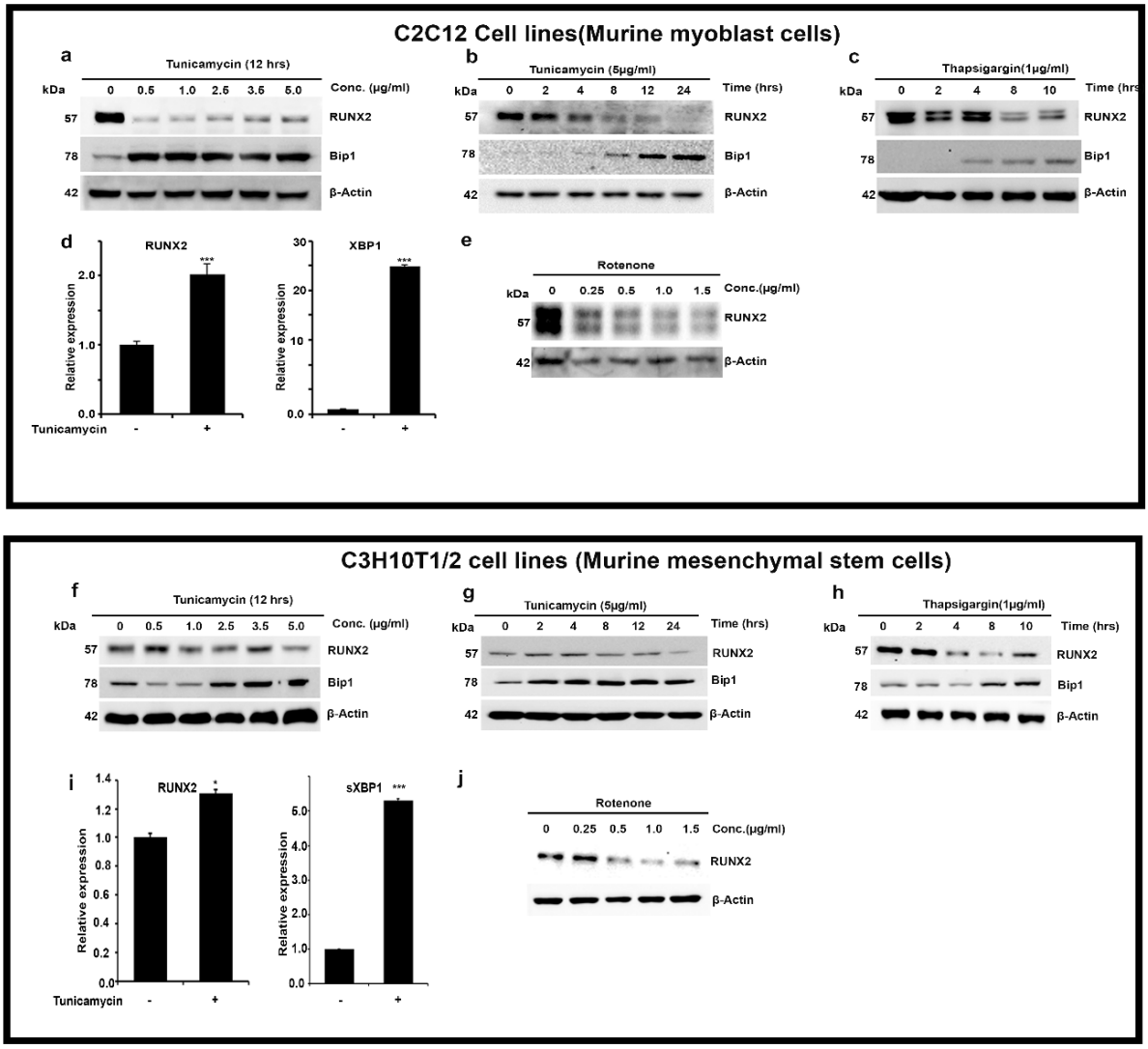

Figure 20: (a) Myoblast cells were treated with tunicamycin by indicated concentrations and subjected to western blotting probed with indicated antibodies (b) Myoblast cells were treated with tunicamycin (5µg/ml) in various time intervals and the cell lysates were probed with RUNX2, BiP1(Stress Marker). (c) Myoblast cells were exposed to thapsigargin (1µg/ml) with different time intervals and RUNX2 and Bip1 protein levels were observed. (d) The mRNA levels of RUNX2 and sXBP1 are measured in tunicamycin treated and untreated cells. (e) Myoblast cells were exposed to oxidative stress (rotenone) and the lysates were subjected to western blotting. (f) Mesenchymal stem cells were treated with tunicamycin by indicated concentrations and subjected to western blotting probed with indicated antibodies (g) Mesenchymal stem cells were treated with tunicamycin (5µg/ml) in various time intervals and the cell lysates were probed with RUNX2, BiP1(Stress Marker). (h) Mesenchymal stem cells were exposed to thapsigargin (1µg/ml) with different time intervals and RUNX2 and Bip1 protein levels were observed. (i) The mRNA levels of RUNX2 and sXBP1 are measured in tunicamycin treated and untreated Mesenchymal stem cells. (j) Myoblast cells were exposed to oxidative stress (rotenone) and the lysates were subjected to western blotting. Mean ± S.E.M.; n=3, *p<0.1, ***p<0.001 versus untreated control.

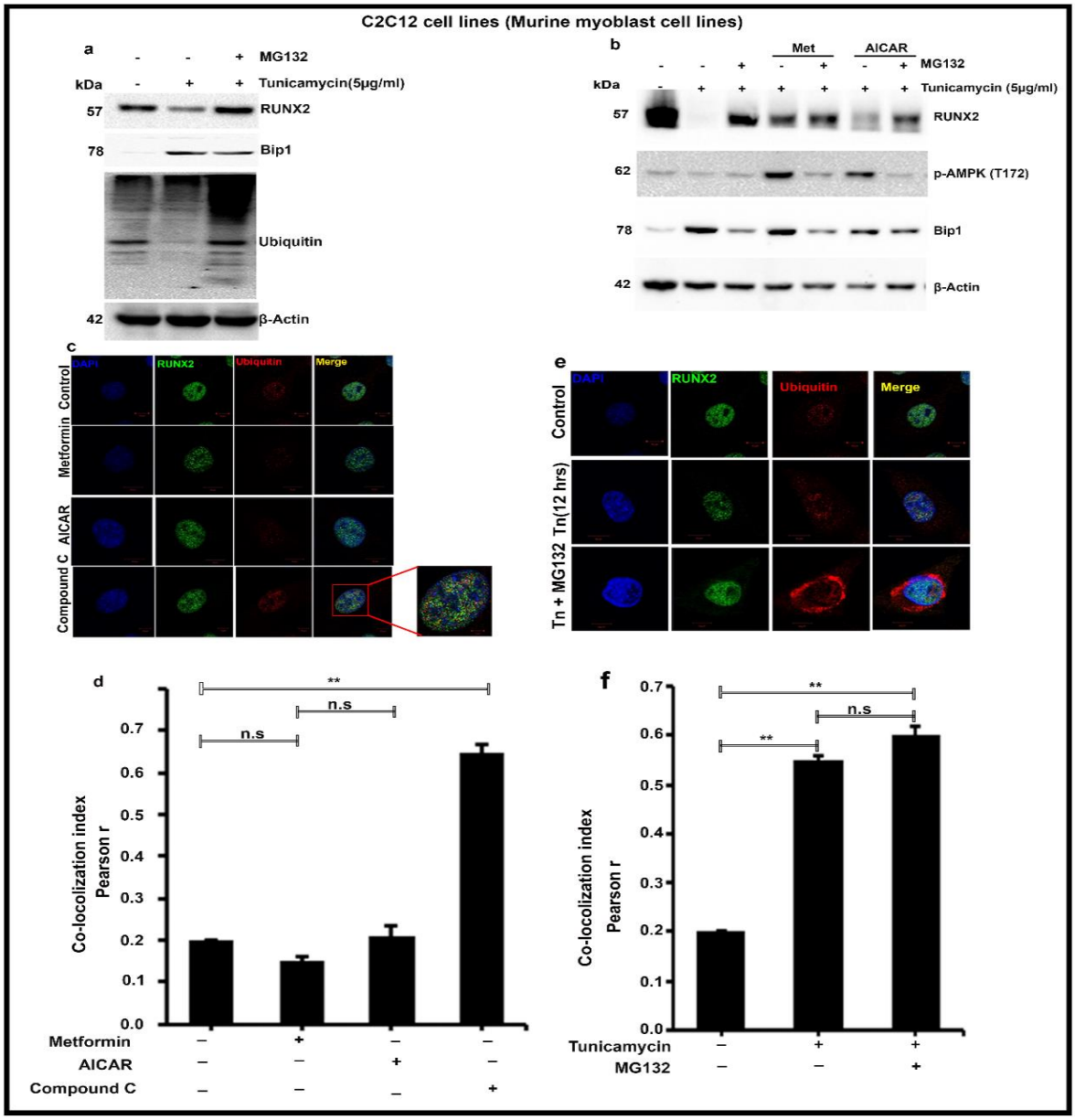

Figure 21: (a) Myoblast cells were pretreated with MG132 followed by tunicamycin treatment. **(b)** Pretreatment with MG132, AMPK activators (AICAR, Metformin) for 60 min followed by treated with tunicamycin (5µg/ml) for 12 hrs. Representative Immunoblotting shows that RUNX2, Bip1, and β-actin expression. **(c)** Myoblast cells were treated with AMPK activators (metformin & AICAR) and inhibitor (Compound C) for 12 hrs and colocalization studies was done with RUNX2 (Alexa Fluor 488) and ubiquitin (Alexa Fluor 546) antibodies. (d) The colocalization was quantified using Image J software. **(e)** The consecutive immunofluorescence analysis was done with control, tunicamycin (5µg/ml) with and without MG132 treated cells for 12 hrs and stained with RUNX2 (Alexa Fluor 488) and ubiquitin (Alexa Fluor 546) antibodies. (f) The colocalization was quantified using Image J software.

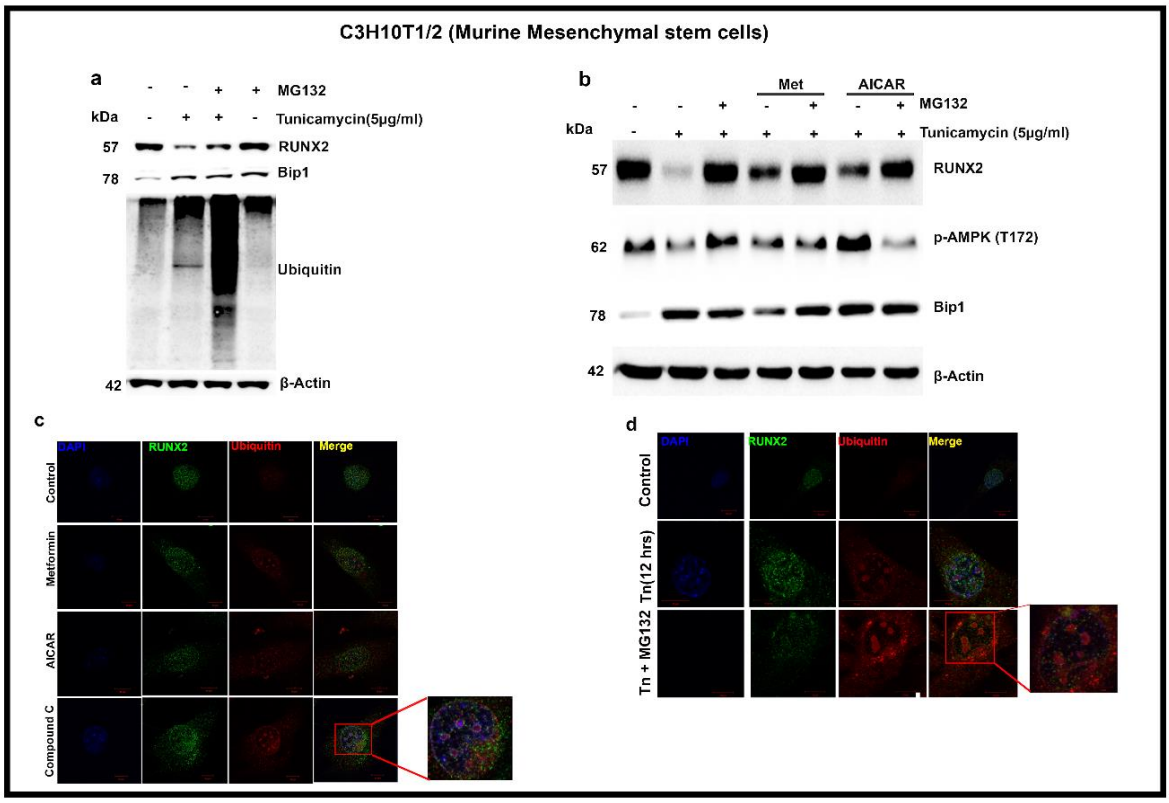

Figure 22: (a) Mesenchymal stem cells (C3H10T1/2) were pretreated with MG132, followed by tunicamycin treatment. **(b)** Pretreatment with MG132, AMPK activators (AICAR, Metformin) for 60 min followed by treated with tunicamycin (5µg/ml) for 12 hrs. Representative Immunoblotting shows that RUNX2, Bip1, p-AMPK and β-actin expression. **(c)** MSCs were treated with AMPK activators (metformin & AICAR) and inhibitor (Compound C) for 12 hrs and colocalization studies was done with RUNX2 (Alexa Fluor 488) and ubiquitin (Alexa Fluor 546) antibodies. (**d)** The consecutive immunofluorescence analysis was done with control, tunicamycin (5µg/ml) with and without MG132 treated cells for 12 hrs and stained with RUNX2 (Alexa Fluor 488) and ubiquitin (Alexa Fluor 546) antibodies.

Treatment with AMPK activators maintained the levels of RUNX2 protein levels and also in the presence of MG132 alone (Figure 21b & 22b). To further confirm these results we have done co-localization studies of RUNX2 and ubiquitin upon the treatment with activators (Metformin & AICAR) and inhibitors (Compound C), which shows that upon inhibition of AMPK activity undergoes RUNX2 interacts with ubiquitin(Figure 21c & 22c). Indicates Loss of AMPK activity undergoes RUNX2 ubiquitination. Which indicates ER stress induced downregulation of AMPK destabilizes the RUNX2 protein levels. We have also induced stress and observed the colocalization of RUNX2 and ubiquitin in stress (Figure 21c & 22d). Collectively, it is revealed that active AMPK is critical for stabilizing RUNX2 levels from proteosomal degradation, which could be due to phosphorylation of S118RUNX2.

7.1.3. RUNX2 S118 phosphorylation protects from stress induced degradation

Our previous results show that AMPK activation is the key factor to maintain RUNX2 protein levels. To further see whether the identified AMPK specific phosphorylation (S118) is essential for RUNX2 stabilization. To confirm this evidential hypothesis, we treated HEK 293T cells overexpressing RUNX2-WT, RUNX2-S118A and RUNX2-S118D with and without tunicamycin. It was revealed that ER stress-induced degradation of RUNX2 is not affected by phosphomimetic RUNX2-S118D over-expressed cells whereas degradation was observed in RUNX2-WT and RUNX2-S118A expressed cells (Figure 23a).

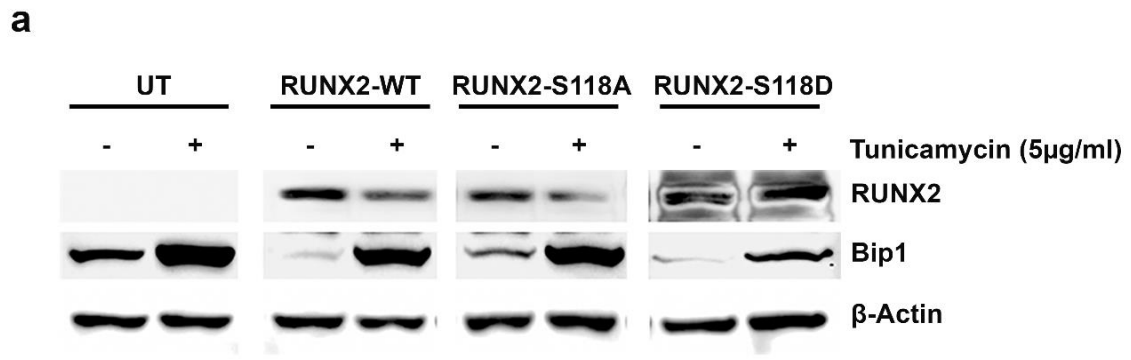

Figure 23: (a) HEK-293T cells were transfected with RUNX2-WT, RUNX2-S118A, and RUNX2-S118D after 24 hrs and the cells were treated with tunicamycin (5µg/ml) for 12 hrs. Western blots shows that RUNX2, Bip1 and β-actin expression.

Discussion

8.1. Discussion:

Many metabolic alterations has been observed during the diabetes disease development, mainly inflammation, oxidative stress, Endoplasmic reticulum stress, etc. there are ample of evidences to promote the significant role of endoplasmic reticulum stress in the evolution of diabetic induced complications[192, 194-197]. Chronic ER stress shows defective in unfolded protein response (UPR) and is associated with variety of pathologies include metabolic syndrome[204]. ER stress induced loss of pancreatic beta cells and insulin resistance was observed in the course of diabetic pathogenesis[205]. Hyperglycemia mediated ER stress like unfolded protein response generation was observed in presence of dextrose and glycolytic intermediates in HUVECs [206]. Glucose, glycolytic & TCA cycle intermediates such as Glycerol dihydroxyacetone and pyruvate can generate ER stress [206]. The hyperglycemic induced ER stress is not affected by anti-oxidants such as ascorbic acid and α-tocopherol [207]. Glucotoxicity induced ER stress shows considerable promising outcome with PKC inhibitors[208]. Many clinical and preclinical studies demonstrates that increased ER stress was observed in obese patients in comparison with lean[209]. Elevated hyperglycemia free fatty acids and LPS (lipopolysaccharide) in circulation are the possible factors to induce ER stress [210].

However it is established that glucotoxicity cause bone adipogenesis in STZ-induced diabetic animal models [211]. Here we hypothesized that elevated glucose in circulation is the main cause of ER stress which further driving mesenchymal stem cell population to adipocytes instead of osteocyte differentiation. Our results demonstrate that tunicamycin and thapsigargin induced ER stress and Rotenone induced oxidative stress shown to be downregulate RUNX2 protein levels (Figure 20a-c & 20f-h) whereas we did not observe RNA levels affected (Figure 20d & 22i). Our further studies shows that RUNX2 is regulating in post translational modifications might regulating the differentiation process. In tunicamycin treatments RUNX2 protein levels restoration was observed in presence of proteosomal inhibitors indicates RUNX2 might be undergoing ubiquitination (Figure 21a & 22a). Further studies is needed to identify the specific ubiquitin protein. Our earlier studies shown that AMPK involved in maintaining the RUNX2 protein level. Further we have observed that AMPK activators restores the protein levels in presence of tunicamycin infers that AMPK activity might be regulating the RUNX2 protein levels in ER stress. Further we hypothesized that RUNX2 S118 phosphorylation by AMPK might be responsible for RUNX2 stability. Our transiently transfected RUNX2 WT , RUNX2 S118A and

phosphomimitic form of RUNX2 S118D followed by tunicamycin treatment in RUNX2 Null cells(HEK 293T) shows that AMPK mediated RUNX2 phosphorylation is essential to maintain RUNX2 protein levels(Figure 23a). Further our colocalization studies of RUNX2 and ubiquitin in presence of AMPK activators (metformin & AICAR) and inhibitor (Compound C) shown that loss of AMPK activity undergoes RUNX2 dephosphorylation followed by RUNX2 degradation. The same we have also observed in tunicamycin treated samples (Figure 21 & 22).

Overall our studies addressed mechanistically hyperglycemia favors the adipogenesis in diabetic patients by downregulating the AMPK activity followed RUNX2 protein levels. That hyperglycemia induced metabolic stress(oxidative & ER stress) might be the possible reasons to downregulate the AMPK activity & RUNX2 protein levels which might be the responsible to drive the mesenchymal stem cells to adipocytes rather osteocytes in diabetic patients.

Summary

9.1. Summary:

Bone marrow is specialized connective tissue involved in hematopoiesis and also provide structural support to muscles and other vital organs. As efficient and precise signaling pathways are indispensable for maintaining normal bone homeostasis while allowing lineage specific commitment, thus studies addressing how these pathways are regulated are of great interest. Mesenchymal stromal cells are non-hematopoietic stem cells, has the ability to differentiate into various adipocytes, osteocytes etc. Interestingly, osteogenic and adipogenic pathways are reciprocally regulated. However, exact mechanism behind this regulation remains elusive.

Differentiation of MSCs to either osteocytes or to adipocytes requires interplay of pathway specific transcription factors. For instance, RUNX2, Dlx5 and Osterix are required for osteogenesis while C/EBP and PPAR gamma promote adipogenesis. Given the constitutive expression of these proteins, how these proteins are being regulated during lineage specific commitment remains less understood. We explained the importance of kinase mediate signaling targeting RUNX2 protein as a key molecule because of the following reasons; 1) RUNX2 is involved in osteogenesis and harbors a putative AMPK motif. 2) AMPK activation is associated with increased bone formation while inhibiting adipogenesis. 3) Hyperglycemia and obesity are associated with loss of AMPK activation. Hence, we reasoned whether AMPK mediated phosphorylation of RUNX2 has any role in regulating RUNX2 functions during cell fate decisions. Here we used *in vitro* differentiation models to monitor AMPK activity and its correlation with RUNX2 levels and also in streptozotocin induced -diabetes model to demonstrate the pathological relevance of AMPK-RUNX2 regulation.

Main findings:

- Our studies provide first line of evidence that bone morphogenic transcription factor RUNX2 is a physiological substrate of AMPK.
- Reduced AMPK activation promotes RUNX2 degradation through proteosomal pathway, while metformin induced AMPK activation stabilizes RUNX2 protein level.
- AMPK activity and RUNX2 levels are positively regulated during MSCs differentiation to osteocytes/adipocytes
- Stabilizing RUNX2 levels by metformin induced AMPK activation, abrogates bone adipogenesis in STZ-induced diabetic models.

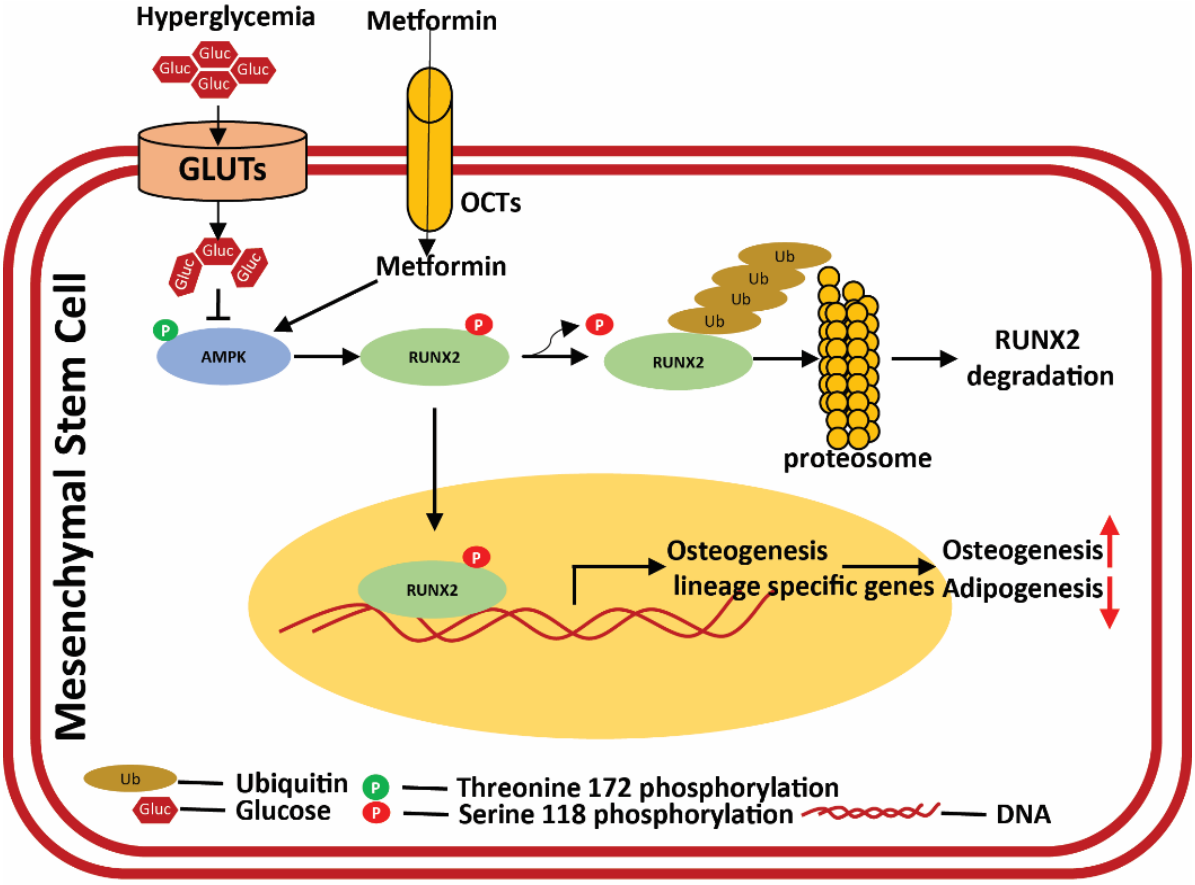

Figure 24: Schematic representations of RUNX2 regulation in mesenchymal stem cell differentiation. Bone microenvironment with high glucose down regulates AMPK activity. AMPK induced phosphorylation of RUNX2 activates its transcriptional activity as well as its stabilization. Reduced AMPK phosphorylation induces RUNX2 proteosomal degradation

In summary our findings advances the knowledge of AMPK mediated signaling converging on RUNX2, thus regulates the differentiation of MSCs to osteocytes/adipocytes and also provide insights in pathological relevance in diabetes induced accumulation of adipocytes in bone. Thus our study provides novel therapeutic interventions aiming to enhance bone health for quality of life.

References

10.1. References

1. Chan, M., *Global report on diabetes* 2016, WHO.
2. Amos, A.F., D.J. McCarty, and P. Zimmet, *The rising global burden of diabetes and its complications: estimates and projections to the year 2010.* Diabet Med, 1997. **14 Suppl 5**: p. S1-85.
3. Wild, S., et al., *Global prevalence of diabetes: estimates for the year 2000 and projections for 2030.* Diabetes Care, 2004. **27**(5): p. 1047-53.
4. Anjana, R.M., et al., *Prevalence of diabetes and prediabetes (impaired fasting glucose and/or impaired glucose tolerance) in urban and rural India: phase I results of the Indian Council of Medical Research-INdia DIABetes (ICMR-INDIAB) study.* Diabetologia, 2011. **54**(12): p. 3022-7.
5. Sadikot, S., *IDF Diabetes Atlas - 8th Edition*. 2017.
6. Poretsky, L., *Principles of diabetes mellitus*. 2nd ed. 2010, New York: Springer. xviii, 887 p.
7. Lakhtakia, R., *The history of diabetes mellitus.* Sultan Qaboos Univ Med J, 2013. **13**(3): p. 368-70.
8. King, K.M. and G. Rubin, *A history of diabetes: from antiquity to discovering insulin.* British Journal of Nursing, 2003. **12**(18): p. 1091-1095.
9. Ahmed, A.M., *History of diabetes mellitus.* Saudi Med J, 2002. **23**(4): p. 373-8.
10. Bellamy, L., et al., *Type 2 diabetes mellitus after gestational diabetes: a systematic review and meta-analysis.* The Lancet, 2009. **373**(9677): p. 1773-1779.
11. Brownlee, M., *Biochemistry and molecular cell biology of diabetic complications.* Nature, 2001. **414**: p. 813.
12. Misra, A., N. Singhal, and L. Khurana, *Obesity, the Metabolic Syndrome, and Type 2 Diabetes in Developing Countries: Role of Dietary Fats and Oils.* Journal of the American College of Nutrition, 2010. **29**(sup3): p. 289S-301S.
13. Andersen, A.R., et al., *Diabetic nephropathy in type 1 (insulin-dependent) diabetes: An epidemiological study.* Diabetologia, 1983. **25**(6): p. 496-501.
14. DeFronzo, R.A., *Pathogenesis of type 2 diabetes mellitus.* Medical Clinics, 2004. **88**(4): p. 787-835.
15. Reaven, G.M., *Role of Insulin Resistance in Human Disease.* Diabetes, 1988. **37**(12): p. 1595-1607.
16. Butler, A.E., et al., *β-Cell Deficit and Increased β-Cell Apoptosis in Humans With Type 2 Diabetes.* Diabetes, 2003. **52**(1): p. 102-110.
17. Dimitriadis, G., et al., *Insulin effects in muscle and adipose tissue.* Diabetes Res Clin Pract, 2011. **93 Suppl 1**: p. S52-9.

18. Cahova, M., H. Vavrinkova, and L. Kazdova, *Glucose-fatty acid interaction in skeletal muscle and adipose tissue in insulin resistance.* Physiol Res, 2007. **56**(1): p. 1-15.

19. Sears, B. and M. Perry, *The role of fatty acids in insulin resistance.* Lipids Health Dis, 2015. **14**: p. 121.

20. Boden, G., *Obesity, insulin resistance and free fatty acids.* Curr Opin Endocrinol Diabetes Obes, 2011. **18**(2): p. 139-43.

21. Moon, J.S. and K.C. Won, *Pancreatic alpha-Cell Dysfunction in Type 2 Diabetes: Old Kids on the Block.* Diabetes Metab J, 2015. **39**(1): p. 1-9.

22. Habegger, K.M., et al., *The metabolic actions of glucagon revisited.* Nat Rev Endocrinol, 2010. **6**(12): p. 689-97.

23. Quesada, I., et al., *Physiology of the pancreatic alpha-cell and glucagon secretion: role in glucose homeostasis and diabetes.* J Endocrinol, 2008. **199**(1): p. 5-19.

24. Roder, P.V., et al., *Pancreatic regulation of glucose homeostasis.* Exp Mol Med, 2016. **48**: p. e219.

25. Boden, G., *Free fatty acids, insulin resistance, and type 2 diabetes mellitus.* Proc Assoc Am Physicians, 1999. **111**(3): p. 241-8.

26. Falholt, K., et al., *Carbohydrate and lipid metabolism of skeletal muscle in type 2 diabetic patients.* Diabet Med, 1988. **5**(1): p. 27-31.

27. Saltiel, A.R. and C.R. Kahn, *Insulin signalling and the regulation of glucose and lipid metabolism.* Nature, 2001. **414**(6865): p. 799-806.

28. Jellinger, P.S., *Metabolic consequences of hyperglycemia and insulin resistance.* Insulin, 2009. **4**(1): p. 2-14.

29. Kim, W. and J.M. Egan, *The role of incretins in glucose homeostasis and diabetes treatment.* Pharmacol Rev, 2008. **60**(4): p. 470-512.

30. Seino, Y., M. Fukushima, and D. Yabe, *GIP and GLP-1, the two incretin hormones: Similarities and differences.* J Diabetes Investig, 2010. **1**(1-2): p. 8-23.

31. Kjems, L.L., et al., *The influence of GLP-1 on glucose-stimulated insulin secretion: effects on beta-cell sensitivity in type 2 and nondiabetic subjects.* Diabetes, 2003. **52**(2): p. 380-6.

32. Godinho, R., et al., *The Place of Dipeptidyl Peptidase-4 Inhibitors in Type 2 Diabetes Therapeutics: A "Me Too" or "the Special One" Antidiabetic Class?* J Diabetes Res, 2015. **2015**: p. 806979.

33. Manandhar, B. and J.M. Ahn, *Glucagon-like peptide-1 (GLP-1) analogs: recent advances, new possibilities, and therapeutic implications.* J Med Chem, 2015. **58**(3): p. 1020-37.

34. D'Alessio, D.A. and T.P. Vahl, *Glucagon-like peptide 1: evolution of an incretin into a treatment for diabetes.* Am J Physiol Endocrinol Metab, 2004. **286**(6): p. E882-90.

35. Patti, M.E. and S. Corvera, *The role of mitochondria in the pathogenesis of type 2 diabetes.* Endocr Rev, 2010. **31**(3): p. 364-95.

36. Sivitz, W.I. and M.A. Yorek, *Mitochondrial dysfunction in diabetes: from molecular mechanisms to functional significance and therapeutic opportunities.* Antioxid Redox Signal, 2010. **12**(4): p. 537-77.

37. Lefranc, C., et al., *Mitochondrial oxidative stress in obesity: Role of the Mineralocorticoid Receptor.* J Endocrinol, 2018.

38. Vankoningsloo, S., et al., *Mitochondrial dysfunction induces triglyceride accumulation in 3T3-L1 cells: role of fatty acid beta-oxidation and glucose.* J Lipid Res, 2005. **46**(6): p. 1133-49.

39. De Pauw, A., et al., *Mitochondrial (dys)function in adipocyte (de)differentiation and systemic metabolic alterations.* Am J Pathol, 2009. **175**(3): p. 927-39.

40. Wang, C.H., et al., *Mitochondrial dysfunction leads to impairment of insulin sensitivity and adiponectin secretion in adipocytes.* FEBS J, 2013. **280**(4): p. 1039-50.

41. Hardy, O.T., M.P. Czech, and S. Corvera, *What causes the insulin resistance underlying obesity?* Curr Opin Endocrinol Diabetes Obes, 2012. **19**(2): p. 81-7.

42. Karpe, F., J.R. Dickmann, and K.N. Frayn, *Fatty acids, obesity, and insulin resistance: time for a reevaluation.* Diabetes, 2011. **60**(10): p. 2441-9.

43. Arner, P. and M. Rydén, *Fatty Acids, Obesity and Insulin Resistance.* Obesity Facts, 2015. **8**(2): p. 147-155.

44. Meng, S., et al., *Metformin Activates AMP-activated Protein Kinase by Promoting Formation of the αβγ Heterotrimeric Complex.* Journal of Biological Chemistry, 2014.

45. Grisouard, J., et al., *Mechanisms of metformin action on glucose transport and metabolism in human adipocytes.* Biochem Pharmacol, 2010. **80**(11): p. 1736-45.

46. Lee, J.O., et al., *Metformin Regulates Glucose Transporter 4 (GLUT4) Translocation through AMP-activated Protein Kinase (AMPK)-mediated Cbl/CAP Signaling in 3T3-L1 Preadipocyte Cells.* Journal of Biological Chemistry, 2012. **287**(53): p. 44121-44129.

47. Klip, A. and L.A. Leiter, *Cellular Mechanism of Action of Metformin.* Diabetes Care, 1990. **13**(6): p. 696-704.

48. Giannarelli, R., et al., *Reducing insulin resistance with metformin: the evidence today.* Diabetes Metab, 2003. **29**(4 Pt 2): p. 6S28-35.

49. Wang, C., et al., *Metformin suppresses lipid accumulation in skeletal muscle by promoting fatty acid oxidation.* Clin Lab, 2014. **60**(6): p. 887-96.

50. Bodmer, M., et al., *Metformin, Sulfonylureas, or Other Antidiabetes Drugs and the Risk of Lactic Acidosis or Hypoglycemia.* A nested case-control analysis, 2008. **31**(11): p. 2086-2091.

51. Hauner, H., *The mode of action of thiazolidinediones.* Diabetes Metab Res Rev, 2002. **18 Suppl 2**: p. S10-5.

52. Kelly, A.S. and A.J. Bank, *The cardiovascular effects of the thiazolidinediones: a review of the clinical data.* J Diabetes Complications, 2007. **21**(5): p. 326-34.

53. Bailey, C.J., *Thiazolidinediones*, in *xPharm: The Comprehensive Pharmacology Reference*. 2007, Elsevier: New York. p. 1-2.

54. Szollosi, A., M. Nenquin, and J.C. Henquin, *Pharmacological stimulation and inhibition of insulin secretion in mouse islets lacking ATP-sensitive K+ channels.* Br J Pharmacol, 2010. **159**(3): p. 669-77.

55. Wu, P.-C., et al., *Meglitinides increase the risk of hypoglycemia in diabetic patients with advanced chronic kidney disease: a nationwide, population-based study.* Oncotarget, 2017. **8**(44): p. 78086-78095.

56. Proks, P., et al., *Sulfonylurea Stimulation of Insulin Secretion.* Diabetes, 2002. **51**(suppl 3): p. S368-S376.

57. Green, B.D., P.R. Flatt, and C.J. Bailey, *Dipeptidyl peptidase IV (DPP IV) inhibitors: A newly emerging drug class for the treatment of type 2 diabetes.* Diab Vasc Dis Res, 2006. **3**(3): p. 159-65.

58. Wilcox, G., *Insulin and Insulin Resistance.* Clinical Biochemist Reviews, 2005. **26**(2): p. 19-39.

59. Gross, J.L., et al., *Diabetic Nephropathy: Diagnosis, Prevention, and Treatment.* Diabetes Care, 2005. **28**(1): p. 164-176.

60. Bansal, V., J. Kalita, and U.K. Misra, *Diabetic neuropathy.* Postgraduate Medical Journal, 2006. **82**(964): p. 95-100.

61. Duh, E.J., J.K. Sun, and A.W. Stitt, *Diabetic retinopathy: current understanding, mechanisms, and treatment strategies.* JCI Insight, 2017. **2**(14): p. e93751.

62. Pappachan, J.M., et al., *Diabetic cardiomyopathy: Pathophysiology, diagnostic evaluation and management.* World Journal of Diabetes, 2013. **4**(5): p. 177-189.

63. Jackuliak, P. and J. Payer, *Osteoporosis, Fractures, and Diabetes.* International Journal of Endocrinology, 2014. **2014**: p. 820615.

64. Trautner, C., et al., *Incidence of lower limb amputations and diabetes.* Diabetes Care, 1996. **19**(9): p. 1006-9.

65. Singh, V.P., et al., *Advanced glycation end products and diabetic complications.* Korean J Physiol Pharmacol, 2014. **18**(1): p. 1-14.

66. de Rekeneire, N., et al., *Diabetes, hyperglycemia, and inflammation in older individuals: the health, aging and body composition study.* Diabetes Care, 2006. **29**(8): p. 1902-8.

67. Katon, W., et al., *Depression Increases Risk of Dementia in Patients with Type 2 Diabetes: The Diabetes & Aging Study.* Archives of general psychiatry, 2012. **69**(4): p. 410-417.

68. Giacco, F. and M. Brownlee, *Oxidative stress and diabetic complications.* Circulation research, 2010. **107**(9): p. 1058-1070.

69. Iseki, K., et al., *Evidence for high risk of cerebral hemorrhage in chronic dialysis patients.* Kidney Int, 1993. **44**(5): p. 1086-90.

70. Campbell, K.N., L. Raij, and P. Mundel, *Role of Angiotensin II in the Development of Nephropathy and Podocytopathy of Diabetes.* Current diabetes reviews, 2011. **7**(1): p. 3-7.

71. Ni, W.J., L.Q. Tang, and W. Wei, *Research progress in signalling pathway in diabetic nephropathy.* Diabetes Metab Res Rev, 2015. **31**(3): p. 221-33.

72. Sorrentino, F.S., et al., *The importance of glial cells in the homeostasis of the retinal microenvironment and their pivotal role in the course of diabetic retinopathy.* Life Sciences, 2016. **162**: p. 54-59.

73. Chen, Q., et al., *Fate decision of mesenchymal stem cells: adipocytes or osteoblasts?* Cell Death Differ, 2016. **23**(7): p. 1128-39.

74. Carbonare, L.D., et al., *Comparison of Trabecular Bone Microarchitecture and Remodeling in Glucocorticoid-Induced and Postmenopausal Osteoporosis.* Journal of Bone and Mineral Research, 2009. **16**(1): p. 97-103.

75. Ferraù, F. and M. Korbonits, *Metabolic comorbidities in Cushing's syndrome.* European Journal of Endocrinology, 2015. **173**(4): p. M133-M157.

76. Moerman, E.J., et al., *Aging activates adipogenic and suppresses osteogenic programs in mesenchymal marrow stroma/stem cells: the role of PPAR-γ2 transcription factor and TGF-β/BMP signaling pathways.* Aging cell, 2004. **3**(6): p. 379-389.

77. Rosen, C.J. and M.L. Bouxsein, *Mechanisms of Disease: is osteoporosis the obesity of bone?* Nature Clinical Practice Rheumatology, 2006. **2**: p. 35.

78. Di Bernardo, G., et al., *Sera of overweight people promote in vitro adipocyte differentiation of bone marrow stromal cells.* Stem Cell Research & Therapy, 2014. **5**(1): p. 4.

79. Qian, C., et al., *High-Fat Diet/Low-Dose Streptozotocin-Induced Type 2 Diabetes in Rats Impacts Osteogenesis and Wnt Signaling in Bone Marrow Stromal Cells.* PLOS ONE, 2015. **10**(8): p. e0136390.

80. Domínguez-Bendala, J., et al., *Concise Review: Mesenchymal Stem Cells for Diabetes.* Stem Cells Translational Medicine, 2012. **1**(1): p. 59-63.

81. Caplan, A.I. and S.P. Bruder, *Mesenchymal stem cells: building blocks for molecular medicine in the 21st century.* Trends in Molecular Medicine, 2001. **7**(6): p. 259-264.

82. Luu, Y.K., et al., *Mechanical signals as a non-invasive means to influence mesenchymal stem cell fate, promoting bone and suppressing the fat phenotype.* IBMS BoneKEy, 2009. **6**(4): p. 132-149.

83. Beresford, J.N., et al., *Evidence for an inverse relationship between the differentiation of adipocytic and osteogenic cells in rat marrow stromal cell cultures.* J Cell Sci, 1992. **102 (Pt 2)**: p. 341-51.

84. Akune, T., et al., *PPARgamma insufficiency enhances osteogenesis through osteoblast formation from bone marrow progenitors.* J Clin Invest, 2004. **113**(6): p. 846-55.

85. Olefsky, J.M., *Treatment of insulin resistance with peroxisome proliferator–activated receptor γ agonists.* Journal of Clinical Investigation, 2000. **106**(4): p. 467-472.

86. Jones, J.R., et al., *Deletion of PPARγ in adipose tissues of mice protects against high fat diet-induced obesity and insulin resistance.* Proceedings of the National Academy of Sciences of the United States of America, 2005. **102**(17): p. 6207-6212.

87. Wu, Z., et al., *PPARgamma induces the insulin-dependent glucose transporter GLUT4 in the absence of C/EBPalpha during the conversion of 3T3 fibroblasts into adipocytes.* Journal of Clinical Investigation, 1998. **101**(1): p. 22-32.

88. Durst, K.L. and S.W. Hiebert, *Role of RUNX family members in transcriptional repression and gene silencing.* Oncogene, 2004. **23**(24): p. 4220-4.

89. Rennert, J., et al., *The evolution of Runx genes I. A comparative study of sequences from phylogenetically diverse model organisms.* BMC Evolutionary Biology, 2003. **3**: p. 4-4.

90. Ito, Y., S.-C. Bae, and L.S.H. Chuang, *The RUNX family: developmental regulators in cancer.* Nature Reviews Cancer, 2015. **15**: p. 81.

91. Kagoshima, H., et al., *The Runt domain identifies a new family of heteromeric transcriptional regulators.* Trends Genet, 1993. **9**(10): p. 338-41.

92. Kamachi, Y., et al., *Purification of a mouse nuclear factor that binds to both the A and B cores of the polyomavirus enhancer.* Journal of Virology, 1990. **64**(10): p. 4808-4819.

93. Schroeder Tania, M., D. Jensen Eric, and J. Westendorf Jennifer, *Runx2: A master organizer of gene transcription in developing and maturing osteoblasts.* Birth Defects Research Part C: Embryo Today: Reviews, 2005. **75**(3): p. 213-225.

94. Fujita, T., et al., *Runx2 induces osteoblast and chondrocyte differentiation and enhances their migration by coupling with PI3K-Akt signaling.* The Journal of Cell Biology, 2004. **166**(1): p. 85-95.

95. Levanon, D. and Y. Groner, *Structure and regulated expression of mammalian RUNX genes.* Oncogene, 2004. **23**: p. 4211.

96. Stock, M. and F. Otto, *Control of RUNX2 isoform expression: the role of promoters and enhancers.* J Cell Biochem, 2005. **95**(3): p. 506-17.

97. Banerjee, C., et al., *Differential regulation of the two principal Runx2/Cbfa1 n-terminal isoforms in response to bone morphogenetic protein-2 during development of the osteoblast phenotype.* Endocrinology, 2001. **142**(9): p. 4026-39.

98. Ducy, P. and G. Karsenty, *Two distinct osteoblast-specific cis-acting elements control expression of a mouse osteocalcin gene.* Mol Cell Biol, 1995. **15**(4): p. 1858-69.

99. Bruderer, M., et al., *Role and regulation of RUNX2 in osteogenesis.* Eur Cell Mater, 2014. **28**: p. 269-86.

100. Qin, X., et al., *Cbfb regulates bone development by stabilizing Runx family proteins.* J Bone Miner Res, 2015. **30**(4): p. 706-14.

101. Thirunavukkarasu, K., et al., *Two Domains Unique to Osteoblast-Specific Transcription Factor Osf2/Cbfa1 Contribute to Its Transactivation Function and Its Inability To Heterodimerize with Cbfβ.* Molecular and Cellular Biology, 1998. **18**(7): p. 4197-4208.

102. Ziros, P.G., E.K. Basdra, and A.G. Papavassiliou, *Runx2: of bone and stretch.* Int J Biochem Cell Biol, 2008. **40**(9): p. 1659-63.

103. Rennert, J., et al., *The evolution of Runx genes I. A comparative study of sequences from phylogenetically diverse model organisms.* BMC Evolutionary Biology, 2003. **3**(1): p. 4.

104. Huang, G., et al., *Dimerization with PEBP2β protects RUNX1/AML1 from ubiquitin–proteasome-mediated degradation.* The EMBO Journal, 2001. **20**(4): p. 723-733.

105. Kundu, M., et al., *Cbfbeta interacts with Runx2 and has a critical role in bone development.* Nat Genet, 2002. **32**(4): p. 639-44.

106. Miller, J., et al., *The core-binding factor beta subunit is required for bone formation and hematopoietic maturation.* Nat Genet, 2002. **32**(4): p. 645-9.

107. Yoshida, C.A., et al., *Core-binding factor beta interacts with Runx2 and is required for skeletal development.* Nat Genet, 2002. **32**(4): p. 633-8.

108. Jiao, H., E. Xiao, and D.T. Graves, *Diabetes and Its Effect on Bone and Fracture Healing.* Current osteoporosis reports, 2015. **13**(5): p. 327-335.

109. Shin, H.D., et al., *Novel promoter polymorphism in RUNX2 is associated with serum triglyceride level.* Mol Cells, 2008. **26**(5): p. 459-61.

110. Goodman, W.G. and M.T. Hori, *Diminished bone formation in experimental diabetes. Relationship to osteoid maturation and mineralization.* Diabetes, 1984. **33**(9): p. 825-31.

111. Lu, H., et al., *Diabetes interferes with the bone formation by affecting the expression of transcription factors that regulate osteoblast differentiation.* Endocrinology, 2003. **144**(1): p. 346-52.

112. Cheng, S.L., et al., *MSX2 promotes osteogenesis and suppresses adipogenic differentiation of multipotent mesenchymal progenitors.* J Biol Chem, 2003. **278**(46): p. 45969-77.

113. Fowlkes, J.L., et al., *Runt-Related Transcription Factor 2 (RUNX2) and RUNX2-Related Osteogenic Genes Are Down-Regulated throughout Osteogenesis in Type 1 Diabetes Mellitus.* Endocrinology, 2008. **149**(4): p. 1697-1704.

114. Rzonca, S.O., et al., *Bone Is a Target for the Antidiabetic Compound Rosiglitazone.* Endocrinology, 2004. **145**(1): p. 401-406.

115. Benvenuti, S., et al., *Rosiglitazone stimulates adipogenesis and decreases osteoblastogenesis in human mesenchymal stem cells.* J Endocrinol Invest, 2007. **30**(9): p. RC26-30.

116. Vianna, A.G.D., C.P. Sanches, and F.C. Barreto, *Review article: effects of type 2 diabetes therapies on bone metabolism.* Diabetol Metab Syndr, 2017. **9**: p. 75.

117. Botolin, S., et al., *Increased bone adiposity and peroxisomal proliferator-activated receptor-gamma2 expression in type I diabetic mice.* Endocrinology, 2005. **146**(8): p. 3622-31.

118. Irwin, R., et al., *Normal bone density obtained in the absence of insulin receptor expression in bone.* Endocrinology, 2006. **147**(12): p. 5760-7.

119. Li, H., et al., *Insulin potentiates the proliferation and bone morphogenetic protein-2-induced osteogenic differentiation of rat spinal ligament cells via extracellular signal-regulated kinase and phosphatidylinositol 3-kinase.* Spine (Phila Pa 1976), 2008. **33**(22): p. 2394-402.

120. D'Souza, D.R., et al., *Hyperglycemia regulates RUNX2 activation and cellular wound healing through the aldose reductase polyol pathway.* J Biol Chem, 2009. **284**(27): p. 17947-55.

121. Molinuevo, M.S., et al., *Effect of metformin on bone marrow progenitor cell differentiation: in vivo and in vitro studies.* J Bone Miner Res, 2010. **25**(2): p. 211-21.

122. Zhen, D., Y. Chen, and X. Tang, *Metformin reverses the deleterious effects of high glucose on osteoblast function.* J Diabetes Complications, 2010. **24**(5): p. 334-44.

123. Wang, W., et al., *High glucose stimulates adipogenic and inhibits osteogenic differentiation in MG-63 cells through cAMP/protein kinase A/extracellular signal-regulated kinase pathway.* Mol Cell Biochem, 2010. **338**(1-2): p. 115-22.

124. Lee, H.L., et al., *Tumor necrosis factor-alpha increases alkaline phosphatase expression in vascular smooth muscle cells via MSX2 induction.* Biochem Biophys Res Commun, 2010. **391**(1): p. 1087-92.

125. Jang, W.G., et al., *Metformin induces osteoblast differentiation via orphan nuclear receptor SHP-mediated transactivation of Runx2.* Bone, 2011. **48**(4): p. 885-93.

126. Adhami, M., et al., *Runx2 regulates the gene network associated with insulin signaling and energy homeostasis.* Cells Tissues Organs, 2011. **194**(2-4): p. 232-7.

127. Garcia-Hernandez, A., et al., *High glucose concentrations alter the biomineralization process in human osteoblastic cells.* Bone, 2012. **50**(1): p. 276-88.

128. Zhang, Y. and J.H. Yang, *Activation of the PI3K/Akt pathway by oxidative stress mediates high glucose-induced increase of adipogenic differentiation in primary rat osteoblasts.* J Cell Biochem, 2013. **114**(11): p. 2595-602.

129. Dong, X., et al., *FFAs-ROS-ERK/P38 pathway plays a key role in adipocyte lipotoxicity on osteoblasts in co-culture.* Biochimie, 2014. **101**: p. 123-31.

130. Ehnert, S., et al., *Factors circulating in the blood of type 2 diabetes mellitus patients affect osteoblast maturation - description of a novel in vitro model.* Exp Cell Res, 2015. **332**(2): p. 247-58.

131. Lin, M.-E., et al., *Runx2 Expression in Smooth Muscle Cells Is Required for Arterial Medial Calcification in Mice.* The American Journal of Pathology, 2015. **185**(7): p. 1958-1969.

132. Poon, C.C., et al., *In vitro vitamin K(2) and 1alpha,25-dihydroxyvitamin D(3) combination enhances osteoblasts anabolism of diabetic mice.* Eur J Pharmacol, 2015. **767**: p. 30-40.

133. Bhatta, A., et al., *Deregulation of arginase induces bone complications in high-fat/high-sucrose diet diabetic mouse model.* Molecular and cellular endocrinology, 2016. **422**: p. 211-220.

134. Sui, B., et al., *Mesenchymal progenitors in osteopenias of diverse pathologies: differential characteristics in the common shift from osteoblastogenesis to adipogenesis.* Scientific Reports, 2016. **6**: p. 30186.

135. Stechschulte, L.A., et al., *Protein Phosphatase PP5 Controls Bone Mass and the Negative Effects of Rosiglitazone on Bone through Reciprocal Regulation of PPARγ and RUNX2.* Journal of Biological Chemistry, 2016.

136. Chen, S.C., et al., *Metformin suppresses adipogenesis through both AMP-activated protein kinase (AMPK)-dependent and AMPK-independent mechanisms.* Mol Cell Endocrinol, 2017. **440**: p. 57-68.

137. Rosa, M., et al., *Leptin induces osteoblast differentiation of human valvular interstitial cells via the Akt and ERK pathways.* Acta Diabetol, 2017. **54**(6): p. 551-560.

138. Hardie, D.G., F.A. Ross, and S.A. Hawley, *AMPK: a nutrient and energy sensor that maintains energy homeostasis.* Nat Rev Mol Cell Biol, 2012. **13**(4): p. 251-62.

139. Kim, J., et al., *AMPK activators: mechanisms of action and physiological activities.* Experimental &Amp; Molecular Medicine, 2016. **48**: p. e224.

140. Lee, J.O., et al., *Metformin Regulates Glucose Transporter 4 (GLUT4) Translocation through AMP-activated Protein Kinase (AMPK)-mediated Cbl/CAP Signaling in 3T3-L1 Preadipocyte Cells.* The Journal of Biological Chemistry, 2012. **287**(53): p. 44121-44129.

141. Jäger, S., et al., *AMP-activated protein kinase (AMPK) action in skeletal muscle via direct phosphorylation of PGC-1a.* Proceedings of the National Academy of Sciences, 2007. **104**(29): p. 12017-12022.

142. Zhao, M. and D.J. Klionsky, *AMPK-Dependent Phosphorylation of ULK1 Induces Autophagy.* Cell Metabolism, 2011. **13**(2): p. 119-120.

143. Luo, Z., M. Zang, and W. Guo, *AMPK as a metabolic tumor suppressor: control of metabolism and cell growth.* Future oncology (London, England), 2010. **6**(3): p. 457-470.

144. Ruderman, N.B., et al., *AMPK, insulin resistance, and the metabolic syndrome.* The Journal of Clinical Investigation, 2013. **123**(7): p. 2764-2772.

145. Semenkovich, C.F., *Insulin resistance and atherosclerosis.* J Clin Invest, 2006. **116**(7): p. 1813-22.

146. Chondronikola, M., et al., *Brown Adipose Tissue Improves Whole-Body Glucose Homeostasis and Insulin Sensitivity in Humans.* Diabetes, 2014. **63**(12): p. 4089-4099.

147. Blondin, D.P., et al., *A critical appraisal of brown adipose tissue metabolism in humans.* Clinical Lipidology, 2015. **10**(3): p. 259-280.

148. Sidossis, L. and S. Kajimura, *Brown and beige fat in humans: thermogenic adipocytes that control energy and glucose homeostasis.* The Journal of Clinical Investigation, 2015. **125**(2): p. 478-486.

149. Ruderman, N.B., et al., *AMPK, insulin resistance, and the metabolic syndrome.* J Clin Invest, 2013. **123**(7): p. 2764-72.

150. Lindholm, C.R., et al., *A high-fat diet decreases AMPK activity in multiple tissues in the absence of hyperglycemia or systemic inflammation in rats.* J Physiol Biochem, 2013. **69**(2): p. 165-75.

151. Mottillo, E.P., et al., *Lack of Adipocyte AMPK Exacerbates Insulin Resistance and Hepatic Steatosis through Brown and Beige Adipose Tissue Function.* Cell Metab, 2016. **24**(1): p. 118-29.

152. Tao, R., et al., *AMPK exerts dual regulatory effects on the PI3K pathway.* Journal of Molecular Signaling, 2010. **5**: p. 1-1.

153. Yu, X., et al., *Leptinomimetic effects of the AMP kinase activator AICAR in leptin-resistant rats: prevention of diabetes and ectopic lipid deposition.* Diabetologia, 2004. **47**(11): p. 2012-21.

154. Kelly, M., et al., *AMPK activity is diminished in tissues of IL-6 knockout mice: the effect of exercise.* Biochem Biophys Res Commun, 2004. **320**(2): p. 449-54.

155. Kramer, H.F., et al., *AS160 regulates insulin- and contraction-stimulated glucose uptake in mouse skeletal muscle.* J Biol Chem, 2006. **281**(42): p. 31478-85.

156. Marsin, A.S., et al., *Phosphorylation and activation of heart PFK-2 by AMPK has a role in the stimulation of glycolysis during ischaemia.* Curr Biol, 2000. **10**(20): p. 1247-55.

157. Vestergaard, P., *Discrepancies in bone mineral density and fracture risk in patients with type 1 and type 2 diabetes—a meta-analysis.* Osteoporosis International, 2007. **18**(4): p. 427-444.

158. Janghorbani, M., et al., *Systematic review of type 1 and type 2 diabetes mellitus and risk of fracture.* Am J Epidemiol, 2007. **166**(5): p. 495-505.

159. Yamamoto, M., et al., *Diabetic patients have an increased risk of vertebral fractures independent of BMD or diabetic complications.* J Bone Miner Res, 2009. **24**(4): p. 702-9.

160. Xi, G., C.J. Rosen, and D.R. Clemmons, *IGF-I and IGFBP-2 Stimulate AMPK Activation and Autophagy, Which Are Required for Osteoblast Differentiation.* Endocrinology, 2016. **157**(1): p. 268-281.

161. Huang, S., et al., *An improved protocol for isolation and culture of mesenchymal stem cells from mouse bone marrow.* Journal of Orthopaedic Translation, 2015. **3**(1): p. 26-33.

162. Satija, N.K., et al., *Mesenchymal stem cells: molecular targets for tissue engineering.* Stem Cells Dev, 2007. **16**(1): p. 7-23.

163. Hardie, D.G., *AMP-activated protein kinase: an energy sensor that regulates all aspects of cell function.* Genes Dev, 2011. **25**(18): p. 1895-908.

164. Keshava Prasad, T.S., et al., *Human Protein Reference Database--2009 update.* Nucleic Acids Res, 2009. **37**(Database issue): p. D767-72.

165. Gwinn, D.M., et al., *AMPK phosphorylation of raptor mediates a metabolic checkpoint.* Mol Cell, 2008. **30**(2): p. 214-26.

166. Veldhuis-Vlug, A.G. and C.J. Rosen, *Mechanisms of marrow adiposity and its implications for skeletal health.* Metabolism, 2017. **67**: p. 106-114.

167. Mohseny, A.B., et al., *Functional characterization of osteosarcoma cell lines provides representative models to study the human disease.* Lab Invest, 2011. **91**(8): p. 1195-205.

168. Garcia, D. and R.J. Shaw, *AMPK: Mechanisms of Cellular Energy Sensing and Restoration of Metabolic Balance.* Mol Cell, 2017. **66**(6): p. 789-800.

169. Hie, M., et al., *Insulin-dependent diabetes mellitus decreases osteoblastogenesis associated with the inhibition of Wnt signaling through increased expression of Sost and Dkk1 and inhibition of Akt activation.* Int J Mol Med, 2011. **28**(3): p. 455-62.

170. McCarthy, A.D., A.M. Cortizo, and C. Sedlinsky, *Metformin revisited: Does this regulator of AMP-activated protein kinase secondarily affect bone metabolism and prevent diabetic osteopathy.* World J Diabetes, 2016. **7**(6): p. 122-33.

171. Enomoto, H., et al., *Runx2 deficiency in chondrocytes causes adipogenic changes in vitro.* J Cell Sci, 2004. **117**(Pt 3): p. 417-25.

172. Chen, L., D.J. Magliano, and P.Z. Zimmet, *The worldwide epidemiology of type 2 diabetes mellitus—present and future perspectives.* Nature Reviews Endocrinology, 2011. **8**: p. 228.

173. Kang, J., et al., *Secoisolariciresinol diglucoside inhibits adipogenesis through the AMPK pathway.* Eur J Pharmacol, 2018. **820**: p. 235-244.

174. Li, C., et al., *Design, syntheses and lipid accumulation inhibitory activities of novel resveratrol mimics.* Eur J Med Chem, 2018. **143**: p. 114-122.

175. Imran, K.M., D. Yoon, and Y.S. Kim, *A pivotal role of AMPK signaling in medicarpin-mediated formation of brown and beige.* Biofactors, 2018. **44**(2): p. 168-179.

176. Wang, S.J., W.Y. Lu, and K.Y. Liu, *Adiponectin receptor agonist AdipoRon suppresses adipogenesis in C3H10T1/2 cells through the adenosine monophosphateactivated protein kinase signaling pathway.* Mol Med Rep, 2017. **16**(5): p. 7163-7169.

177. Zhao, J., et al., *AMPKalpha1 deficiency suppresses brown adipogenesis in favor of fibrogenesis during brown adipose tissue development.* Biochem Biophys Res Commun, 2017. **491**(2): p. 508-514.

178. Wang, Y.G., et al., *AMPK promotes osteogenesis and inhibits adipogenesis through AMPK-Gfi1-OPN axis.* Cell Signal, 2016. **28**(9): p. 1270-82.

179. Chen, S.C., et al., *Metformin suppresses adipogenesis through both AMP-activated protein kinase (AMPK)-dependent and AMPK-independent mechanisms.* Molecular and Cellular Endocrinology, 2017. **440**: p. 57-68.

180. Wang, E.A., et al., *Bone morphogenetic protein-2 causes commitment and differentiation in C3H10T1/2 and 3T3 cells.* Growth Factors, 1993. **9**(1): p. 57-71.

181. Otto, F., et al., *Cbfa1, a candidate gene for cleidocranial dysplasia syndrome, is essential for osteoblast differentiation and bone development.* Cell, 1997. **89**(5): p. 765-71.

182. Rosen, E.D., et al., *PPAR gamma is required for the differentiation of adipose tissue in vivo and in vitro.* Mol Cell, 1999. **4**(4): p. 611-7.

183. Aguiari, P., et al., *High glucose induces adipogenic differentiation of muscle-derived stem cells.* Proc Natl Acad Sci U S A, 2008. **105**(4): p. 1226-31.

184. Wang, P., et al., *Metformin Induces Osteoblastic Differentiation of Human Induced Pluripotent Stem Cell-derived Mesenchymal Stem Cells.* J Tissue Eng Regen Med, 2017.

185. Wei, W., et al., *PGC1beta mediates PPARgamma activation of osteoclastogenesis and rosiglitazone-induced bone loss.* Cell Metab, 2010. **11**(6): p. 503-16.

186. Kugimiya, F., et al., *GSK-3beta controls osteogenesis through regulating Runx2 activity.* PLoS One, 2007. **2**(9): p. e837.

187. Wee, H.J., et al., *Serine phosphorylation of RUNX2 with novel potential functions as negative regulatory mechanisms.* EMBO Rep, 2002. **3**(10): p. 967-74.

188. Huang, Y.F., et al., *c-Jun N-terminal kinase 1 negatively regulates osteoblastic differentiation induced by BMP2 via phosphorylation of Runx2 at Ser104.* J Bone Miner Res, 2012. **27**(5): p. 1093-105.

189. Shen, R., et al., *Cyclin D1-cdk4 induce runx2 ubiquitination and degradation.* J Biol Chem, 2006. **281**(24): p. 16347-53.

190. Rajgopal, A., et al., *Mitotic control of RUNX2 phosphorylation by both CDK1/cyclin B kinase and PP1/PP2A phosphatase in osteoblastic cells.* J Cell Biochem, 2007. **100**(6): p. 1509-17.

191. Chen, C., et al., *Human beta cell mass and function in diabetes: Recent advances in knowledge and technologies to understand disease pathogenesis.* Molecular Metabolism, 2017. **6**(9): p. 943-957.

192. Busik, J.V., S. Mohr, and M.B. Grant, *Hyperglycemia-Induced Reactive Oxygen Species Toxicity to Endothelial Cells Is Dependent on Paracrine Mediators.* Diabetes, 2008. **57**(7): p. 1952-1965.

193. Piperi, C., et al., *Crosstalk between Advanced Glycation and Endoplasmic Reticulum Stress: Emerging Therapeutic Targeting for Metabolic Diseases.* The Journal of Clinical Endocrinology & Metabolism, 2012. **97**(7): p. 2231-2242.

194. Ozcan, L. and I. Tabas, *Calcium signalling and ER stress in insulin resistance and atherosclerosis.* Journal of internal medicine, 2016. **280**(5): p. 457-464.

195. Dong, Y., et al., *Role of endoplasmic reticulum stress signalling in diabetic endothelial dysfunction and atherosclerosis.* Diabetes & vascular disease research, 2017. **14**(1): p. 14-23.

196. Tsiotra, P.C. and C. Tsigos, *Stress, the endoplasmic reticulum, and insulin resistance.* Ann N Y Acad Sci, 2006. **1083**: p. 63-76.

197. Hou, Z.Q., et al., *Involvement of chronic stresses in rat islet and INS-1 cell glucotoxicity induced by intermittent high glucose.* Mol Cell Endocrinol, 2008. **291**(1-2): p. 71-8.

198. O'Sullivan-Murphy, B. and F. Urano, *ER Stress as a Trigger for β-Cell Dysfunction and Autoimmunity in Type 1 Diabetes.* Diabetes, 2012. **61**(4): p. 780-781.

199. Byon, C.H., et al., *Oxidative Stress Induces Vascular Calcification through Modulation of the Osteogenic Transcription Factor Runx2 by AKT Signaling.* The Journal of Biological Chemistry, 2008. **283**(22): p. 15319-15327.

200. Lin, C.H., et al., *Oxidative stress induces imbalance of adipogenic/osteoblastic lineage commitment in mesenchymal stem cells through decreasing SIRT1 functions.* Journal of Cellular and Molecular Medicine, 2018. **22**(2): p. 786-796.

201. Nakatani, Y., et al., *Involvement of endoplasmic reticulum stress in insulin resistance and diabetes.* J Biol Chem, 2005. **280**(1): p. 847-51.

202. Giacco, F. and M. Brownlee, *Oxidative stress and diabetic complications.* Circ Res, 2010. **107**(9): p. 1058-70.

203. Kim, H., et al., *Activation of AMP-activated protein kinase inhibits ER stress and renal fibrosis.* Am J Physiol Renal Physiol, 2015. **308**(3): p. F226-36.

204. Lee, J. and U. Ozcan, *Unfolded Protein Response Signaling and Metabolic Diseases.* The Journal of Biological Chemistry, 2014. **289**(3): p. 1203-1211.

205. Eizirik, D.L., A.K. Cardozo, and M. Cnop, *The role for endoplasmic reticulum stress in diabetes mellitus.* Endocr Rev, 2008. **29**(1): p. 42-61.

206. Sheikh-Ali, M., et al., *Hyperglycemia-induced endoplasmic reticulum stress in endothelial cells.* Nutrition, 2010. **26**(11-12): p. 1146-50.

207. Sheikh-Ali, M., et al., *Effects of antioxidants on glucose-induced oxidative stress and endoplasmic reticulum stress in endothelial cells.* Diabetes Res Clin Pract, 2010. **87**(2): p. 161-6.

208. Sakaki, K. and R.J. Kaufman, *Regulation of ER stress-induced macroautophagy by protein kinase C.* Autophagy, 2008. **4**(6): p. 841-843.

209. Sharma, N.K., et al., *Endoplasmic Reticulum Stress Markers Are Associated with Obesity in Nondiabetic Subjects.* The Journal of Clinical Endocrinology and Metabolism, 2008. **93**(11): p. 4532-4541.

210. Wang, D., Y. Wei, and M.J. Pagliassotti, *Saturated Fatty Acids Promote Endoplasmic Reticulum Stress and Liver Injury in Rats with Hepatic Steatosis.* Endocrinology, 2006. **147**(2): p. 943-951.

211. Botolin, S. and L.R. McCabe, *Bone loss and increased bone adiposity in spontaneous and pharmacologically induced diabetic mice.* Endocrinology, 2007. **148**(1): p. 198-205.

Publications

List of publications

1. **Suresh C,** Chennakesavulu S, Gayatri MB, Reddy AB*. A Novel Phosphorylation by AMP-activated Kinase regulates RUNX2 from Ubiquitination in Osteogenesis over Adipogenesis. *Cell death and disease.* (2018) **(Accepted for publication)**

2. Devi A, Chennakesavulu S, **Suresh C**, Reddy AB*. Chapter-17 "Nutraceuticals in Health and Disease". "Functional food and human health". (2018) *Springer-Nature Inc.* (Book chapter ISBN: 978-981-13-1122-2)

Anti-plagiarism certificate

Dynamic Regulation of RUNX2 and AMPK in Metabolic Disorders and Stress

by Chava Suresh

Submission date: 21-Jun-2018 04:17PM (UTC+0530)
Submission ID: 977499956
File name: Chava_Suresh_Thesis12LAPH14.docx (15.29M)
Word count: 15496
Character count: 96558

Dynamic Regulation of RUNX2 and AMPK in Metabolic Disorders and Stress

ORIGINALITY REPORT

10%	7%	8%	4%
SIMILARITY INDEX	INTERNET SOURCES	PUBLICATIONS	STUDENT PAPERS

PRIMARY SOURCES

1	Submitted to National University of Singapore Student Paper	2%
2	Submitted to Indian Institute of Technology, Madras Student Paper	1%
3	Rana, Sandeep, Elizabeth C. Blowers, and Amarnath Natarajan. "Small Molecule Adenosine 5′-Monophosphate Activated Protein Kinase (AMPK) Modulators and Human Diseases", Journal of Medicinal Chemistry Publication	<1%
4	"10th World Congress 15-18 October 2017 Rotterdam, The Netherlands", Journal of Developmental Origins of Health and Disease, 2017 Publication	<1%
5	Acin-Perez, R.. "Protein Phosphorylation and Prevention of Cytochrome Oxidase Inhibition by ATP: Coupled Mechanisms of Energy	<1%